This is to certify that the

dissertation entitled

Analysis of Front Mounted Three-Point Hitch
Geometry On Front-Wheel Assisted Tractors

presented by

Milton Mintsong Mah

has been accepted towards fulfillment
of the requirements for

_____Ph.D._____ degree in _Agric. Engr._

Thomas H Burkhardt
Major professor

Date _June 15, 1990_

PLACE IN RETURN BOX to remove this checkout from your record.
TO AVOID FINES return on or before date due.

DATE DUE	DATE DUE	DATE DUE

MSU Is An Affirmative Action/Equal Opportunity Institution

c:\circ\datedue.pm3-p.1

ANALYSIS OF FRONT MOUNTED THREE-POINT HITCH

GEOMETRY ON FRONT-WHEEL ASSISTED TRACTORS

By

Milton Mintsong Mah

A DISSERTATION

Submitted to
Michigan State University
in partial fulfillment of the requirements
for the degree of

DOCTOR OF PHILOSOPHY

in

Agricultural Engineering

Department of Agricultural Engineering

1990

A

mor

dri

can

imp

to c

How

tract

theo

perf

impr

dime

front

was c

hitche

to pre

These

in two

data to

measu

ABSTRACT

ANALYSIS OF FRONT MOUNTED THREE-POINT HITCH GEOMETRY ON FRONT-WHEEL ASSISTED TRACTORS

By

Milton Mintsong Mah

Front-wheel assisted (FWA) tractors have been used for providing more drawbar pull, higher power, and better field efficiency than two-wheel drive tractors. An FWA tractor equipped with front mounted implements can increase tractive forces from the tractor's front wheels. The front implement serves as ballast to aid vehicle stability and eliminates the need to carry front weights. As a result tractor power is better utilized. However, the front mounted hitch systems should have an impact on the tractor's performance. The general goal of this research was to develop theoretical and experimental means to determine the extent to which the performance of an FWA tractor with front and rear hitches can be improved by adjusting hitch configurations, ballast ratios, and implement dimensions.

A mathematic model was developed to describe the geometries of front and rear three-point hitches. The tractor's dynamic load distribution was calculated using the hitch geometries and the forces applied to the hitches. Finally, two equations published in the ASAE Yearbook were used to predict the pull developed by the tractor wheels and the tractive efficiency. These equations were coded into a computer program which could be used in two modes. The data analysis mode was used to analyze experimental data to predict tractive efficiency which would be difficult or impossible to measure with instruments. The simulation mode was used to predict the

effects of changing hitch dimensions, ballast ratios, and implement dimensions on the tractor's dynamic load distribution.

The field experiment results lead to the conclusion that using an average value of soil cone index to predict pull developed by the tractor's wheels was not adequate. The sensitivity test of cone index revealed that the variation of cone index greatly influenced the predicted value of tractor pull. There are opportunities for improving tractor performance on loose soil. The simulation results showed that dynamic load distribution was affected by the adjustment of most front three-point hitch dimensions. On the other hand, most of the rear hitch dimensions had no effect on dynamic load distribution. The dynamic load ratio changed proportionally to the change of ballast.

Date : *June 15, 1990*

Approved : *Thomas H Burkhardt*

Major Professor

Approved : *Larry Segerlind*

Department Chairperson

To my beloved family, Carina, Alexandre, and Alice

who

prog

indi

profe

inno

guid

this

supp

(CNP

prog

mora

durir

read

ACKNOWLEDGMENTS

I would like to express my sincere appreciation to all of those people who provided encouragement and assistance throughout my graduate program. I would like to extend a special thanks to the following individuals:

* Dr. Thomas Burkhardt, my major professor, for his personal and professional guidance throughout the duration of my program.

* Dr. John Gerrish, member of my guidance committee, for his innovative suggestions during the implementation of testing instruments.

* Dr. Robert Wilkinson and Dr. Ronald Rosenberg, members of my guidance committee, for their professional contribution to my studies.

* Ford New Holland, Inc., for supplying the plowing system used in this research and for their financial support during the research period.

* The Universidade Federal de Viçosa, Brasil, for their financial support during the first part of my program.

* The Conselho Nacional de Desenvolvimento Científico e Tecnológico (CNPq), Brasil, for their financial support during the first part of my program.

* My brother and sister, Marcos and Gamin, for their financial and moral support during my program.

* My friend, Dr. John Goeschl, for his suggestion and assistance during the writing of this dissertation, which greatly improved the readability of this dissertation.

* Last and the most, to my beloved wife, Carina, for her unlimited encouragement and personal sacrifice, so that I could complete this study.

TABLE OF CONTENTS

4.

5. S

6. F

LIST OF TABLES

LIST OF FIGURES

mar

culti

and

As tr

draw

tract

4WD

wher

beco

equi

diser

and

the r

Thes

simil

4WD

'acco

fuel

1. INTRODUCTION

The single axle drive (2WD) tractor has dominated the farm tractor market for years. Its main advantage has been its versatility in row crop cultivation, tillage, and utility operations. As farm size increases, larger and higher powered tractors become more important in tillage operations. As tractor power increases, it becomes difficult to utilize that power at the drawbar with conventional 2WD tractors. The four-wheel drive (4WD) tractor is a popular solution to this problem. Research has shown that the 4WD tractor can improve traction, and can save fuel and time, especially when operating in poor field conditions.

A variation of 4WD tractor called the front-wheel assist (FWA), is becoming popular. This tractor is a modified 2WD tractor which is equipped with a front wheel drive. The front wheel drive can be engaged or disengaged from the operator's platform. The front wheels are steerable and are smaller than the rear wheels. This gives the FWA tractor many of the maneuverability benefits of a 2WD tractor, but with greater traction. These FWA tractors hold an advantage in pull to mass ratio over the similarly powered 2WD tractors. They also are more cost effective than the 4WD counterparts.

Advantages of the FWA systems in comparison to 2WD systems (according to manufacturers) include increased pull, drawbar power, and fuel efficiency. Also wheel slip, rear tire wear, and soil compaction are

redu

FW

seve

effe

few

trac

on a

star

the

the

of t

beh

Thu

thre

intr

from

from

issu

Am

dec

FW

rea

reduced. In addition there is better stability against overturning and the FWA vehicles have increased drive train life.

Due to the popularity of FWA tractors, researchers have conducted several investigations of FWA tractor performance. They have studied the effect of tire size, tire type and other parameters. However, there are very few studies, if any, about the geometry of the three-point hitch in FWA tractors.

The geometry of the three-point hitch used in FWA tractors is based on an ASAE (American Society of Agricultural Engineers) standard. This standard was primarily designed for 2WD tractors, and it was adopted by the ASAE in 1959. Since then, there have been ten revisions. Nevertheless, the design of chassis mechanics for the FWA tractor is different from that of the 2WD tractor. Consequently, the weight distribution and dynamic behavior of FWA tractors must be different from those of 2WD tractors. Thus, the FWA tractor requires a reconsideration of the geometry of the three-point hitch in order to obtain optimal tractive efficiency.

Front mounted three-point hitch systems have recently been introduced in the United States (Figure 1.1). An FWA tractor equipped with front mounted implements can increase tractive forces from the tractor's front wheels. An article (entitled "Dear Murphy...") in the January 1984 issue of Implement & Tractor noted that a front mounted hitch made by American owned companies in Europe has been used there for over a decade. It was also noted that improved traction and reduced slippage on FWA tractors could result if implements were attached to both front and rear hitches at the same time.
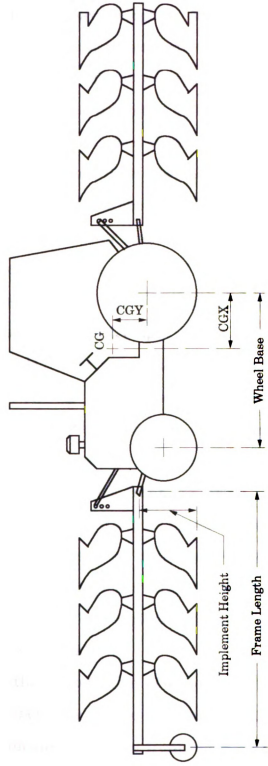
Figure 1.1- Front and rear mounted, reversible moldboard plows.

Before the introduction of the front mounted three-point hitch, a tractor could only work with a limited size of fully mounted implement due to its inability to lift heavy weights. With the front mounted three-point hitch, a tractor can use two implements at the same time and thus increase the working efficiency without overloading the hitching capability. The front implement serves as ballast to aid vehicle stability and eliminates the need to carry front weights. As a result tractor power is better utilized.

A dual three-point hitch also allows a tractor to work with two different implements simultaneously. There are numerous possibilities of using dual implements. For instance, a front mounted sprayer and rear mounted planter, or a front mounted field cultivator and rear mounted planter could perform two operations in one field trip. A front mounted sprayer tank and rear mounted sprayer could better distribute loads to the rear and front axles. The potential advantages of using dual implements are reduced working time, increased productivity, reduced fuel consumption, reduced soil compaction and improved working quality. On the other hand, some specific implements would provide better working control for the operator with front mounting. For example, an operator would rather work with a front mounted row crop cultivator than with a rear mounted one, because he could control both tractor and implement while facing forward. Another example is that front mounted shovels could smooth tire tracks on rough terrain, thus increasing the tire life and reducing operator discomfort.

However, the introduction of front mounted three-point hitches has raised concerns about the tractor and implement design and field operating system. By all means these new front mounted hitch systems should have

an impact on the strength requirements of the tractor's front chassis, as well as on performance, stability and drivability.

and

tra

FW

and

fou

inst

slip

(e.g

pro

Am

note

of t

perf

and

expe

conf

cond

FW

atter

hydr

2. LITERATURE REVIEW

Ballast ratios, hitch configurations, dynamic loads, and performance and many other aspects have been studied in 2WD, 4WD, and FWA tractors, but the specific problem of front and rear hitch configuration on FWA tractors has not been addressed in published literature. A theoretical and practical background for this problem, however, can be drawn from four major lines of research, plus a fifth subject area related to instrumentation.

First, the practical and theoretical treatment of motion resistance, slip, and tractive efficiency (TE) of a given wheel , based on soil properties (e.g. cone index), tire design, tire inflation, and vertical load, has progressed to the point of having at least some standards accepted by American Society of Agricultural Engineers (ASAE). It is important to note that these principles of individual wheel performance are independent of tractor design. Second, there are numerous studies comparing the performance of 2WD, 4WD, and/or FWA tractors. Conflicts in the results and conclusions of these studies have led to considerable discussion and experimentation with ballast ratios and peripheral wheel velocity ratios; conflicting conclusions remain. Third, several studies have been conducted regarding optimization of ballast and hitch positions on 4WD and FWA tractors per se, but primarily with rear loads only. Fourth, a few attempts have been made to develop real-time, computer controlled, hydraulically adjustable hitches using signals from various transducers to

ad

lite

an

wi

pre

bec

inc

pub

ref

2.1

whe

trac

pres

Mar

due

tract

of th

limit

esser

other

adjust dynamic loads to optimize tractive efficiency. A fifth area of literature regarding the design of instrumentation, computer hardware, and algorithms necessary to conduct the experiments for the present study will be discussed in Chapter 6.

Both refereed and non-refereed publications (many of them presentations at ASAE meetings) are included in the present review because of the scarcity of published studies in many of these areas, inconsistencies in the reported results and conclusions of some refereed publications, and the lack of comprehensive literature citations in many refereed publications.

2.1 Effects of tire design, inflation pressure, loading, and soil properties on tractive efficiency

The recognition of energy losses due to motion resistance and drive wheel slip and their significance for efficient operation of agricultural tractors has long been recognized. The tractor drawbar predictor chart as presented in the ASAE Yearbook's Data D230.4 Agricultural Machinery Management Data, illustrates the penalty for non-optimal slip operation due to incorrect ballasting and/or drawbar pull for a two-wheel drive tractor. Excessive ballast reduces slip but also increases motion resistance of the tractor, thus reducing overall tractive efficiency. Since there is only limited published data regarding these parameters in FWA tractors, and essentially none regarding FWA's with front hitches, one must draw upon other sources of information.

2

e
f
r
sc

2..

res
Lut
resi

2.1.1 Rigid wheel theory

Barger et al. (1963) discussed the methodology and developed equations to theoretically calculate the motion resistance of traction devices. The equations were based on the dynamic wheel load, wheel size, and cohesive and frictional properties of the soil. The use of the equations is limited as the soil properties are difficult to determine accurately. These concepts and equations with respect to thrust and dynamic weight relationships for rigid wheels were further developed by Burt & Bailey (1975), Bailey et al. (1976), and Bailey & Burt (1976).

Later, Bekker (1983) presented methods, tests, and numerical examples for prediction of design and performance parameters in agroforestry vehicles. He presented a simplified expression for calculating the rolling resistance coefficient, but use of the equation still required values for soil and tire parameters that were not readily available.

2.1.2 Pneumatic wheel theory

One of the more simplified expressions for determining motion resistance of a wheel with a pneumatic tire was developed by Wismer and Luth (1974). Using dimensional analysis, they showed that the motion resistance of a towed tire could be predicted from:

$$F = W\left[\frac{1.2}{c_n} + 0.04\right] \tag{2.1}$$

where:

F = towed force, N

W = dynamic wheel load, N

c_n = wheel numeric

to

de

was

2.1.

app:

reg;

perf

$$c_n = \frac{CIbd}{W} \qquad (2.2)$$

b　　= unloaded tire section width, cm

d　　= unloaded tire diameter, cm

CI　　= cone index as defined by ASAE Standard S313.1, N/cm^2

While equation 2.1 was used to predict traction characteristics of a towed wheel with a pneumatic tire on soil, Wismer and Luth (1974) also developed another equation for the driving wheel.

$$\frac{P}{W} = 0.75 \left(1 - e^{-0.3\, c_n\, s} \right) - \left(\frac{1.2}{c_n} + 0.04 \right) \qquad (2.3)$$

where:

P　　= driving wheel pull, parallel to soil surface, N

s　　= wheel slip, decimal fraction

and all other terms were as defined for a towed wheel. Wheel slip was defined as follows:

$$s = 1 - \frac{V_a}{V_t} \qquad (2.4)$$

where:

V_a　　= actual travel speed, km/h

V_t　　= theoretical travel speed, km/h

2.1.3 Pneumatic wheel performance

Several factors determine the extent to which a given wheel would approach optimal, theoretical performance. There are numerous studies regarding the effects of tire design, inflation pressure, and loading on the performance of single wheels with pneumatic tires.

r

p

e

o

N

p

(

po

fie

tir

me

for

has

app

ind

mea

dist

abou

figu

eval

esta

refer

by t

Only selected samples of some publications will be given here, since many of these review and cite previous, historically important papers. Performance effects of standard, commercially available tread designs, for example, were studied by Taylor (1976). The effects of tire width and diameter on tractive performance were studied by Dwyer & Heigho (1984). More recently similar studies of radial tires have led to the tractive performance predictive equations by Brixus (1987) and by Upadhyaya et al. (1987).

Ellis (1977) reported that agricultural tire deflections average about 19 percent under conditions of rated load and inflation pressure for normal field conditions. He defined the deflection as the ratio of the reduction in tire section height at ground contact to the undeflected tire section height measured above the rim flange area. With the increased loads approved for slow speed operations, tire deflections will approach 25 percent. This has been found to be about the practical limit for agricultural tires in any application where normal service life is expected. On the other hand, he indicated that the dynamic loaded radius was slightly larger than the one measured statically. When in motion, there was a lifting action due to the distribution of stresses in the moving tire which resulted an increase of about 3 to 3.5 percent in the tire section height compared with the static figure.

Gee-Clough and McAllister (1982) conducted a series of field tests to evaluate the effects of wheel ballasting on a tractor's power output. They established a dynamic rear axle load as the optimum value and used as the reference point throughout their tests. They concluded that power delivered by the tractor increased as the rear axle load approached its optimum value

bu

its

eff

on

an

83.

sli

the

dif

ran

the

fou

tra

tha

mir

or

10

nec

det

eff

by

be

pre

eff

but the rate of increase decreased when the axle load was at 70% or more of its optimum value.

Burt and Bailey (1982) reported on efforts to optimize tractive efficiency while holding net traction constant. They varied the static load on a 20.8-R38 radial tire throughout the range recommended by the Tire and Rim Association. They also varied the inflation pressure using 28, 55, 83, and 110 kPa. They compared the tractive efficiency at both 10 and 20% slip. Results showed that tractive efficiency can be optimized by selecting the appropriate levels of dynamic load and inflation pressure. The relative difference in tractive efficiency between optimum and minimum was in the range of 6 to 10%, depending upon soil conditions.

Burt et al. (1983) conducted a similar study under field conditions at the University of Natal, Republic of South Africa. These tests were run at four levels of inflation pressure at each of four levels of dynamic load. Net traction was held at 10 kN for each operating condition. Results showed that the difference in tractive efficiency between the maximum and the minimum was dependent upon soil condition and tire construction (radial or bias). The observed difference (i.e. maximum - minimum) ranged from 10 to 21%. They also reported that the maximum tractive efficiency did not necessarily occur at the minimum level of slip.

Lyne and Burt (1987) developed a computerized system for determining the dynamic load and inflation pressure for optimum tractive efficiency under dynamic conditions and within the ranges recommended by Tire and Rim Association. They affirmed that the tractive efficiency can be optimized by selecting the proper values of dynamic load and inflation pressure. The difference between the optimum and minimum tractive efficiency depended upon the net traction demanded, the soil type, and the

so
inc
pre

2.2

tes
dyr
opt

2.2

ma
con
dri
pos
opt
loos
forr
Hov
mec
in t
prol

soil condition. Under some operating conditions, they achieved a 30% increase in tractive efficiency by selecting the dynamic load and inflation pressure for optimum efficiency.

2.2 Comparisons of 2WD, 4WD, and FWA tractor performance

Papers comparing 2WD, 4WD, and/or FWA tractors often discuss tests with each tractor at different front-to-rear (f/r) ballast ratios or dynamic loads. Although these studies are not necessarily aimed at optimization of performance, they offer some information along these lines.

2.2.1 Soil bin tests of multiple wheel passes

Some attempts to predict performance of 4WD tractors have been made using multiple passes of single wheels. Burt et al. (1980) used continuously changing dynamic loads during first and second passes of a drive wheel over the same track in a soil bin as a means of evaluating possible tandem wheel drives. They found only limited opportunities for optimization of f/r load ratios in firm soil but slightly better opportunities in looser soils. In a later study (Bailey & Burt, 1981) the advantages of some form of tandem drive over single wheel or dual wheel drives were shown. However, since the second passes of the wheel were not linked mechanically to the first, no possibility for dynamic f/r interactions existed in these studies, thus the results have limited application to the present problem.

i

c

r

2

a

u

cc

co

(u

co

to

he

hav

res

bet

osci

2.2.3

trac

pres

FW

loss

oper

2.2.2 Performance of 2WD vs 4WD tractors

Introduction of the 4WD tractor led to numerous comparisons which generally showed an advantage of the 4WD over 2WD under various conditions. For example, Rackham & Blight (1985) conducted an extensive review of published papers about the advantage of the 4WD tractors over 2WD. They concluded that on a firm, flat surface, 4WD offers very little advantage; but as soil conditions become progressively softer so the usefulness of 4WD increases. Clark (1984) reviewed several papers comparing the performance of various 2WD and 4WD tractors, then conducted experiments with a 4WD tractor in the 2WD and 4WD modes (unfortunately with the same ballast ratio). Nevertheless these results also confirm that drawbar pull and ground speed were greatly improved (e.g. 60 to 125%) in the 4WD mode, along with a 25% to 57% reduction in fuel use per hectare. Although TE was not calculated directly, it can be presumed to have been higher in the 4WD mode. One important point in these and other results is that different operating speeds may affect the relationships between unevenness of the ground, variations in pull resistance, and the oscillation and/or deformation frequencies of the tractor-implement system.

2.2.3 Performance of 2WD vs FWA tractors

The possible advantages of FWA tractors over conventional 2WD tractors have also been studied by several researchers. Bashford (1984) presented the results of comparative tests with different drawbar loads on a FWA tractor operated in the 2WD mode and FWA mode based on the power loss due to slip and motion resistance. He concluded that, for the tractor operating in the FWA mode, slip power loss is relatively independent of

ba

ba

du

in

ra

in

an

wh

dis

san

Tra

gea

this

per

was

diffe

for a

Figu

incr

appr

acco

level

0.32.

drive

ballast distribution. However, with the tractor operating in the 2WD mode, ballast distribution is very important. On the other hand, the power losses due to motion resistance as related to vehicle traction ratio are relatively independent of drive mode and ballast distribution.

Bashford (1984) again studied the effects of two static (ballasted) load ratios (f/r = 41/59 & 26/74) on the performance of an FWA tractor operating in the 2WD and FWA modes, pulling only a rear drawbar load consisting of another tractor. Tests were performed on two different soil conditions in a wheat stubble field, one a moderately firm soil condition with the field only disked, and a looser soil condition following plowing and disking of the same field. Different ratios of drawbar pull to gross tractor load (Vehicle Traction Ratios, or VTR) were generated by driving the tractor in different gears at different engine speeds. The results are summarized below and in this summary his parameter called Axle Power Loss will be expressed as a percentage of Total Axle Power (TAP).

Power loss due to Motion Resistance (MR) as a percentage of TAP was essentially independent of the drive modes and load ratios, but was different on the two soil conditions. For the firm soil condition it accounted for approximately 40% of TAP at VTR = 0.1 (these values estimated from Figures 1 & 2 of Bashford, 1984). It decreased substantially as VTR increased, but began to level off asymptotically toward a value of approximately 22% of TAP as VTR approached 0.25. On the looser soil MR accounted for 48% of TAP at VTR = 0.1, and likewise declined and began to level off toward a value of approximately 22% of TAP as VTR approached 0.32.

Power loss due to slip as a percentage of TAP was affected by the drive modes and by ballast ratio in the 2WD mode, but not by ballast ratio in

the FWA mode. With the tractor in the FWA mode, slip accounted for approximately 6% of TAP on both the firm and looser soil, and increased almost linearly toward approximately 19% of TAP on the firm soil and 24% of TAP on the loose soil at VTR = 0.35. With the tractor in the 2WD mode and with a ballast ratio of 26/74 slip began at values of approximately 7 and 8% of TAP and increased to 20 and 28% of TAP on the firm and loose soils, respectively. Although the values of slip in the 2WD mode were higher than the corresponding slip when front wheels were powered, the slopes of the increase in slip with VTR were similar. However, with a ballast ratio of 41/59 in the 2WD mode, slip increased more steeply from 8% of TAP at VTR = 0.1 to 21% at VTR = 0.3 on the firm soil, and curved non-linearly from 11% to more than 35% as VTR passed 0.25.

Power converted to Drawbar Pull (DP) as a percentage of TAP (i.e. Tractive Efficiency) was highest in the FWA mode at all values of VTR and was independent of ballast ratio. In the firm soil it formed a broad convex curve from approximately 61% at VTR = 0.1, to a maximum of approximately 68% of TAP at VTR = 0.27, then declined to 64% at VTR = 0.35. In the 2WD mode with a ballast ratio of 26/74 on firm soil the DP curve had values uniformly 4% lower than those of the FWA mode for all VTR values. Changing the ballast ratio to 41/59 on firm soil lowered the initial value of DP to 52% of TAP at VTR = 0.1, with the maximum DP of 58% occurred at VTR = 0.22, and caused a steeper decline of DP to 54% while VTR increased from 0.22 to 0.29. The looser soil condition lowered the VTR values of all of these curves to maxima of 60%, 56%, and 48% respectively.

This study did not address the issue of dynamic loading. The total static load was maintained at 5105 Kg, however one is left to assume that the towed load (i.e. a second tractor) did not add significant static vertical

load. No information is given about the rear hitch configuration, thus it is not possible to estimate how much the dynamic load ratio differed from the static ratio over the different values of VTR. Regardless of these considerations, the results of this study appear to be somewhat in conflict with the earlier study by Woerman & Bashford (1983) and that of Mueller & Freer (1986), discussed below.

Kucera et al. (1985) obtained results which appear to conflict with other studies of 2WD and FWA tractor performance, especially with respect to fuel efficiency per hectare. They concluded that when each was operated at its respective optimal ballast ratio, the 2WD could equal or surpass the FWA tractor. They also reviewed a number of papers with a wide range of conflicting results, but cautioned that in many cases the two types were not optimally configured. While these 2WD vs FWA comparisons do not bear directly on the present study, they do point out the general lack of a systematic way of setting, measuring and/or calculating tractor configurations.

Shell et al. (1986) also compared what they believed were optimally balanced 2WD and FWA tractors, and reached the opposite conclusion from Kucera et al. (1985), namely that fuel efficiency of the FWA was better at all pull levels tested in three soil types.

Mueller and Freer (1986) presented test comparisons of FWA versus conventional 2WD CASE-IH tractors. They reported that the FWA tractors were superior to their 2WD counterparts in pulling performance. An issue emphasized in that paper was the importance of the proper weight ratio on FWA tractors and the critical nature of weight ratio to the measured performance.

Babacz et al. (1986) conducted an extensive series of tests with an instrumented FWA tractor to determine the ballast distribution that led to the highest tractive efficiency for operation in the 2WD and FWA models. A subsequent step was to compare tractor performance in these two modes when operating at optimum ballast distribution. Relative performance reported for operation in good, intermediate, and poor tractive conditions showed that the optimum ballast distribution for the FWA mode required 60-64% of the tractor static weight on the rear axle, a result which was in agreement with what other researchers had found. Felsenstein et al. (1987) continued tests similar to those reported by Babacz et al. They concluded that the FWA mode with optimum ballast generally outperformed the 2WD mode. However, the optimization curve is relatively flat compared to that of 2WD tractors.

2.3 Configuration optimization studies in 4WD and FWA tractors

Murillo-Soto & Smith (1977, 1978) used a 1:10.9 scale 4WD model in a soil box with sand or clay loam to establish that front to rear (f/r) static load ratio (i.e. ballast ratio), drawbar vertical position (which affected dynamic weight transfer), and different f/r wheel peripheral velocities could affect tractive efficiency. They adjusted the ballast ratio and effective drawbar height and used an equation established in their 1977 paper to calculate absolute dynamic weight transfer. The dynamic f/r load ratios were not measured and are difficult to calculate from their published data since the absolute total weight of the model was not given.

The primary result of their study was that tractive efficiency increased as angular velocity of the axle supporting the larger dynamic

load was increased. Since the front and rear tires of this test model were equal in size, the actual f/r ballast ratios and hitch positions for this model would not likely apply directly to a FWA tractor with its smaller front wheels. This same problem of comparing results from one tire size to another occurs in many of the studies discussed below.

Another important observation was that even under ideal conditions (i.e. 1:1 f/r ratios of load and of angular axle velocities on dry sand) weight transfer was about 5% lower than theoretical predictions. This discrepancy increased as the ratios of loads and angular velocities deviated from 1.0, and was attributed to shaking and vibration (i.e. angular acceleration of the tractor), front-to-rear oscillations in slippage (i.e. "push-pull" effect), and desynchronization of the tire lugs. This is suggestive that in addition to optimizing the sum of slippage and motion resistance, optimal static load distributions and hitch configurations may improve TE by minimizing these oscillatory power losses.

Erickson & Larsen (1983) also focused on the problems of oscillations in f/r load ratios and/or power ratios, and the associated variations in TE under field conditions. Heavy draft loads increased the oscillation problems, which became unmanageable under conditions of turning. They did not confirm the "push-pull" effect suggested by the soil bin model studies of Murillo-Soto & Smith (1977, 1978), but do confirm that power losses from oscillatory motion may greatly reduce performance below theoretical predictions under real operating conditions.

In many other studies only static ballasting was considered, for example Shell et al. (1986) used fuel efficiency during field tests to determine some relationships between total mass (three levels) and ballast ratios (three levels) in an FWA tractor on three soil types. Their results are

suggestive that some of the discrepancies in published optimal ballast ratios resulted because the ratios used were not properly matched to the total mass.

Woerman & Bashford (1983) presented TE data for an FWA tractor [assuming a rear drawbar load] showing an optimal f/r dynamic load ratio of about 40/60 and optimal f/r wheel peripheral velocity ratio of about 1.03. TE was improved, and differences in the various tractor configurations were minimized (i.e. the optimization curves were flattened) when the tractor was operated at a speed of about 8 km/h as compared to 4-5 km/h. This resulted because of a substantial decrease in slip accompanied by a smaller relative increase in rolling resistance.

Mueller & Freer (1986) used a mechanical front drive (MFD) tractor (i.e. Case-IH 3594) with an unspecified rear drawbar load. They found that some ballast ratios resulted in slightly lower amounts of rear wheel slip than others over a range of drawbar pulls (see Table 2.1). The differences were more noticeable on the firm soil (i.e alfalfa sod).

Table 2.1 - Rear wheel slippage summarized from tests "CTT436S" and "CTT436T" of Mueller & Freer, 1986

| Soil condition | F/R Axle Load Ratio | | | |
DP range (lbs)	25/75	30/70	40/60	45/55
Alfalfa sod 4700 - 10300	16.8	16.7	13.9	15.7
Tilled soil 2900 - 11300	11.9	11.0	12.5	12.9

2.4 Attempts to design and test real-time adjustable hitches

Summarizing the above sample studies it is clear that many factors interact to determine the performance of an FWA tractor. These include soil and tire properties, total mass, static ballast, dynamic loading, tractor speed, possibly front-to-rear oscillations, and possibly angular momentum. One approach to dealing simultaneously with these interactions in real time is with computer controlled adjustments of various parts of the tractor-implement system.

Smith & Khalid (1982) attempted to minimize oscillations in weight transfer in two scale models (i.e. 1/10.9 and 1/5.7) fitted with computer controlled hitch systems whose vertical position was adjusted in real time in response to signals from torque transducers on the front and rear axles. While these systems did respond as planned by optimizing the f/r division of power, they concluded (primarily on the basis of other published studies) that this adjustment would not increase TE, but may reduce uneven wear on the drive system.

Dodd et al. (1986) attempted to optimize rear wheel load in a 2WD tractor using a computer controlled 3-point hitch in which the height of the upper link position was adjusted hydraulically. Proper angles of the hitch configuration were maintained by sliding the upper hitch point through an angled slot which approximated the effect of adjusting the upper link length. The effect of this adjustment was to alter the virtual hitch point in response to signals from appropriate load transducers [described in Reynolds et al. (1982)] and a mathematical model which included instantaneous calculations of cone index and optimal loading to improve TE. Field studies indicated that the hitch responded as expected, but actual

field evaluation for improved tractor performance had not been completed. These authors also mention another study of an automated hitch adjustment system for 4WD tractors [i.e."McNab (1982)"], but failed to cite the publication reference. Cowell & Herbert (1988) used a variable-length upper link to improve the depth control of a fully mounted implement. However, they did not address the effects of three-point hitch geometry on tractor's dynamic behavior.

2.5 Summary

Past researchers have focused on several factors which affect tractive efficiency such as soil types, tire characteristics and inflation pressures, static ballasting ratios, rear hitch configurations, and the resulting dynamic loading. Many of these observations were made in the course of studies designed to compare the tractive efficiency of 2WD with 4WD and/or FWA tractors. An overview of these studies results in several impressions.

First, it is clear that hitch configurations and ballast ratios affect the performance (including TE) of 2WD tractors, but considerably less so for 4WD and FWA tractors. Indeed, in optimization studies of 4WD and FWA tractors the range between the highest and lowest values of TE were only a few percent, whereas there were greater differences for a given 2WD tractor.

Second, in comparison tests where each type of tractor was optimally configured the differences in TE between 2WD and 4WD or FWA tractors were a few percent smaller. Note, that a 4WD or FWA tractor may have greater value to the user beyond that of moderately better TE because of added advantages in plowing speed, implement pulling capacity, or other

characteristics relevant to a particular type of farming operation. However, it does forewarn that the opportunity for optimization of TE by hitch configurations and/or ballasting in FWA tractors may be limited.

Finally, since none of the publications dealt with combined front and rear hitches and implements on FWA tractors, a number of questions remain open, for example:

1) How do the combined front and rear hitches affect dynamic loading, TE, handling, and other performance characteristics of FWA tractors in comparison to those with a rear hitch and implement only?

2) Is the range of opportunity for optimization of a given FWA tractor with front and rear equipment greater than, the same as, or less than the same tractor with rear equipment only?

If one finds that there is good opportunity for optimization then:

3) How should the front and rear hitches be configured in general, and how would this vary with different types of implements, soils and other factors?

4) How should the tractor be ballasted for optimal TE with front and rear hitches, and with different implements?

The remaining chapters of this dissertation will address some steps intended to answer these questions, and hopefully provide the means of achieving the best performance from this new type of agricultural tool.

3. GOALS, OBJECTIVES, CONSTRAINTS AND ASSUMPTIONS

3.1 Goals

The general goals of this research are to develop theoretical and experimental means to:

1) Determine the extent to which the performance, especially tractive efficiency (TE), of an FWA tractor with front and rear hitches can be improved by adjusting hitch configurations, ballast ratios, or other properties of the tractor implement system as outlined in section 2.5.

2) Provide a basis for attaining whatever optimization is possible.

3.2 Objectives

The primary objectives necessary to accomplish the above goals are:

1) Develop a mathematical model of an FWA tractor with both front and rear, three-point hitches. This model, would utilize static dimensions and properties of the tractor and hitch system, along with dynamic forces and movements of system components during field operation, to calculate those parameters, such as dynamic loads and wheel slippage that are necessary to evaluate performance, e.g. tractive efficiency (TE).

2) Develop the instrumentation, data acquisition system and software necessary to obtain the measurement data from field tests, and to

develop the software necessary to evaluate that data utilizing the model from the first objective.

3) Conduct sufficient field tests to determine if the model and measured parameters are adequate to analyze and predict performance for this type of tractor system.

4) If the third objective is favorable, then the model and field measurements will be used to evaluate the potential opportunities for optimization in this type of tractor system and make specific recommendations for experiments, modifications, or other developments to achieve these ends.

3.3 Constraints

Several things constrainted the development of this simulation model in order to maintain the compatibility of the tractor and implements and to maintain safe working conditions. The constraints were:

1) The simulated geometry of rear three-point hitch had to be compatible with the ASAE standard for the implements. At present ASAE standards have not been published for front hitch geometry, thus in this study the manufacturer's dimensions were used as a starting point.

2) The dimensions of the simulated rear implement's mast had to follow the specification of the ASAE standard. The front implement's mast dimensions have also not been standardized by ASAE; thus, in this study the front mast dimensions were set the same as the rear.

3) The simulated hitching geometry had to promote soil penetration for the implements.

4) The hitching geometry had to promote stability at working depth without excessive penetration.

5) The arrangement of ballast could not violate the working safety code.

6) The addition of ballast could not cause load beyond the tire specification.

7) The tractor's weight distribution on both axles, with the addition of ballast, could not exceed the maximum permissible load, either in static or in dynamic situation.

8) The tractor's total weight with ballast could not exceed the specification of Roll Over Protection Structure (ROPS).

3.4 Assumptions

Several assumptions simplified the design procedure and simulation model:

1) The implement's working depth was assumed constant after it reached the steady state, regardless of the field conditions.

2) The irregularity on the soil surface was assumed to be negligible. However, the field inclination was not ignored.

3) The upper link point on the mast of the front implement was an oval shaped slot which permitted relative motion between the link pin and the mast. Before the implement reached the working steady state, the upper link was in tension. The link pin was assumed to be at one end of the slot (Figure 3.1). However, it was

assumed that when the front implement reached working steady state, the link pin moved to the opposite position (Figure 3.2). With a proper adjustment of the front three-point hitch and implement, the front upper link should not experience any load.

4) The rolling radii of tractor wheels were measured with implements in the raised position. The rolling radii while the implement was actually working are likely to be slightly smaller. However, this difference was assumed to be negligible.

5) The difference of rolling radius caused by the field topography was considered to be negligible.

6) The center of gravity of each wheel ballast was assumed to be at the center of the wheel.

7) The front axle load was considered to be distributed equally to both wheels. The difference caused by the in-furrow travel was considered to be negligible.

8) The tractor was assumed to be advancing at constant ground speed when it reached the working steady state.

9) Gibson and Biller (1974) verified how the fuel and hydraulic fluids affect the location of the center-of-gravity of the tractor. They concluded that these effects were negligible. Their assumption was used in this research.

10) The weight of the data acquisition system and the tractor operator was included in the total tractor weight. However, the weight difference between different operators was considered to be negligible.
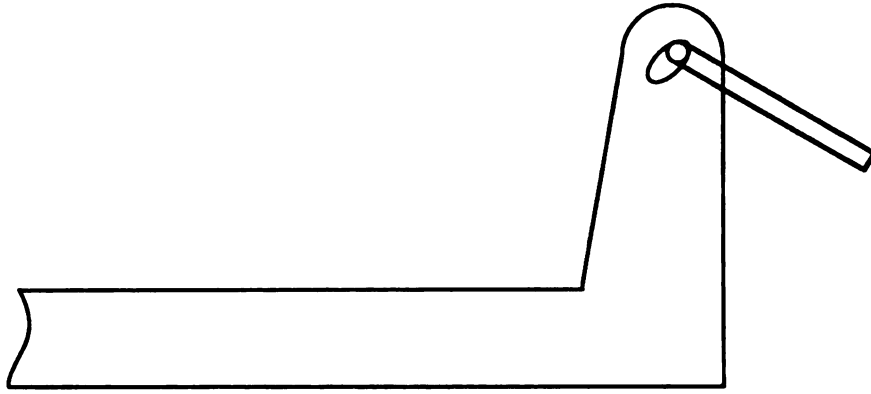
Figure 3.1 - Position of upper link pin at the front three-point hitch before the implement reaches steady working state.
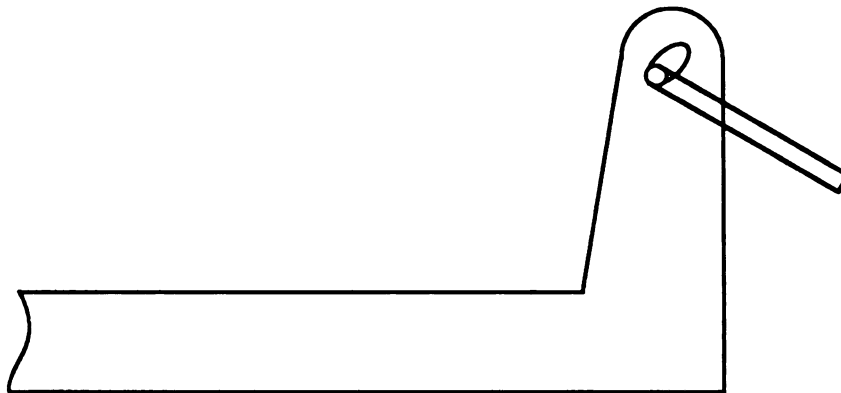
Figure 3.2 - Position of upper link pin at the front three-point hitch after the implement reaches steady working state.

11) The components of the data acquisition system were spread inside the tractor cab, with the majority of its weight located behind the rear axle. The position of the operator seat could be adjusted to fit the operator's body dimension and driving habit; however, the position was always over or before the rear axle. Thus, it was assumed that the total weight of the data acquisition system and operator acted directly on the rear axle.

4. MATHEMATIC MODEL

4.1 Kinematical analysis

The geometries of front and rear three-point hitches must be designed so that they could provide conditions for an implement's penetration, working stability, and in-field manipulation along with optimal performance. The following model is designed to predict theoretically how hitch geometry will affect these parameters, and to serve as a means of evaluating data from field experiments and optimization tests.

4.1.1 Reference position and sign conventions for the tractor

The reference position used through this dissertation was the position in which the tractor operator sits on the seat and faces toward the front of the tractor. In this case, the right-hand side was referred to the operator's right-hand side and the same rule to the left-hand side.

The tractor's transverse angle was defined as positive when it was counter-clockwise at the reference position. The tractor's pitch angle (longitudinal) was defined as positive when the tractor is going uphill.

4.1.2 Sign conventions for the front and rear hitches and implements

The angle of any given link (i.e. upper or lower, front or rear) relative to the ground is considered positive if the hitch point of the link is higher than the link point. The angle between a vertical reference line drawn

through the lower link point and a line drawn from the lower link point to the upper point is positive if the latter line slopes away from the vertical line toward the tractor center. Likewise, the angle of the main longitudinal axis of an implement relative to the ground is positive if the end of the axis away from the hitch point is higher than the hitch point.

Note, in the various figures that follow (with the tractor facing left), these conventions have the effect that positive angles will be oriented clockwise in the rear hitch system, but will be oriented counterclockwise in the front hitch system.

4.1.3 Mechanism for the rear three-point hitch

There are three working positions for the three-point hitch which deserve special consideration when designing its geometry. The first position is that in which the implement is lifted for transportation (Figure 4.1). In this position, the distance between the hitch point and the soil surface (RHH) must provide sufficient clearance for the implement so that the tractor can maneuver in the field. The second position is that in which the implement merely touches the soil surface (Figure 4.2). In this position, the implement frame angle (ϕ_r) must be positive in order to promote a penetration force into the soil. The third position is that when the implement reaches steady working state (Figure 4.3). In this position, the frame must remain parallel to the soil surface and the frame angle must be 0° during the working period so that the implement can keep the working depth constant.

Figure 4.1 - Geometry of rear three-point hitch, with plow in transportation position

Figure 4.2 - Geometry of rear three-point hitch, with plow in penetration position

Figure 4.3 - Geometry of rear three-point hitch, with plow in working position

From Figure 4.1 the following equations can be obtained.

$$\alpha_r = \sin^{-1}\left\{\frac{RHH - (RRR - RLY)}{AD}\right\} \tag{4.1}$$

$$\beta_r = \tan^{-1}\left\{\frac{RLX - RTX}{RLY + RTY}\right\} \tag{4.2}$$

where:

α_r = rear lower link angle relative to soil surface, degrees

RHH = perpendicular distance from rear hitch point to soil surface, cm

RRR = rear wheel rolling radius, cm

RLY = vertical distance from rear axle center line to rear lower link point, cm

AD   = effective length of rear lower link as shown in Figure 4.4, cm

β_r = the angle formed by a line connecting the centers of the rear upper and rear lower link points in relation to a vertical line through the lower link point, degrees

RLX = horizontal distance from rear axle center line to rear lower link point, cm

RTX = horizontal distance from rear axle center line to rear upper link point, cm

RTY = vertical distance from rear axle center line to rear upper link point, cm

By the sign convention used in this dissertation, the angle β_r shown in Figure 4.1 is negative, whereas the angle α_r is positive. The diagonal distance **BD** of the rear three point hitch, and the angle formed by the diagonal line **BD** and the lower link **AD**, δ_r, can be calculated by analyzing the geometry of Figure 4.1.

$$BD = \sqrt{AB^2 + AD^2 - 2*AB*AD*\cos(90° - \alpha_r + \beta_r)} \qquad (4.3)$$

$$\delta_r = \cos^{-1}\left\{\frac{AD^2 + BD^2 - AB^2}{2*AD*BD}\right\} \qquad (4.4)$$

where:

AB = distance from rear lower link point to rear upper link point, cm

Finally, the rear implement angle, ϕ_r, and the rear upper link angle, θ_r, are obtained by the following equations.

$$\gamma_r = \cos^{-1}\left\{\frac{BD^2 + CD^2 - BC^2}{2*BD*CD}\right\} \qquad (4.5)$$

$$\phi_r = \omega_r = 90° + \alpha_r - \delta_r - \gamma_r \qquad (4.6)$$

$$\psi_r = 90° - \gamma_r - \omega_r \qquad (4.7)$$

$$\theta_r = \cos^{-1}\left\{\frac{BC^2 + BD^2 - CD^2}{2*BC*BD}\right\} - \psi_r \qquad (4.8)$$

where:

γ_r = angle between rear diagonal line and rear implement mast, degrees

BC = rear upper link length, cm

CD = rear implement mast height, cm

ϕ_r = rear implement frame angle relative to soil surface, degrees

ω_r = rear implement mast angle relative to the line perpendicular to soil surface, degrees

ψ_r = rear diagonal line angle relative to soil surface, degrees

θ_r = rear upper link angle relative to soil surface, degrees
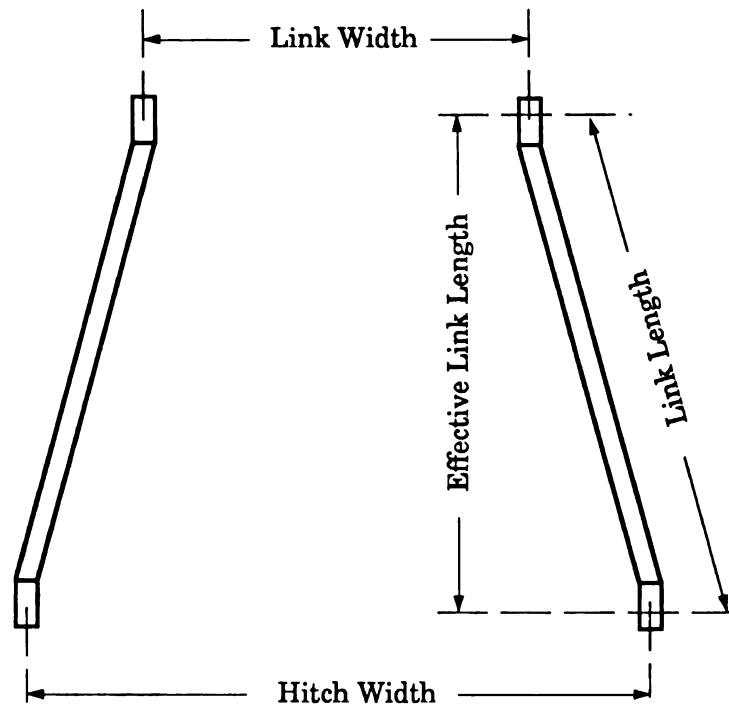
Figure 4.4 - Effective lower link length

4.1.4 Mechanism for the front three-point hitch

The same three special working positions for the rear hitch also deserve special consideration when designing the front three-point hitch geometry (Figures 4.5 to 4.7). However, there are differences due to some different moving requirements for the front implement.

The steady state working position still requires a 0° frame angle for the front implement (Figure 4.7). However, the angle ϕ_f at the penetration position (Figure 4.6) must be negative so that there is a penetration angle on the implement. The requirement for transportation is the same as the rear hitch (Figure 4.5).
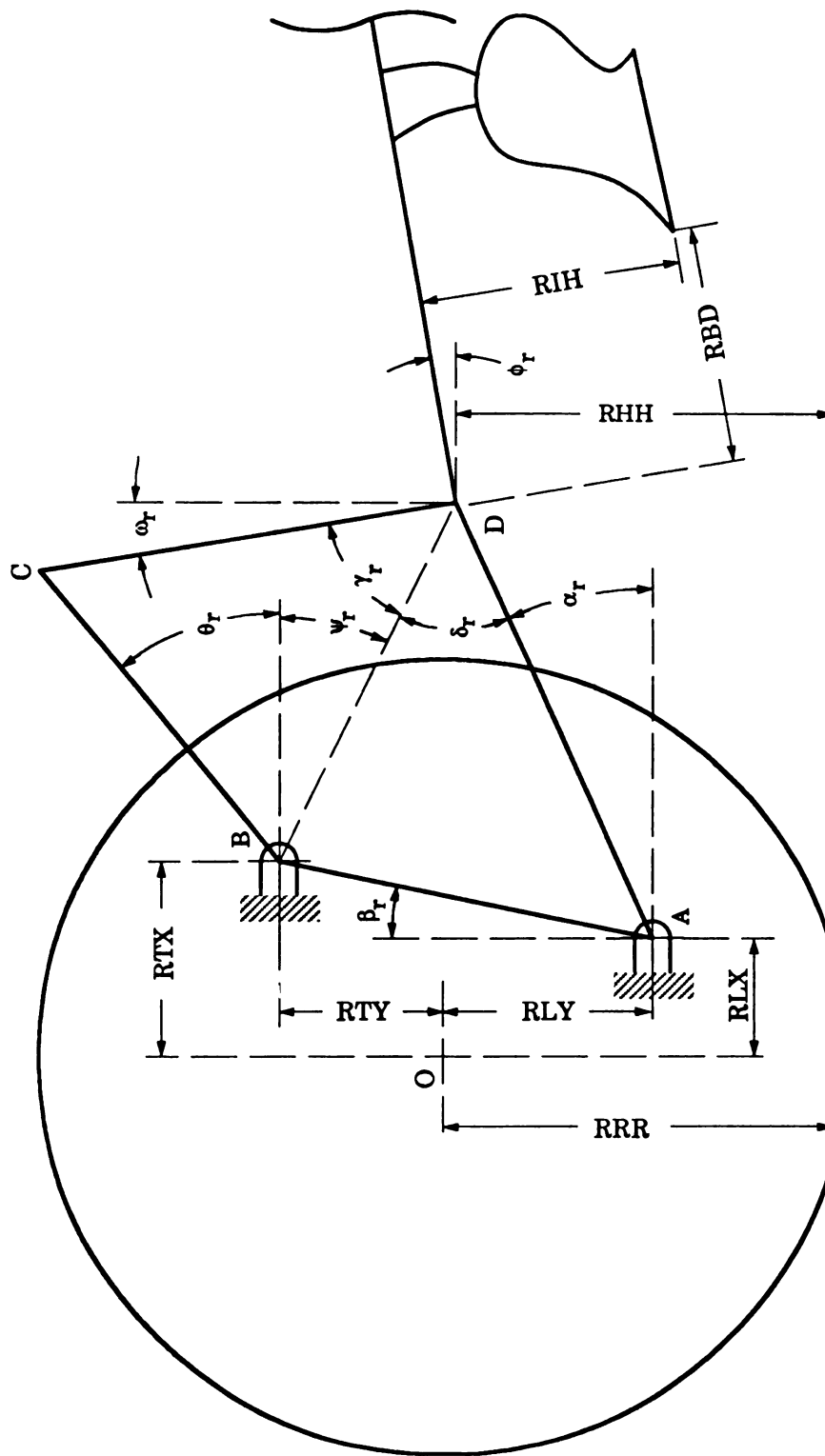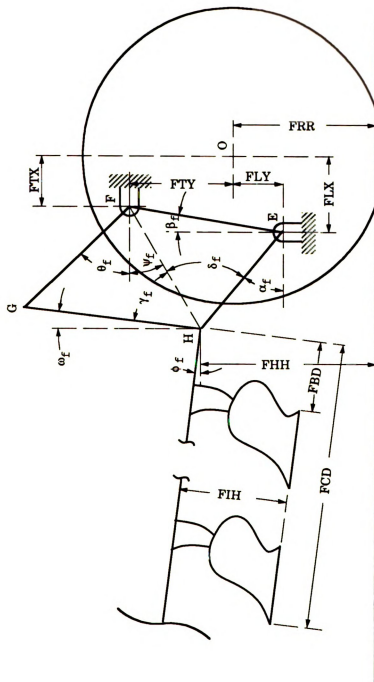
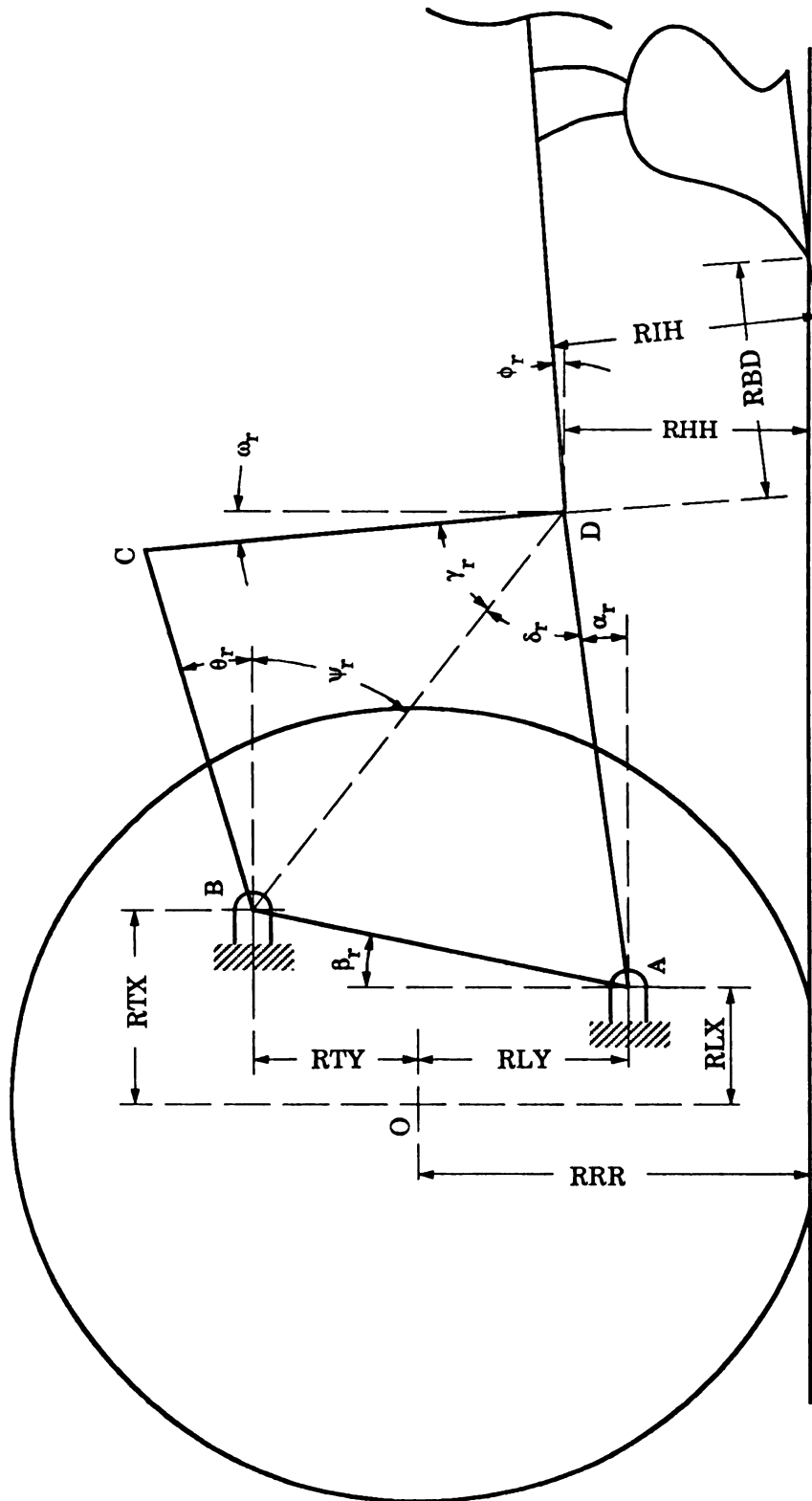Figure 4.5 - Geometry of front three-point hitch, with plow in transportation position

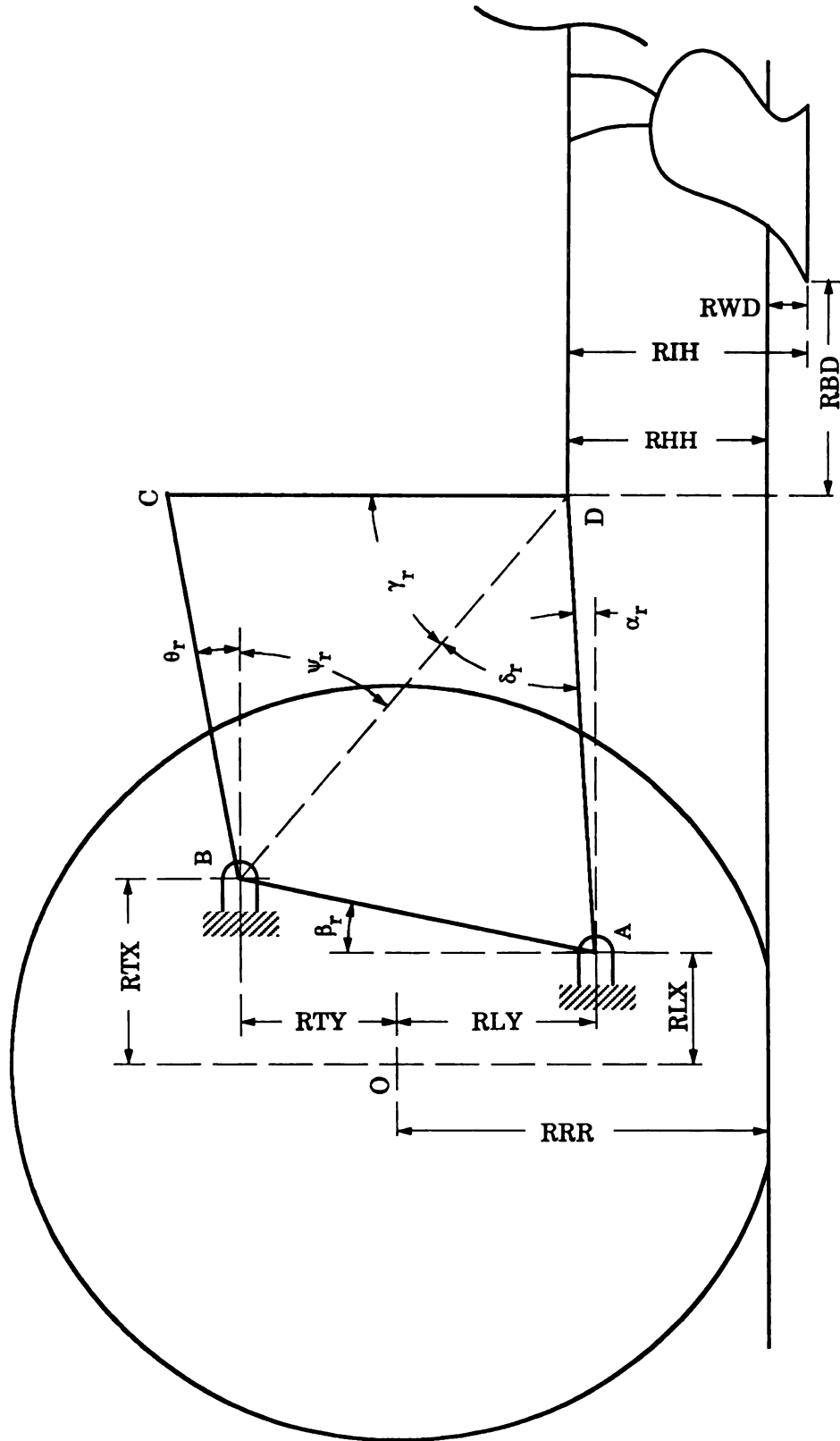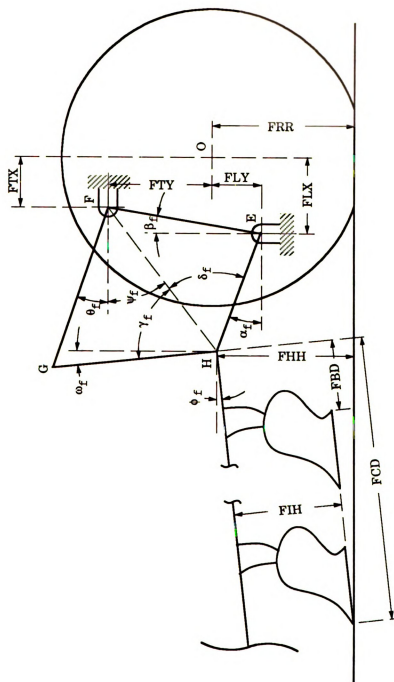Figure 4.6 - Geometry of front three-point hitch, with plow in penetration position
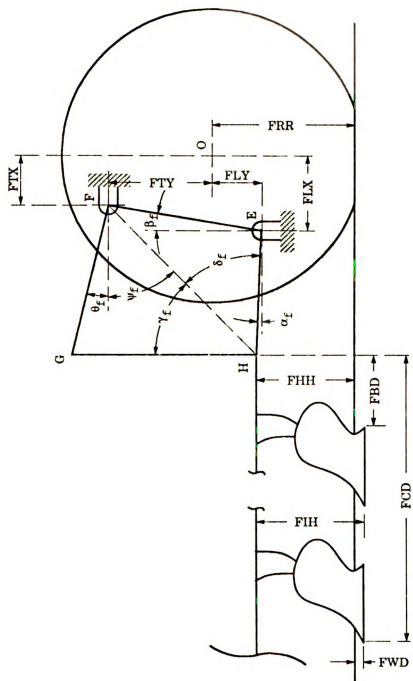
Figure 4.7 - Geometry of front three-point hitch, with plow in working position

From Figure 4.5 the following equations can be obtained.

$$\alpha_f = \sin^{-1}\left\{\frac{FHH - (FRR - FLY)}{EH}\right\} \tag{4.9}$$

$$\beta_f = \tan^{-1}\left\{\frac{FLX - FTX}{FLY + FTY}\right\} \tag{4.10}$$

where:

α_f = front lower link angle relative to soil surface, degrees

FHH   = perpendicular distance from front hitch point to soil surface, cm

FRR   = front wheel rolling radius, cm

FLY   = vertical distance from front axle center line to front lower link point, cm

EH   = effective length of front lower link as shown in Figure 4.4, cm

β_f = the angle formed by a line connecting the centers of the front upper and front lower link points in relation to a vertical line through the lower link point, degrees

FLX   = horizontal distance from front axle center line to front lower link point, cm

FTX   = horizontal distance from front axle center line to front upper link point, cm

FTY   = vertical distance from front axle center line to front upper link point, cm

By the sign convention used in this dissertation, the angle β_f shown in Figure 4.5 is positive, and the angle α_f is also positive. The diagonal distance FH of the front three point hitch, and the angle formed by the diagonal line FH and the lower link EH, δ_f, can be calculated by analyzing the geometry of Figure 4.5.

$$FH = \sqrt{EF^2 + EH^2 - 2*EF*EH*cos(90° - \alpha_f + \beta_f)} \qquad (4.11)$$

$$\delta_f = cos^{-1}\left\{\frac{FH^2 + EH^2 - EF^2}{2*FH*EH}\right\} \qquad (4.12)$$

where:

EF = distance from front lower link point to front upper link point, cm

Finally, the front implement angle, ϕ_f, and the front upper link angle, θ_f, are obtained by the following equations.

$$\gamma_f = cos^{-1}\left\{\frac{FH^2 + GH^2 - FG^2}{2*FH*GH}\right\} \qquad (4.13)$$

$$\phi_f = \omega_f = 90° + \alpha_f - \delta_f - \gamma_f \qquad (4.14)$$

$$\psi_f = 90° - \gamma_f - \omega_f \qquad (4.15)$$

$$\theta_f = cos^{-1}\left\{\frac{FG^2 + FH^2 - GH^2}{2*FG*FH}\right\} - \psi_f \qquad (4.16)$$

where:

γ_f = angle between front diagonal line and front implement mast, degrees

FG = front upper link length, cm

GH = front implement mast height, cm

ϕ_f = front implement frame angle relative to soil surface, degrees

ω_f = front implement mast angle relative to the line perpendicular to soil surface, degrees

ψ_f = front diagonal line angle relative to soil surface, degrees

θ_f = front upper link angle relative to soil surface, degrees

4.2 Analysis of chassis mechanics

The location of the center of resistance CR is fixed for a given implement at a certain working condition. The direction and magnitude of the soil resistance force also are fixed.

The Figure 4.8 shows forces acting on the rear of the tractor. With input of three forces, T_r, V_r and C_r, and the upper link pitch angle θ_r, the virtual pull point VP_r can be determined. At the same time, the direction of the soil resistance force is also determined.

For the front three-point hitch, knowing three forces, T_f, V_f and C_f, and the angle θ_f (Figure 4.9) is not enough to determine the virtual push point. However, these four inputs along with front three-point hitch geometry provide a means of calculating tractor dynamic load.

The initial model for load distribution is based on the tractor's longitudinal plane, assuming that there is no sideways roll. Analyzing Figure 4.10, an equation relating forces perpendicular to the soil surface can be obtained:

$$R_r + R_f = W * \cos\theta_g + V_r + V_f - C_r * \sin\theta_r - C_f * \sin\theta_f \qquad (4.17)$$

where:

R_r = dynamic load on rear axle, N

R_f = dynamic load on front axle, N

W = tractor weight, N

θ_g = ground slope at tractor travel direction, degrees

V_r = vertical force acting on rear lower links, N

V_f = vertical force acting on front lower links, N

C_r = axial force acting on rear upper link, N

C_f = axial force acting on front upper link, N
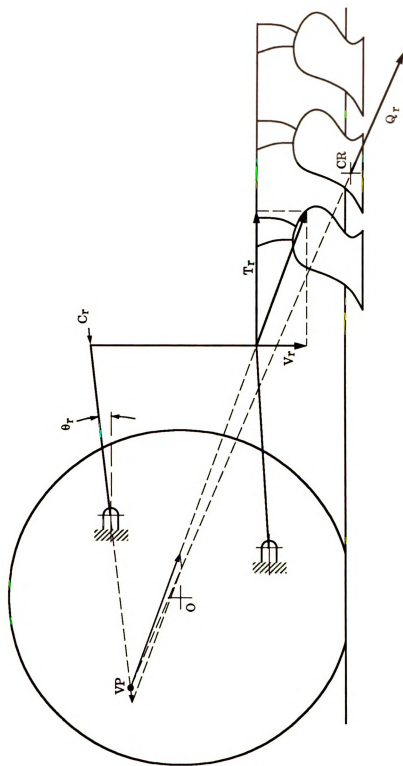
Figure 4.8 - Forces acting on the rear three-point hitch and the virtual line of pull

Figure 4.9 - Forces acting on the front three-point hitch and implement

θ_r, θ_f = as defined in Section 4.1.3 and 4.1.4, degrees

The sum of moments about point C can be obtained from Figure 4.10. The equation 4.18 is derived based on the convention that clockwise moments are positive and counter-clockwise are negative. Since the forces acting on the links were defined as positive for tensile force and negative for compressive force, the signs in the equation must agree with this definition.

$$R_f*BASE - V_f*(EH*cos\alpha_f + FLX + BASE) - T_f*FHH$$
$$- C_f*cos\theta_f*(FG*sin\theta_f + FTY + FRR) +$$
$$C_f*sin\theta_f*(FG*cos\theta_f + FTX + BASE) -$$
$$W*cos\theta_g*CGX + W*sin\theta_g*(CGY + RRR) -$$
$$C_r*sin\theta_r*(BC*cos\theta_r + RTX) + C_r*cos\theta_r*(BC*sin\theta_r$$
$$+ RTY + RRR) + T_r*RHH + V_r*(AD*cos\alpha_r + RLX)$$
$$= 0 \hspace{2cm} (4.18)$$

where:

BASE = tractor wheel base, cm

CGX = horizontal distance from the tractor's center of gravity to tractor's rear axle, cm

CGY = vertical distance from the tractor's center of gravity to tractor's rear axle, cm

The remaining symbols used in equation 4.18 are described in Sections 4.1.3 and 4.1.4.
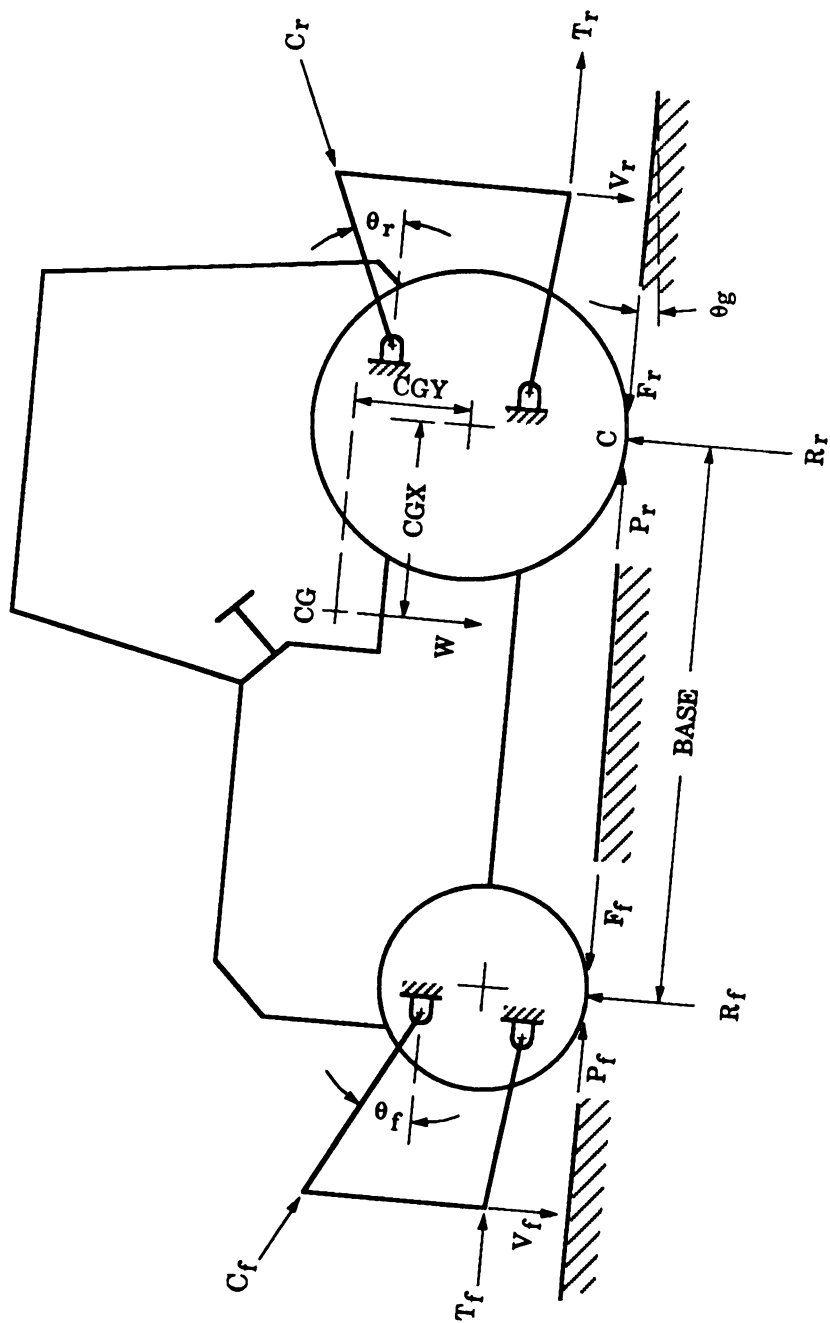
Figure 4.10 - Forces acting on the tractor

Thus, R_r and R_f can be calculated by equations 4.17 and 4.18. After the calculations, the rear axle is rotated to the actual working condition where one wheel is in the furrow, and thus is lower than the other which is on unplowed ground (Figure 4.11). The resulting load distribution to the lower and higher wheels, R_{rl} and R_{rh}, will then be calculated by equations 4.19 and 4.20. However, the front axle load is evenly divided between the two front wheels due to the action of the pivot point where the front axle is attached.
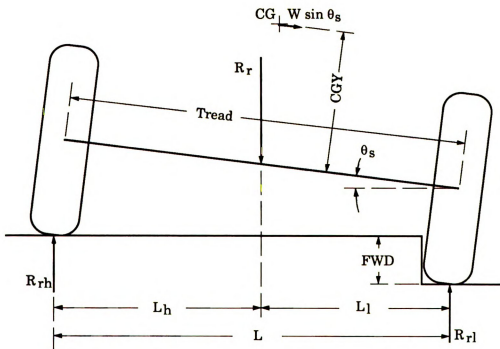
Figure 4.11 - Dynamic load distribution on tractor rear wheels

$$R_{rl} = R_r * \frac{L_h}{L} + \frac{W*\sin\theta_s*CGY}{L} \qquad (4.19)$$

$$R_{rh} = R_r * \frac{L_l}{L} - \frac{W*\sin\theta_s*CGY}{L} \qquad (4.20)$$

where:

$$L \quad = \sqrt{Tread^2 - FWD^2} \qquad (4.21)$$

$$L_h \quad = \frac{1}{2}L + \frac{RRR * FWD}{Tread} \qquad (4.22)$$

$$L_l \quad = \frac{1}{2}L - \frac{RRR * FWD}{Tread} \qquad (4.23)$$

$\theta_s \quad$ = tractor's roll angle

$$= \sin^{-1}\left\{\frac{FWD}{Tread}\right\}$$

Tread = tractor's rear wheels tread, cm

FWD = front implement working depth (Figure 4.7), cm

The optimal three-point hitch geometry should promote a certain R_r/R_f ratio in order to obtain the best tractive efficiency for an FWA tractor. If this condition is not met, the geometries of both front and rear three-point hitch should be redesigned until the optimal R_r/R_f ratio is obtained.

4.3 Predictions of performance

4.3.1 Predictions of slippage

The equations above can be used to calculate the dynamic load on the front and rear wheels for any given combination of hitch configuration and static weight distribution. Thus, the first aspect of performance, namely

slippage (s) of each wheel on a soil with a given value of cone index (CI), can be calculated for given values of pull by equation 4.24.

$$s = \frac{1}{0.3 * c_n} \ln \left\{ \frac{0.75}{0.75 - (\frac{P}{R} + \frac{1.2}{c_n} + 0.04)} \right\} \tag{4.24}$$

where:

c_n = wheel numeric, defined in Section 2.1.2

P = pull delivered by the wheel, N

R = dynamic load on the wheel, N

4.3.2 Predictions of tractive efficiency

The second aspect of performance, namely tractive efficiency (TE) for the tractor must now be calculated in a stepwise manner on a per wheel basis. Using the calculated values of slippage for each wheel from equation 4.24, an individual TE for each wheel can be calculated using equation 4.25.

$$TE = (1 - s) \left\{ 1 - \frac{\frac{1.2}{c_n} + 0.04}{0.75 (1 - e^{-0.3 \, c_n \, s})} \right\} \tag{4.25}$$

Based on the individual values of TE, the power delivered to each wheel (HP) can be calculated by equation 4.26.

$$HP = \frac{P * V}{TE} \tag{4.26}$$

where:

HP = input power to each wheel, kw

V = tractor's advance speed, m/sec

Finally a value of tractive efficiency (TE_t) for the tractor can be obtained as a quotient of the sum of the power developed by the wheels

(Σ P*V) and the sum of input powers to the wheels (Σ HP) as shown in equation 4.27.

$$TE_t = \frac{\Sigma P*V}{\Sigma HP}$$

(4.27)

5. SIMULATION MODEL

The equations described in Chapter 4, along with appropriate solution procedures and the usual input/output subroutines have been incorporated into a computer program. Appendix B shows the Pascal-like pseudo code of this program. The logic of this program is outlined in the flow charts presented in the subsequent sections. The computer code is written in such a way that the model can be used in two different modes.

5.1 Program structure and model inputs

A block diagram showing the interactions of the main subroutines is illustrated in Figure 5.1. The main routine is designed to serve as an interface between users and the model. With a main option menu shown on the computer output device (usually it is the monitor screen), the user would initiate the selection of option by typing an appropriate number. After the validation of option selected, the corresponding subroutine would be initiated.

There are six options available in the program. Three are devoted to the input, retrieval, editing, and saving of tractor and implement parameters and the field working conditions. The fourth option is used to analyze field test results and the fifth one is used for optimizing the tractor performance. The last option handles the finalization of program execution and exiting of the program.

51
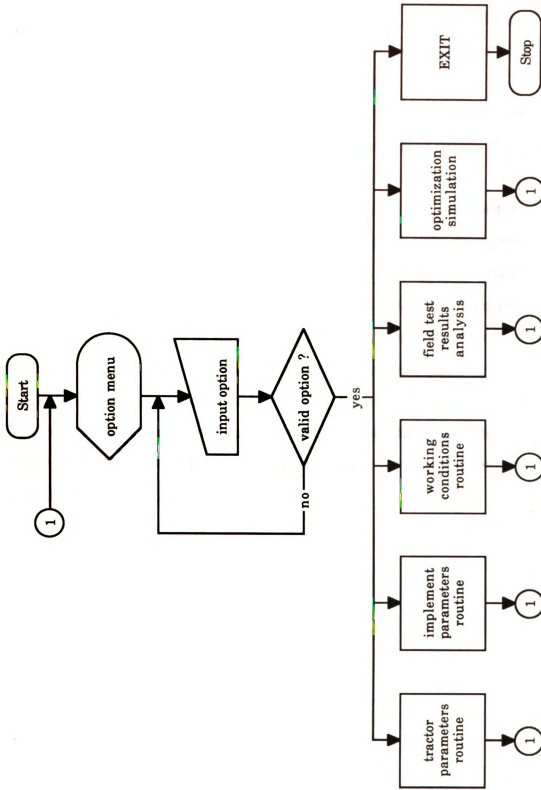
Figure 5.1 - Block diagram of simulation program

The logic for the input, retrieval, editing, and saving of the input parameters is illustrated in Figure 5.2. Since the handling of data regarding the tractor, the implements, and the working conditions have similar logic, they are presented in one flowchart.

The input parameters for either the data analysis or simulation mode can be entered into the model either as templates (Tables B.1, B.2, and B.3 in Appendix B), or as step-by-step keyboard entries in response to interactive statements presented by the program in the same order as those of the templates seen in the tables mentioned in this paragraph. The templates have an advantage that they can be set up in any text editing program (e.g. a word processor), stored as text files, and then loaded into the model from memory or disk, usually this is faster than the step-by-step keyboard entry. The stepwise keyboard entry, however, minimizes the likelihood of typographic errors, especially those which might affect the data column positions which are critical to FORTRAN data handling. In either way it is possible to change the value of a given parameter by invoking the editing subroutines.
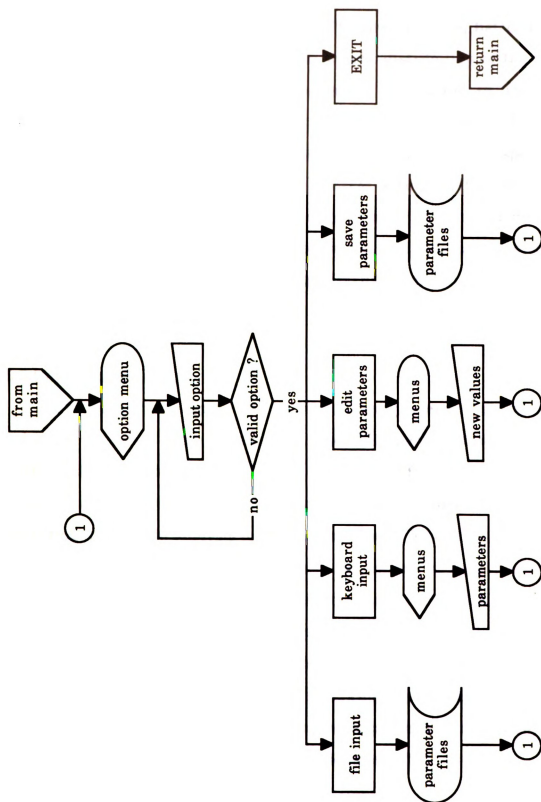
Figure 5.2 - Flow chart of parameter handling routines

The input parameters are clustered in three sets, each with its own template or keyboard entry subroutine. The first of these, listed in Table B.1, includes the dimensions and static weight distribution of the tractor and dimensions of the hitches. The second set, listed in Table B.2, represents the implement dimensions. The third set, listed in Table B.3, includes the working conditions such as working depth, ground speed, type of soil and cone index, along with the forces acting on the three point hitches. This arrangement makes it easy to enter each set of data with different combinations of tractors, implements, and working conditions in a modular fashion for analysis of experimental data and especially for simulation runs.

5.2 Data analysis mode

The computer program can be used to analyze experimental data to calculate values of some parameters, especially performance parameters such as dynamic load and TE, which would be difficult or impossible to measure with instruments. A flow chart showing the logic of the program operating in the data analysis mode is illustrated in Figure 5.3.

In this mode, one would measure the values of input parameters such as tractor dimensions, static weight distribution, hitch dimensions, implement dimensions, and soil properties. Then experiments would be conducted in which forces acting on the hitches and motion of the tractor and wheels, as well as the implement's working depth would be measured and recorded. These input parameters and experimental data would then be used to calculate the values of dynamic load and TE.
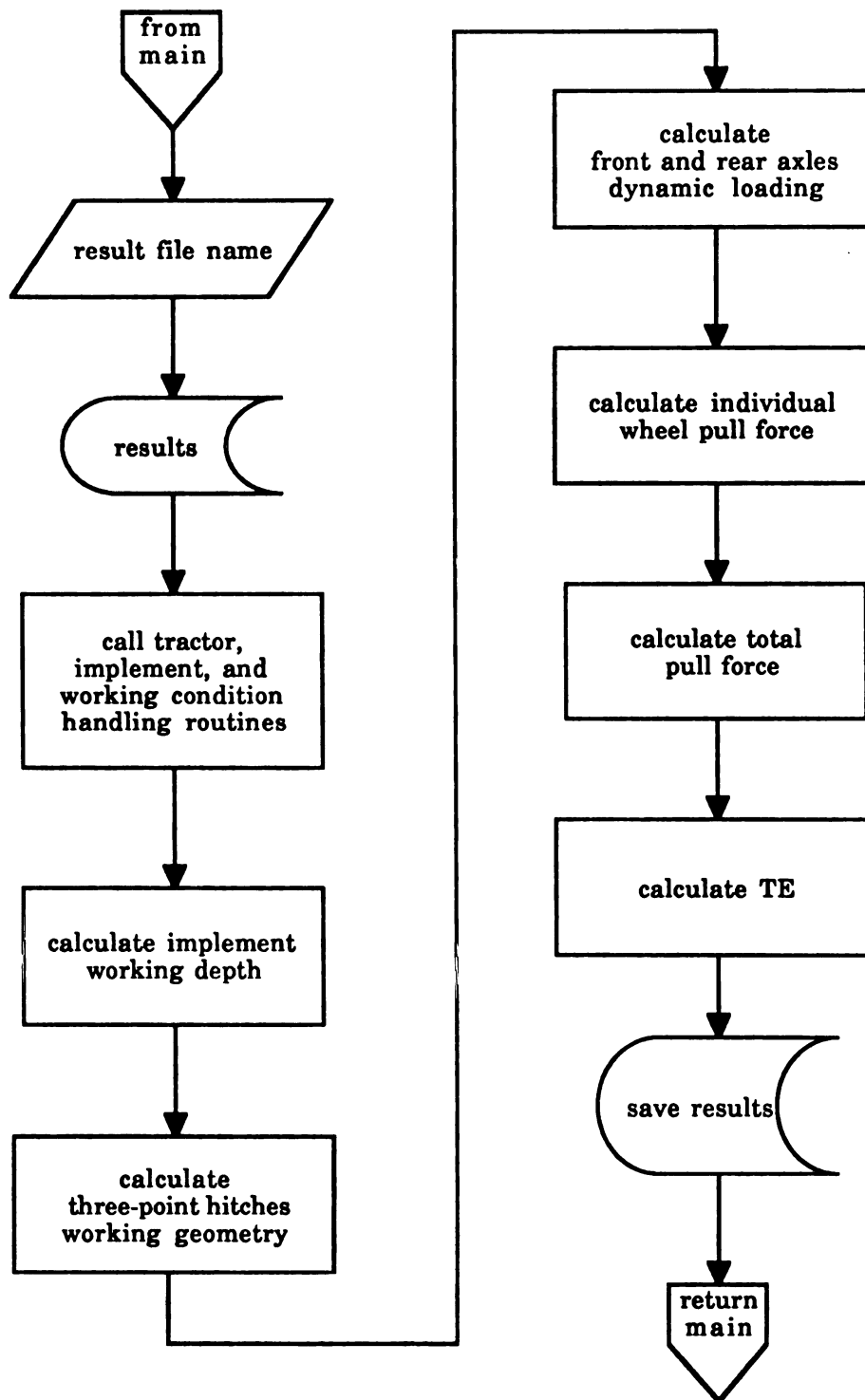
Figure 5.3 - Flow chart of the simulation program operating in the data analysis mode

5.3 Simulation mode

The model can also be used as a type of simulation or optimization model to predict the consequences of changing such parameters as dimensions of hitch components, static ballast, and implement dimensions. A flow chart showing the logic of the program operating in the simulation mode is illustrated in Figure 5.4. As in the case of the data analysis mode, one would begin by entering all of the measured tractor and implement dimensions, desired implement working depth, tractor's static ballast, along with field conditions such as ground slope.

Since experimental data are not being used in the simulation mode, one must enter a set of values for the forces acting on the hitch. Unlike the situation with drawbars where forces transferred to the tractor can be predicted from hitch position and implement pull, the interactions between an implement and a three point hitch are much more complex than the interaction when a drawbar is used. Although the resultant forces applied to a three-point hitch by an implement can be predicted using empirical equations (see ASAE Data D230.4), the analytical decomposition of force components applied to each link can not be done easily. The reason is that forces acting on each link and the center of resistance of implement are functions of three-point hitch geometry, which represents a non-linear relationship between components. Thus some experience is necessary to help the selection of appropriate values. For example, the force components used in this simulation were selected from the field test data to present three different loading modes. Once these values are entered the model will calculate front and rear upper link lengths and dynamic load on each wheel.
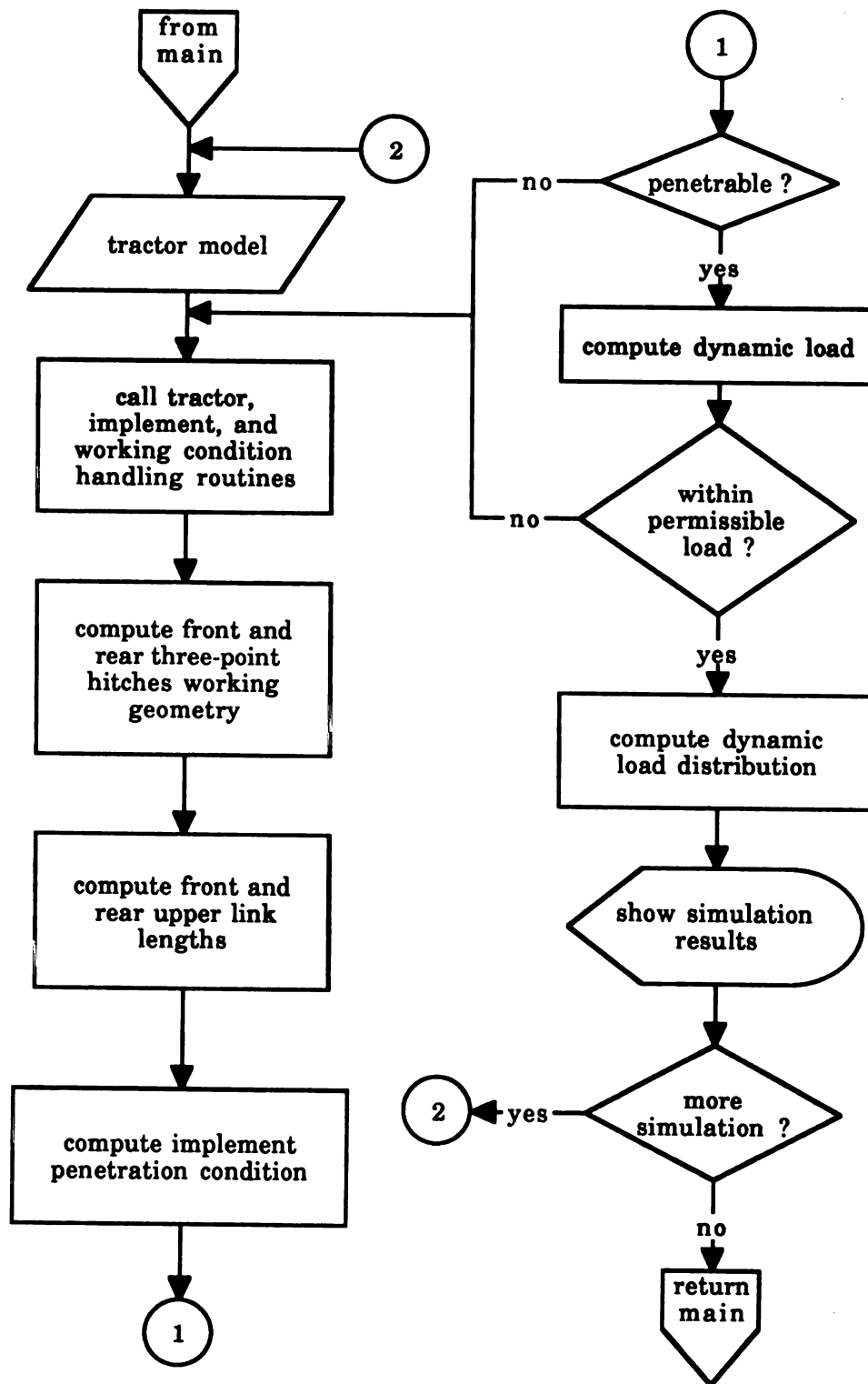
Figure 5.4 - Flow chart of the simulation program operating
in the data simulation mode

Before the simulation, a target value of dynamic load distribution ratio must be selected based on previous experience or the results from other research projects which would result in maximum TE. The calculated dynamic load distribution ratio can then be compared with this value. If the calculated dynamic load distribution ratio would not likely result in maximum TE, then a selected input parameter could be changed interactively and a new set of values of dynamic load calculated. This would be repeated until the calculated value of dynamic load distribution ratio approached the selected target value.

However, the effects of front and rear three-point hitch geometry on dynamic load distribution are not only functions of the hitch dimensions, but also functions of how the forces are applied on the hitch. It would require a great amount of knowledge about these functions to implement an algorithm to decide mathematically how the parameters should be changed during the simulation in order to approach the preset dynamic load distribution. Since the implementation of this algorithm is not possible at this moment due to insufficient knowledge about these functions, the simulation process must be done one iteration at a time and the user must make judgements about which parameter should be changed for the next iteration. Some simulation results are discussed in Chapter 7 regarding this concern. Automated simulation for optimization would be possible only after more detailed research. Also note that the model does not predict values of TE directly because there appears to be no adequate model to predict slippage from soil properties and dynamic load. When the model is used in the experimental analysis mode the values of slippage are obtained from experimental measurements of tractor and wheel motion, thus the

Equations 4.24 and 4.25 can be used to predict the values of tractor wheel pull and TE.

6. FIELD TESTS

6.1 Plowing system

An FWA tractor equipped with a conventional rear three-point hitch and a front mounted three-point hitch was used for the field tests. Two fully mounted, reversible moldboard plows were used for the experiments.

6.1.1 Tractor

The tractor used in this research was a Ford[1] agricultural tractor, model 7610, with front wheel assist. The nominal PTO power of this tractor was 64.1 kW (86 hp). In addition to a standard rear mounted three-point hitch, the test tractor came equipped with a front mounted three-point hitch. The front hitch was manufactured by Ransomes Company of England and imported to the United States. Table 6.1 shows the size of tractor tires, the tire inflation pressures used during the field tests, and the rated permissible loads at corresponding pressure published by the Tire and Rim Association (1986).

6.1.2 Implements

The implements used for the field test were two reversible moldboard plows. They were made by the same company that made the front hitch. Each plow had three bottoms with the nominal cutting width of 35.6 cm (14

---

[1]Trade names are used in this dissertation solely to provide specific information. Mention of a product name does not constitute an endorsement of the product by the author to the exclusion of other products not mentioned.

inches). The only difference between these two plows was in the mounting frame. One was designed for conventional mounting on the rear hitch of the tractor, the other was for front hitch mounting. Both frames were designed to allow addition or reduction in the number of bottoms.

Table 6.1 - Specification of tractor tires

	Tire Size	Inflation Pressure kPa (psi)	Permissible Load N (lb)
Rear	18.4-34.6, 6 ply	111 (16)	22100 (4960)
Front	13.6-24, 6 ply	152 (22)	13200 (2960)

The front plow was mounted so that its angular position could be moved, from the center line of the tractor during transport, to an offset angle toward the right or left of center for plowing. With the front gage wheel running in the previous furrow, the last bottom would leave a new furrow for the tractor wheels. The rear plow was mounted in the conventional way. With either the right or left tractor wheels running in the furrow, the front bottom of the rear plow should cut beginning from the furrow edge. Figure 6.1 shows an overview of the tractor with two plows mounted in working position.
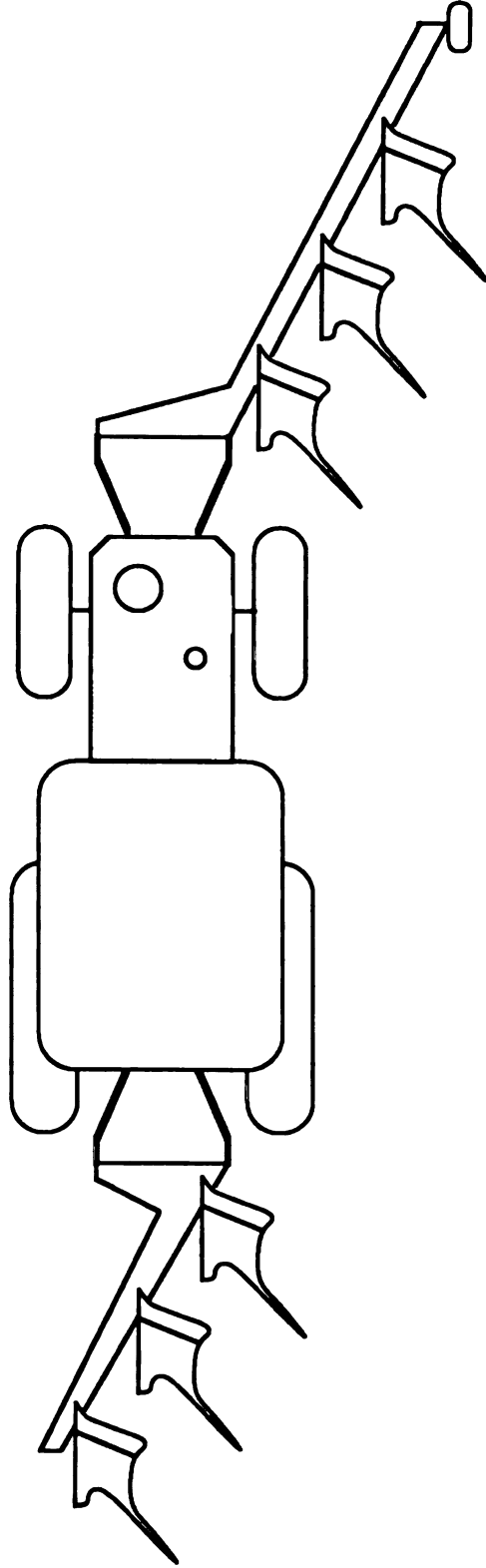
Figure 6.1 - Overview of tractor with front and rear mounted plows

6.1.3 Static weight and rolling radius

The tractor and plows were weighed on a platform scales. The tractor with front hitch and the operator weighed 44200 N (9940 lb). The rear plow with 3 bottoms weighed 10100 N (2260 lb). The front plow with 3 bottoms weighed 11600 N (2600 lb), but was reduced to 9250 N (2080 lb) when one of the bottoms was removed. Table 6.2 shows the tractor total weight and static load distribution on both axles with the three-bottom plow attached to the rear hitch and the two or three-bottom plow attached to the front hitch. Note that the removal of one bottom from the front plow drastically reduced the front axle load.

Table 6.2 - The weight distribution of tractor with plows attached

	no plows	3 front x 3 rear	2 front x 3 rear
Rear axle load, N (lb)	26900 (6040)	33200 (7460)	37300 (8380)
Front axle load, N (lb)	17300 (3900)	32000 (7200)	25600 (5760)
Total weight, N (lb)	44200 (9940)	65200 (14660)	62900 (14140)

The tractor wheels' rolling radii were measured in the field with implements and data acquisition system mounted. The plows were lowered but without cutting the soil. To prevent wheel slippage, the tractor was towed by another tractor at the lowest speed possible. The values were obtained by measuring the linear distance covered by 10 revolutions of the front and rear wheels respectively. Then the rolling radii could be calculated easily by the following equation:

$$r = \frac{L}{20\pi}$$ (6.1)

where:

r   = rolling radius, cm

L   = distance covered by 10 revolutions, cm

Table 6.3 - Tires' rolling radii, unloaded radii, and section widths

	3 front x 3 rear cm (inch)		2 front x 3 rear cm (inch)	
	Rear	Front	Rear	Front
On Land	79.5 (31.3)	57.2 (22.5)	78.5 (30.9)	57.9 (22.8)
In Furrow	76.5 (30.1)	56.6 (22.3)	75.7 (29.8)	57.2 (22.5)
Unloaded	82.7 (32.6)	60.5 (23.8)	82.7 (32.6)	60.5 (23.8)
Sect. Width	46.7 (18.4)	34.5 (13.6)	46.7 (18.4)	34.5 (13.6)

The measurement was made in two different situations: one with two wheels running in an 8-inch deep furrow, the other with the wheels running on unplowed land. The results are presented in Table 6.3 along with unloaded tire radii and section widths which were specified in the Tire and Rim Association Yearbook (1986). Note that the difference between the rolling radius of the in furrow rear wheel and that of the on land rear wheel is significant due to the weight shifting caused by the shift of tractor's center of gravity toward the furrow side. However, the front

wheels don't display this difference because of the action of pivot point where the front axle is attached. The small difference is caused by the weight of front axle and wheels.

6.2 Data acquisition system

A microcomputer based data acquisition system designed to meet Objective 3.2.2 was developed and mounted on the tractor. There were 15 sensors used on the plowing system to monitor the tractor's engine speed, ground speed, front and rear wheels rotational speed, front drive shaft torque, and forces acting on the front and rear three-point hitches. The signal from each sensor was supplied to an appropriate channel of a signal conditioner, then to one of 16 channels of an AI13 analog to digital (A/D) converter, and the digital information was then recorded by a computer as outlined below. Many components developed for this system were utilized and tested in another study in conjunction with Tembo (1986), thus details of these components were presented therein. Note that the sensors used to measure forces acting on the front three-point hitch were the same type as those used on the rear three-point hitch, thus they were calibrated by the same procedure as described in Tembo's thesis and had the same measuring accuracies. Also, the sensor used to measure the torque on the front drive shaft had the same property as the one used to measure the PTO torque by Tembo.

6.2.1 Three-point hitch dynamometer

A series of investigations was undertaken to find the best suited three-point hitch dynamometer for this research. In the past, the majority

of three-point hitch dynamometers developed by several researchers consisted of two subframes, one of which attached to the tractor and the other to the implement. The two frames were connected by a transducer capable of measuring forces between them, (Devine and Johnson, 1979; Langwisch and Frisby, 1976; Johnson and Voorhees, 1979; Kendall, et al. 1984). Although this type of dynamometer was interchangeable among different tractors, it had the disadvantage of adding additional weight to the tractor hitch if it was constructed to withstand loads from large implements. This type of dynamometer also extended the implement rearward, thus altering the tractor's operating characteristics. These disadvantages made this type of dynamometer incompatible with the main objective of this project, which was to analyze the tractor dynamic weight distribution under normal operation with rear and front mounted implements.

Hoag and Yoeger (1974) described an extended ring load cell transducer which measured a vertical and axial force. Luth et al. (1978) described the use of this transducer mounted in the lower draft links of a three-point hitch so as not to alter the original hitch geometry. Bandy et al. (1985) adapted Luth's idea and constructed a dynamometer at Texas A&M University. They cut off the original lower links. An adapter bracket was welded to each link. An extended ring load cell was bolted to each bracket and the original telescoping link from each lower link was welded to the load cell. This dynamometer had the advantage of maintaining the original three-point hitch geometry, as long as we assumed that the alignment of link and bracket was perfect after welding. However, the interchangeability of this dynamometer was limited to those tractors with equal dimensions at the lower links.

In order not to alter the original hitch geometry, the ability to interchange between different tractors had to be sacrificed. Thus, the above type of dynamometer was selected for this research. To simplify the construction process and to avoid any inaccuracy in fabrication, it was decided that the strain gages would be applied directly to the original lower links.

6.2.2 Strain gages - application and cautions

The surfaces of the telescoping parts of the lower links of the rear three-point hitch were milled so that the adjacent faces were perpendicular to each other and the opposite faces were parallel to each other. Because the telescoping link system was not a symmetrical, straight beam, the neutral axis could not be determined geometrically. A stress coating was used to determine the neutral axis.

The upper link had one set of strain gages, and each lower link had two sets of strain gages. Each set had four strain gages forming a full Wheatstone bridge. The advantages of full bridges are higher sensitivity and guaranteed temperature compensation. However, the lead wires must have the same length so that no error is caused by the difference in the wire resistance.

One Wheatstone bridge on each lower link was set to measure the force parallel to the center line of the tractor. The other bridge on each lower link was used to measure the force perpendicular to the link. There was one Wheatstone bridge on the rear upper link to measure the axial force. Signals from these 5 Wheatstone bridges were passed through

appropriate channels of the signal conditioner to channels 1 - 5 of the AI13 A/D converter.

The front upper link had the same configuration and single Wheatstone bridge as the rear upper link. The front lower links were bolted to a rigid frame which could move vertically by the activation of a hydraulic cylinder but could not move laterally. The two links were machined to have parallel surfaces. Two full Wheatstone bridges were attached to each link to function the same as those on the rear links. Signals from the front 5 bridges were conditioned and supplied to channels 10 - 14 of the AI13 A/D converter.

6.2.3 Torquemeter on the front wheel drive shaft

A set of four strain gauges forming a single Wheatstone bridge on the front wheel drive shaft were connected to a combined voltage to frequency (V/F) converter and FM transmitter which, along with rechargeable batteries, were embedded in an aluminum ring on the drive shaft. The FM receiver and frequency to voltage (F/V) converter were mounted inside the tractor cab where the voltage output of the F/V converter was connected to channel 15 of the AI13 A/D converter.

6.2.4 Other sensors

Other sensors, some of which utilized signals from a Dickey john Tractor Performance Monitor II (DjTPMII, described in detail in Tembo, 1986), are summarized as follows where Channel numbers refer to specific channels of the AI13 A/D converter as shown in Figure 6.2.

70
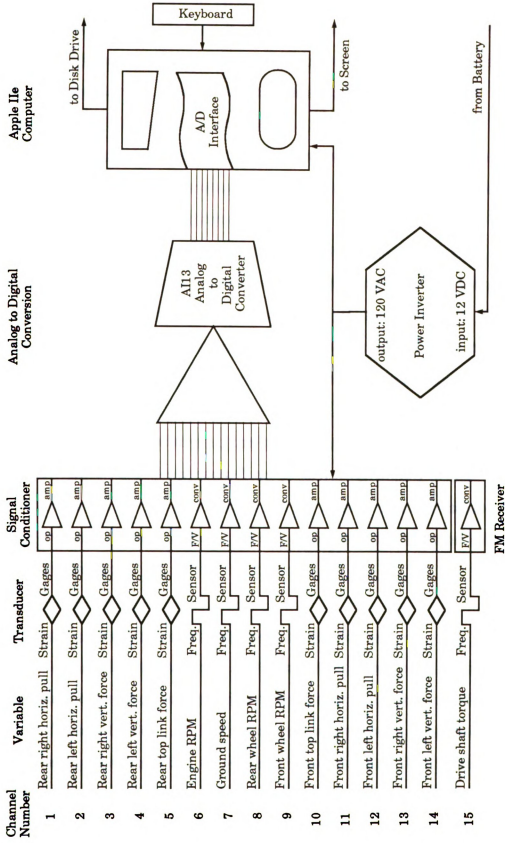
Figure 6.2- Configuration of data acquisition system hardware

Channel Number	Variable	Transducer	Signal Conditioner	Analog to Digital Conversion	Apple IIe Computer
1	Rear right horiz. pull	Strain Gages	op amp		
2	Rear left horiz. pull	Strain Gages	op amp		
3	Rear right vert. force	Strain Gages	op amp		
4	Rear left vert. force	Strain Gages	op amp		
5	Rear top link force	Strain Gages	op amp		
6	Engine RPM	Freq. Sensor	F/V conv		
7	Ground speed	Freq. Sensor	F/V conv		
8	Rear wheel RPM	Freq. Sensor	F/V conv		
9	Front wheel RPM	Freq. Sensor	F/V conv		
10	Front top link force	Strain Gages	op amp		
11	Front right horiz. pull	Strain Gages	op amp		
12	Front left horiz. pull	Strain Gages	op amp		
13	Front right vert. force	Strain Gages	op amp		
14	Front left vert. force	Strain Gages	op amp		
15	Drive shaft torque	Freq. Sensor	F/V conv		

Keyboard

to Disk Drive

to Screen

A/D Interface

AI13 Analog to Digital Converter

Power Inverter
output: 120 VAC
input: 12 VDC

from Battery

FM Receiver

Engine speed in revolutions per minute (RPM) [Channel 6] was obtained from the frequency signal generated by the DjTPMII RPM sensor fitted between the existing mechanical drive sender and the tachometer cable. The signal was processed through an M1080, 10KHz F/V converter and was read by the AI13 A/D converter.

Ground speed, [Channel 7] was obtained from signals generated by the DjTPMII radar unit, processed through an M1080 F/V converter, and also read on the AI13 A/D converter.

To measure front and rear wheel angular velocities (RPM), sprockets were mounted on the axle hubs just inside the right front and right rear wheels. Cylindrical pole piece magnetic pickups (Wabash Inc.) were mounted on brackets and positioned near the periphery of each sprocket. The brackets were very rigid to avoid variations in the distance between the magnetic pickups and the sprockets, and thus minimize noise in the signals. As the wheels turned, the passing of the sprocket teeth and gaps past the magnetic pickup caused an alternating signal whose frequency was proportional to the wheel RPM. These signals were processed through M1080 F/V converters, and the voltage supplied to Channels 8 & 9 of the AI13 A/D converter.

6.2.5 Signal processing, computer, and power source

The signal conditioner, A/D converter, computer, battery power source, and their mounting inside the tractor cab are described in more detail by Tembo (1986). An FM telemetry receiver was added to the system to receive signals from the torquemeter (see 6.2.3). One important point was that each component was chosen to meet the objectives of system

flexibility, documentation, high volume and high speed data storage, durability, and compactness. Because of the ruggedness of the units chosen only moderate precautions regarding enclosure (a plastic film around the Apple II computer) and vibration resistant mounting (e.g. foam plastic padding in wooden box) in the tractor cab was necessary. Special care was taken to provide a stable source of electrical power during operation. This was accomplished by using a high quality 12VDC-120VAC, 60HZ, 500 watt sinusoidal voltage converter powered from a 12VDC free-floating ground battery, disconnected from the tractor charging system during operation. This precaution of disconnecting the battery prevented the possibility of electrical spikes or noise (e.g. from engine RPM fluctuations) from reaching the data acquisition system. More importantly it also prevented the possibility of current leakage from the transducers to the tractor ground. Also, during tractor operation, all data was stored in the RAM memory of the computer, thus avoiding possible errors and damage in the disk drives (see section 6.4 below).

6.3 Sensor calibration

6.3.1 Three-point hitch dynamometer

Details of procedures to calibrate the Wheatstone bridges on the three point hitches are given in Tembo (1986), however several key points are summarized here. As illustrated in Figure 6.3a the horizontal load was applied to each link (i.e. front & back, upper & lower) by a hydraulic cylinder which was carefully aligned so that the force was applied parallel with the tractor center line to simulate the longitudinal draft. The output of

each axial Wheatstone bridge was then correlated to that of a Chatillon HCL hydraulic tensiometer (John Chatillon and Sons). Because the links are not exactly symmetrical nor straight some vertical forces may be generated, and because there is a cross-bar between the right and left lower links some forces may be transferred across to the opposite link. Thus, output from the axial sensor of the opposing link and from the vertical sensors of both the loaded and opposite links were also recorded to evaluate these "cross signals".

When vertical loads were generated in each of the lower links by the test tractor's hydraulic system, the angle of the link was not necessarily exactly horizontal (see Figure 6.3b). Thus, the link angle with respect to horizontal was recorded along with the outputs of the axial and vertical sensors and the Chatillon tensiometer. Again, the axial and vertical sensor "cross signals" from the opposing link were also recorded. An additional precaution was exercised with the front lower links which were bolted to a frame that induced stress in the links. After calibration, the bolts were not tightened or loosened since this would alter the induced stresses.

The possibility of "cross signals" being generated by lateral or side forces was tested, and were found to be negligible.

1 - Loading hydraulic cylinder
2 - Hydraulic hoses
3 - Hydraulic dynamometer
4 - Dynamometer dial
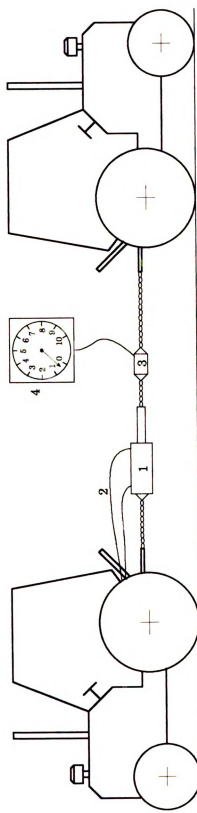
(a)
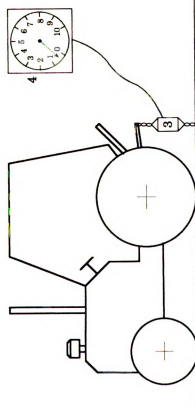
(b)

Figure 6.3 - Strain gages calibration set up: a) simulating the horizontal forces b) simulating the vertical forces

6.3.2 Torquemeter

One end of the tractor drive shaft (approximately 210 cm long) was fixed in a vice, and the other end was supported on a stand with a free turning roller perpendicular to the shaft. The surface of the roller was smooth and hard, thus the friction between the shaft and support was considered negligible. A 91 cm long torque arm was fastened to the free end of the shaft, a series of weights was added. and the output of the torquemeter was recorded. Also, as each weight was added the angle of the torque arm changed slightly, so the angle of the arm with respect to a horizontal line through the center of the shaft was measured in order to calculate the effective arm length and true applied torque.

6.3.3 Other sensors

The primary signals for engine RPM, ground speed, and wheel RPM were in the form of frequencies which, especially in the case of the RPM measurements, were based on mechanical action and thus not in need of calibration. However, each of the F/V converters was calibrated by supplying known frequencies from an accurate signal generator, and measuring the voltage output of the converter.

6.4 Computer software

6.4.1 Data collection program

The data collection program, developed for an Apple IIe microcomputer, was designed to occupy as little memory as possible since the data were stored temporarily in RAM memory during each

experimental run of the tractor. It was important not to use the disk drive during tractor operation to avoid the introduction of noise, data loss, and possible damage to the drive because of mechanical vibration.

The program was also user friendly, and informative, so that the operator knew what the computer was doing at each step. At the beginning of each run the operator could enter the number of data sets to be collected and the interval at which the computer would query the AI13 A/D converter, ranging from 0.05 ms to 1 s. When the tractor reached steady state operation during an experimental run the operator could initiate the data collection procedure with a single keystroke. After each experimental run the program was continued by the operator to verify the data and thus the functionality of the sensors before the data were recorded on a floppy disk. The 12-bit digital data were stored as an ASCII file in order to provide transferability to other computers for analysis.

6.4.2 Data processing program

Data from the field experiments were processed in two steps. First, the data (still in 12-bit digital form) were transferred from disks through an Apple IIe connected directly to a Macintosh computer by a BASIC program written specifically for this purpose. A second program written in FORTRAN 77, with proposed FORTRAN 8x extensions was used to convert the 12-bit digital data into real numbers representing the voltages sent from the signal conditioner to the AI13 A/D converter. These voltage values were then converted by the appropriate calibration equations to represent the parameter measured by each sensor. These parameter values then were

stored on disks for later analysis and interpretation by the simulation model.

The steps in these data transfer and analyses are represented in the following flowchart. (Figure 6.4)

6.5 Field operation

All of the tests were conducted on the Michigan State University farms for two seasons. The field used during the first season (1986 Summer) consisted of a sandy soil with an average cone index of 45 N/cm^2, ranging from 38 to 70. The field used during the second season (1987 Summer) consisted of silty-clay soil with an average cone index of 90 N/cm^2, ranging from 70 to 176. Cone index was randomly sampled in 30 locations in that area of each field where several runs were to be conducted. Moisture content, measured in random samples from the second field, ranged from 7% to 12%, dry base. Both fields were relatively flat with average slopes (longitudinal and lateral to the plowing runs) averaging no more than 1°, with occasional longitudinal slopes up to 4° during portions of some runs.
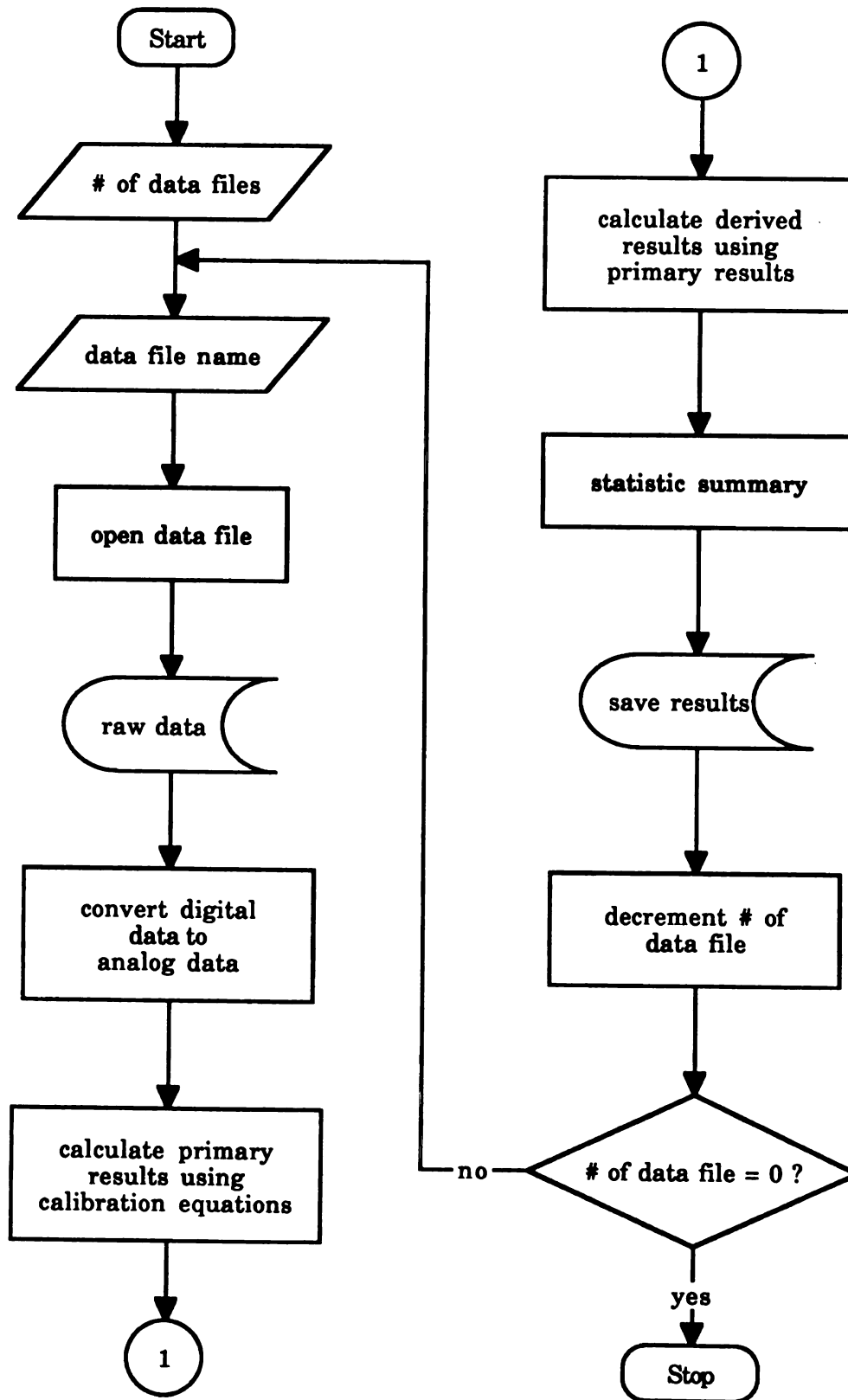
Figure 6.4 - Flow chart for the field data analysis program

In addition to the fifteen variables monitored by the data acquisition system, the tillage depth and width of the front and rear plows were measured after each run, along with pitch angles of the tractor and six links. Tillage depth for the rear plow was determined at three positions along the length of the run, by placing a level on the surface of unplowed ground adjacent to the furrow, and measuring the distance from the lower side of the level to the bottom of the furrow (Figure 6.5). Because the rear plow cuts and covers the furrow formed by the front plow, tillage depth for the front plow could be determined only in that portion of the front furrow which remained between the front and rear plows when the tractor was stopped. Tillage width at three positions along the plowing run was determined as the distance from the new edge of plowed ground to three respective pre-set stakes minus the distances of the previous run (Figure 6.5).

The field tests were designed to measure the effect of varying ground speed, different soil conditions, different combinations of front and rear plow bottom numbers, and the impact of upper link length on the implement's draft, power requirements, and overall field performance. The parameters were varied in the following order:

1) four different ground speeds with other conditions fixed

2) three front bottoms versus two front bottoms

3) different rear and front upper link lengths, in order to obtain different tensile or compressive forces in the upper link

A total of 36 tests for the 1986 season and 24 tests for the 1987 season were conducted. Plow adjustment and hitch geometry, except rear and front upper link lengths, were kept constant.
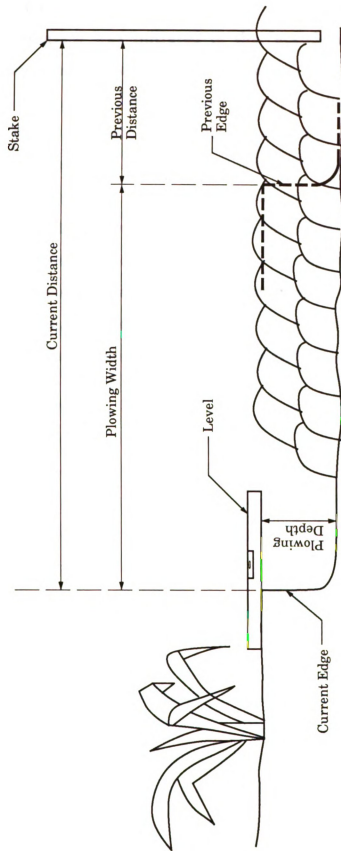
Figure 6.5 - Measurement of plowing width and depth

coll
plov
cond
prog
a to
data
oper
oper
sign
quic
disk
then

At the beginning of each run, with the tractor in position, the data collection program was initiated to the "stand-by" condition, then the plowing run was started. When the tractor's forward speed and plowing conditions were steady, the data collection procedure was executed. The program was set to collect all 15 channels of data at 0.1 second intervals for a total of 500 data sets, thus 50 seconds of plowing time. During the run, data were stored only in the RAM memory of the computer to avoid operating the disk drive while the tractor vibration might disturb its operation. When the data collection was completed, the operator was signaled by the monitor and the tractor was stopped. The data could then be quickly checked, channel by channel on the monitor, and then stored on disk. The measurements of tillage parameters, as described above, were then taken.

7.

th

ch

th

ar

pe

TE

equ

val

calc

load

depe

on a

7.1.1

mea

a st

7. RESULTS AND DISCUSSION

7.1 Special considerations regarding the results of field experiments

Before reporting and interpreting the results of field experiments in this study, it is useful to summarize certain points established in previous chapters. First, the review of published literature (Chapter 2) indicated that the relationships between dynamic load distribution, slippage, pull, and TE are very important in comparisons or optimization of tractor performance.

Second, two of these parameters (i.e. dynamic load distribution and TE) must be calculated stepwise on a per-wheel basis from appropriate equations (Section 4.2). During the course of these calculations, individual values at each wheel for dynamic load, pull, TE, and horsepower, must be calculated using measured values of tractor and hitch dimensions, static load, forces acting on the hitches, tractor speed, wheel numeric (which depends in part on soil cone index), and slip.

Third, the tractor's wheel motion was not measured simultaneously on all wheels during each experiment as discussed below.

7.1.1 Soil cone index and other soil properties

Measurement of cone index was conducted in a manner that several measurements of cone index were made to a depth of 15 cm (6 inches) with a standard instrument at random positions in the test area of each field.

Th

va

the

assu
vari
calcu
any

inst
reac
imp
reac
the
CI n
for
dep

The average values, standard deviations, maximum values, and minimum values are shown in Table 7.1.

Table 7.1 - Average, standard deviation, and range of cone index measurements. (See also Section 6.5)

	Average	Std. Dev.	Maximum	Minimum
Sandy Soil	45	10.5	70	38
Silty-Clay	90	33.1	176	70

Note: 30 values of cone index were collected for each type of soil

There are several possible consequences of both the variability and the method of these measurements.

First, the cone index used in the calculations for each run was assumed to be the average value for the whole field. Considering the variability of these measurements in different parts of the field the calculations involving the wheel numeric (e.g. Equations. 4.21 and 4.22) for any given run could be considerably different from the actual conditions.

Second, the maximum value of force during penetration of the instrument was recorded, regardless of whether that maximum was reached at the top, middle, or bottom of the 6 inches stroke. A general impression during these measurements was that maximum force was reached toward the bottom of the stroke in the sandy soil, but near the top of the stroke in the silty soil which was somewhat crusted. Thus the value of CI may have been correct for wheels on the silty soil surface, but overvalued for wheels on the sandy surface. However, since the front plow cut to a depth of approximately 8 inches, the cone index of the soil under wheels in

the

un

of

Se

7.1

wh

the

slip

rad

incl

and

dyn

appl

esti

the c

the s

surfa

patte

meas

How

test

the furrow might have been overvalued for the silty furrow, and undervalued for the sandy furrow. A sensitivity analysis of possible effects of these variations and assumptions regarding cone index will be shown in Section 7.1.4.

7.1.2 Slippage measurements and estimations

Wheel motion was measured only on the right front and right rear wheels as described in Section 6.2.4, and the amount of slippage in each of these two wheels was calculated using Equation 2.4. The amount of slippage in each left wheel was calculated as an inverse function of rolling radii of these wheels. The geometric inputs (including the lateral inclination resulting from the wheels on one side running in the furrow) and force transfer equations of the model are believed to closely predict the dynamic load distribution. However, considering the possible problems of applying average values of cone index to the soil surface and furrow, the estimation of slippage in the left wheels, based on the measured behavior of the corresponding right wheels, is subject to question (Table 7.2).

Note that the measured slippage of the right wheels was higher on the surface of the sandy soil than in the furrow, and was lower on the surface of the silty-clay soil than in the furrow. These measured slippage patterns are consistent with the suggested variation of cone index measurements as a function of soil depth discussed in Section 7.1.1. However, this discrepancy should be canceled by the opposing runs in each test and thus in the final averages.

Ta

No

the

effe

pul

inc

int

exp

use

by

7.1

ind

Table 7.2 - Average slippage in the right (measured) and left (estimated) wheels running respectively on the soil surface and furrow during opposite direction runs.

	Right wheels (measured)		Left wheels (estimated)	Avg. slip (R+L)/2
		Sandy Soil		
Surface	0.147	Furrow	0.143	0.145
Furrow	0.132	Surface	0.136	0.134
		Silty-clay Soil		
Surface	0.116	Furrow	0.118	0.117
Furrow	0.147	Surface	0.150	0.148

Note: each test consisted of two runs, one in a direction that the right wheels running in the furrow, and the other in the opposite direction with the left wheels running in the furrow.

Fortunately, there are several ways to either minimize or evaluate the potential effects of these averaged soil properties, along with possible effects of longitudinal and lateral slope, on the calculation of slippage and pull and TE. First, these effects were minimized as much as possible by including two runs of opposite direction in each test. Secondly, certain intermediate calculations can be checked against independently obtained experimental results (e.g. Section 7.1.3). Third, sensitivity analyses can be used to evaluate the amplitude of variations in the final calculations caused by variations in any given parameter (e.g. Section 7.1.4).

7.1.3 Total pull, predicted and measured

One means of evaluating the effects of estimated slippage and/or cone index is to note that a predicted value of total pull can be obtained by

su

(E

co

S

sa

w

a

su

T.

Ri
on

Ri
in

summing the calculated horizontal force or "pull" exerted by each wheel (Equation 4.21 rearranged). This predicted value of total pull can then be compared with the total pull determined from the measured hitch forces. Such comparisons of predicted and measured pull in individual runs on sandy and silty soils are illustrated respectively in Figures 7.1 and 7.2, in which S denoted that right wheels (instrumented) are on the land surface, and F in the furrow.

The averages of the data shown in the above two figures are summarized in Table 7.3.

Table 7.3 Average of total pull as predicted from individual wheel data and as measured from hitch forces

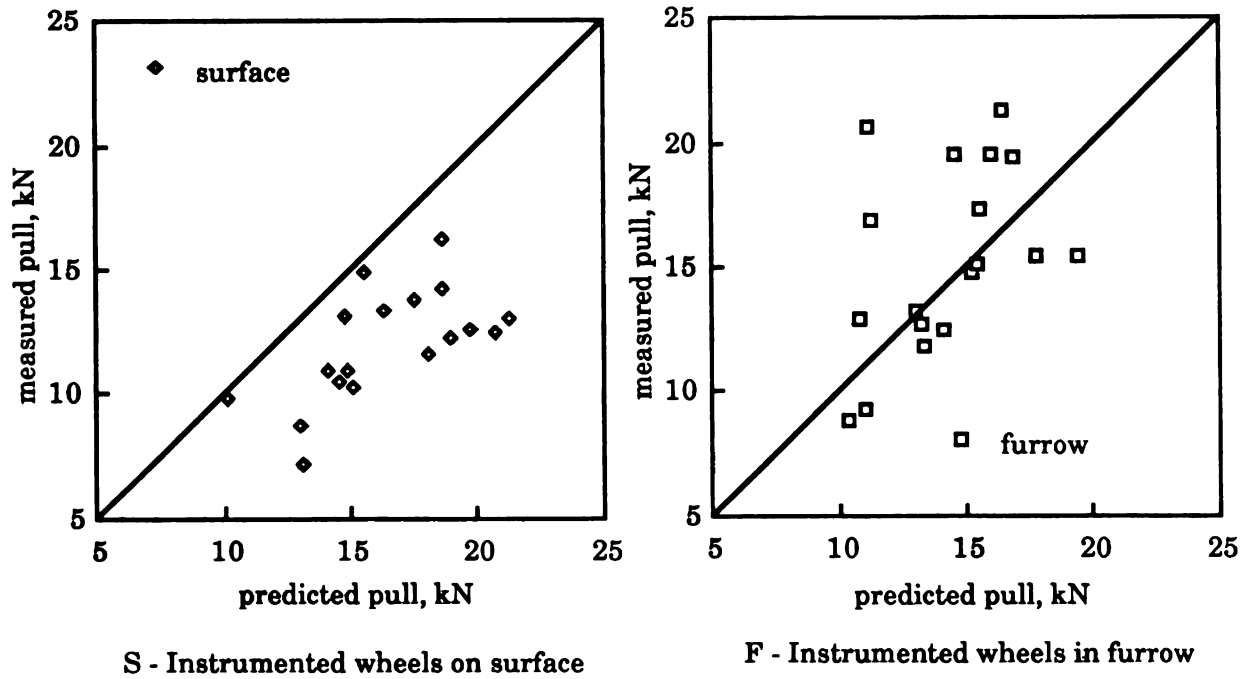|	Sandy Soil		Silty-clay Soil	
	Predicted	Measured	Predicted	Measured
Right wheels on surface	16100	12000	23500	23100
Right wheels in furrow	14400	15400	27100	20400

Figure 7.1 - Measured pull vs predicted pull in sandy soil
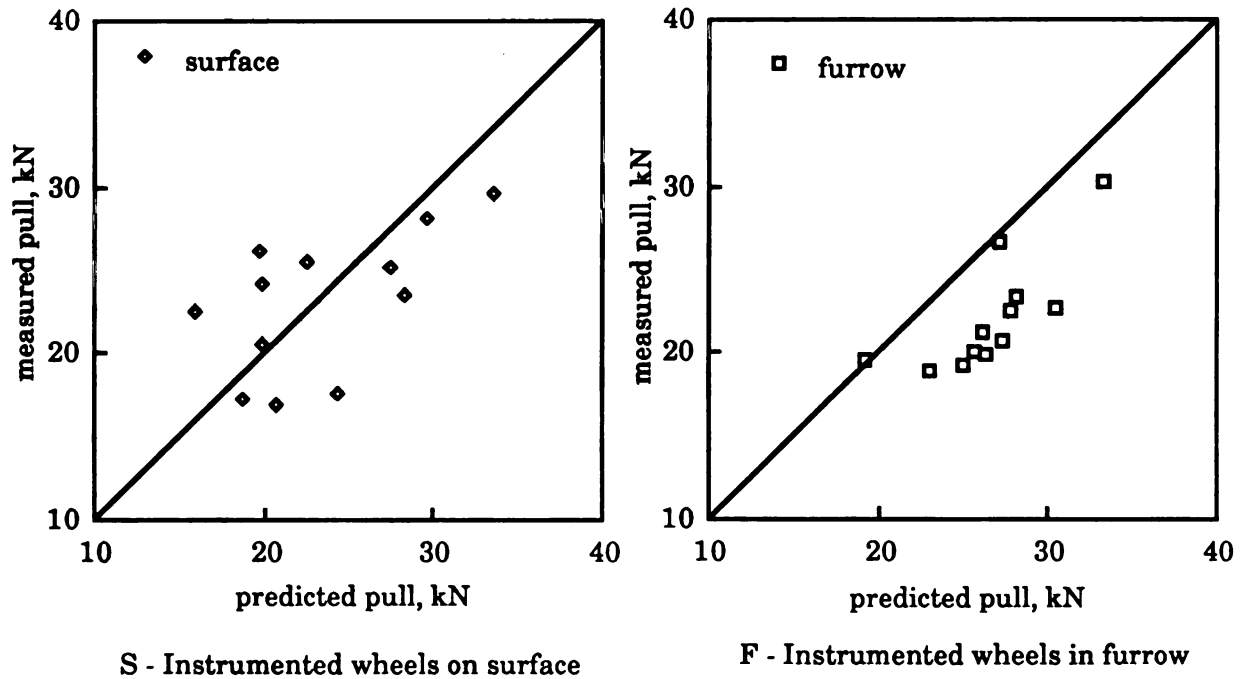

Figure 7.2 - Measured pull vs predicted pull in silty-clay soil

hig

th

th

W

m

pr

re

re

th

rig

the

cor

tha

dur

to

rel

ter

tha

op

va

lir

th

ev

In sandy soil with the right wheels on the surface, predicted pull is higher than the measured pull in nearly all runs (Fig. 7.1-S) and thus in the average (Table 7.3). This is consistent with the high values of slip, and the suggestion that cone index is lower at the surface of the sandy soil. With the right wheels in the furrow the relationship between predicted and measured pull varied from run to run (Figure 7.1-F), but the average predicted pull was nearly the same as measured pull (Table 7.3). These results are also consistent with the suggestion that the maximum force recorded during measurement of cone index occurred near the bottom of the stroke near the level of the furrow.

In silty soil the relationships of predicted and measured pull with the right wheels on the surface versus in the furrow are reversed from those of the sandy soil (Figure 7.2 and Table 7.3). Again, these results are consistent with the suggestion that cone index of the furrow is lower than that of the crusted surface of the silty-clay soil.

In both cases it should be noted that some of the measured slippage during a given run may have included brief periods when the wheels began to spin, and thus would not have been following the mathematical relationship between dynamic load, spin, and pull (i.e Equation 4.21). This tendency of wheels to spin in places where actual cone index was lower than the average would have exaggerated the apparent differences between opposite direction runs. It is less likely that this particular source of variability would have cancelled in the two runs within each test.

Given the above considerations, and the fact that slip has a non-linear effect on the calculated or predicted value of pull, it is not surprising that there remain some differences between predicted and measured pull even when the opposing runs are combined into a single value for each test

(F

so

7.

th
Fi
se
pr
ci
Cl
10

of
50
the
ran
of t
and
var
res

(Figures 7.3 and 7.4). Specifically, the predicted values continue to be somewhat higher than the measured values.

7.1.4 Sensitivity test of cone index on predicted pull

Finally, the extent to which variations of cone index, above and below the average, might influence the calculated values of pull is illustrated in Figures 7.5 and 7.6. In both cases the measured value of pull from 10 selected tests are plotted as closed diamonds, and the corresponding predicted pull based on the appropriate average CI are plotted as open circles. Then, new values of predicted pull were calculated using values of CI which were 33% lower (open squares), 50% greater (closed squares), and 100% greater (open diamonds) than the average CI.

Note that the standard deviation, maximum, minimum, and range of the actual CI measurements (see Table 7.1) were similar to the 33% to 50% variations used in this sensitivity test. Thus the observed variations in the relationship between predicted and measured pull are well within the range that might be expected based on the variability of CI within the areas of the field tests. Nevertheless, problems in the variability of CI in test fields and its effects on slip and pull are common to many other studies (e.g. see variations in pull with time in Figure 7 of Shell & Fox, 1986). Thus, the results of this study should be comparable to others.

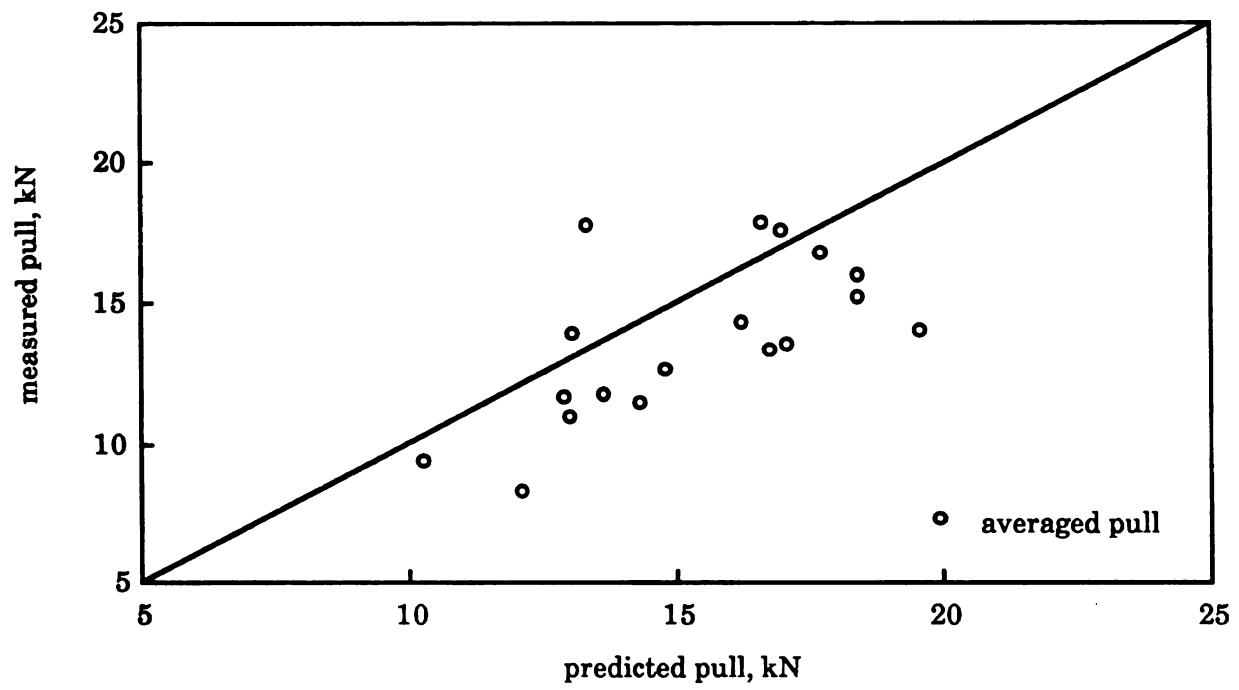measured pull, kN

measured pull, kN

Figure 7.3 - Averaged, measured pull vs predicted pull in sandy soil
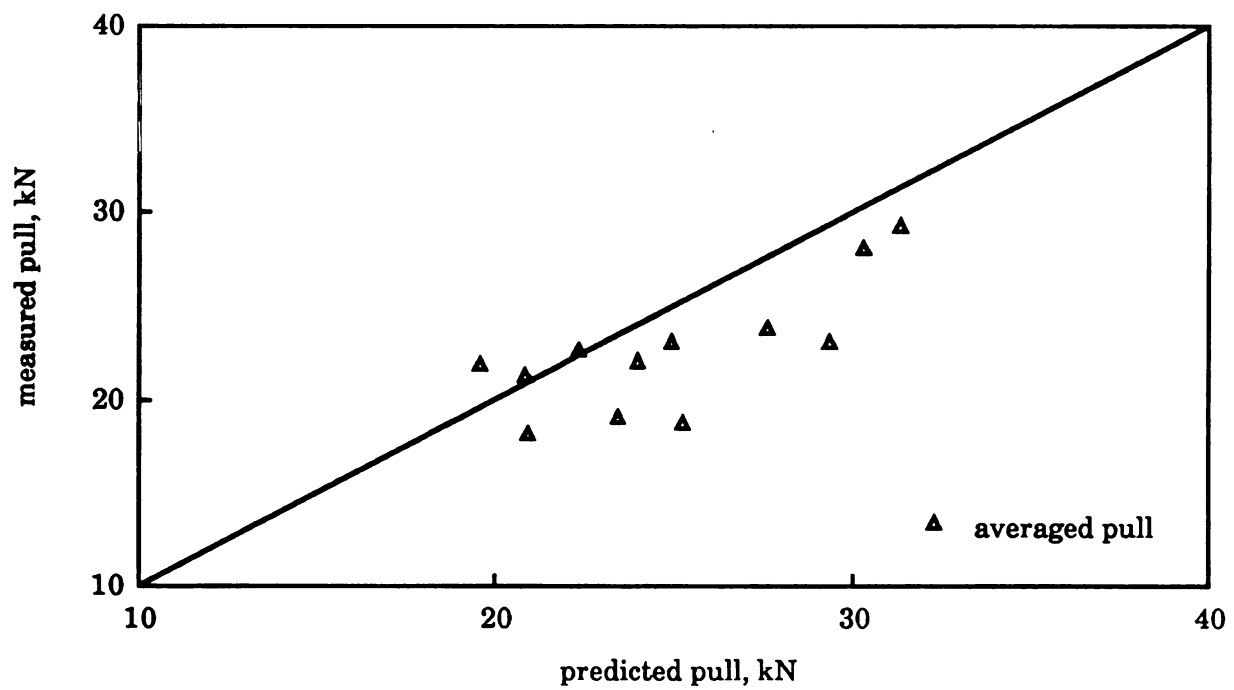
Figure 7.4 - Averaged, measured pull vs predicted pull in silty-clay soil
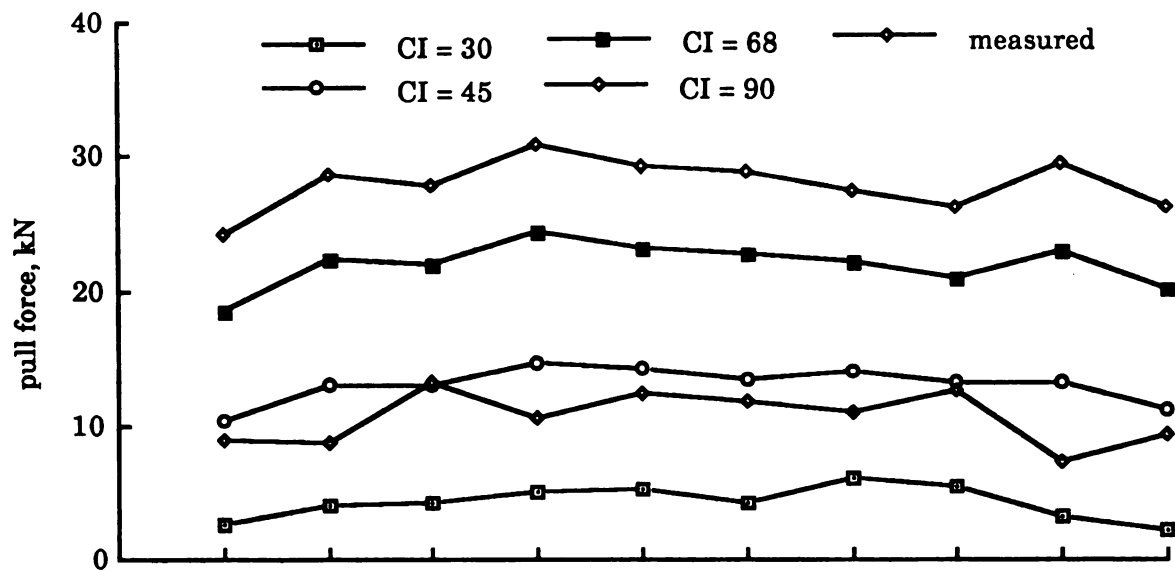
Figure 7.5 - Sensitivity test of CI on predicted pull in sandy soil
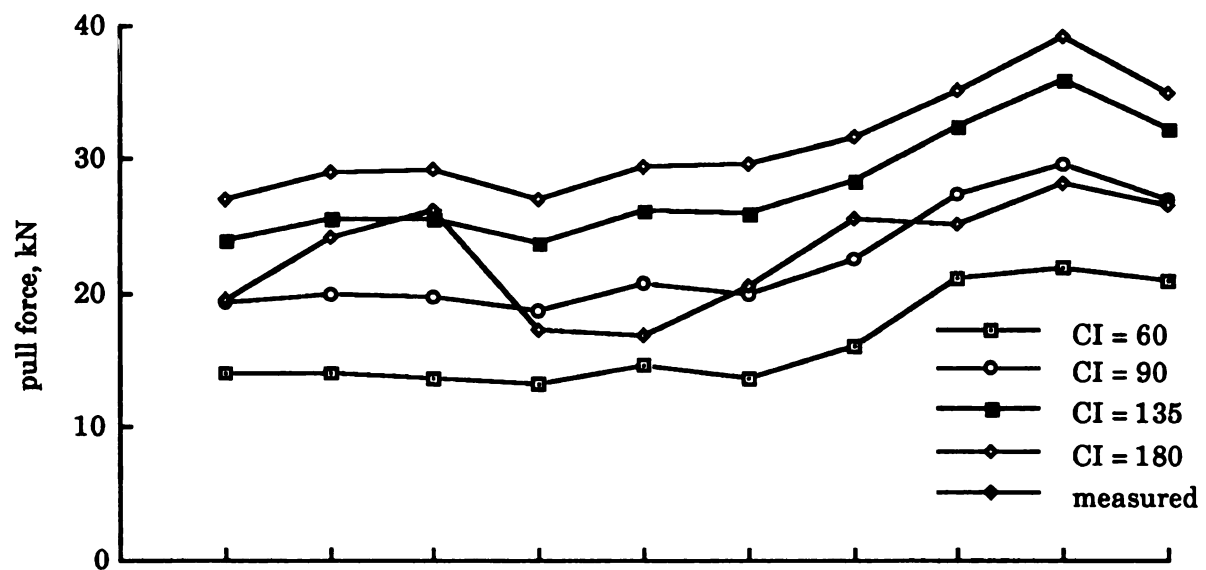
Figure 7.6 - Sensitivity test of CI on predicted pull in silty-clay soil

c

7

f

v

r

t

f

s

r

r

re

p

7.

7.

ind

Fig

res

stu

19

19

Figures 7.7 and 7.8 illustrate the influence of cone index on the calculated values of pull. The values of predicted pull used to plot Figures 7.3 and 7.4 were calculated by the use of averaged cone index for both in-furrow and on-surface wheels. However, different values of cone index were used for each wheel while calculating the values of predicted pull in preparation of Figures 7.7 and 7.8. The criterion of variation was based on the discussion presented in Section 7.1.1. In sandy soil, the cone index used for in-furrow wheels was the average measured value (i.e. 45), while on-surface wheels used a smaller cone index (i.e. 30). On the other hand, the measured cone index (i.e. 90) was used for on-surface wheels and the reduced value (i.e. 60) was used for in-furrow wheels in silty-clay soil. The results show that the modification has brought the values of the predicted pull closer to those of the measured pull.

7.2 Comparison of field results with other studies

7.2.1 Relationship between total (average) slip and total pull

Total or average slippage in all types of tractors increases with increased pull. This relationship in the present study is illustrated in Figures 7.9 and 7.10 on sandy and silty-clay soils respectively. These results are of the same magnitude and slope as those reported in other studies of 4WD or FWA tractors (e.g. Meuller & Freer 1986, Wismer & Luth 1972), and have comparable or even less variability (e.g. Wismer & Luth 1972, Bashford, 1984).
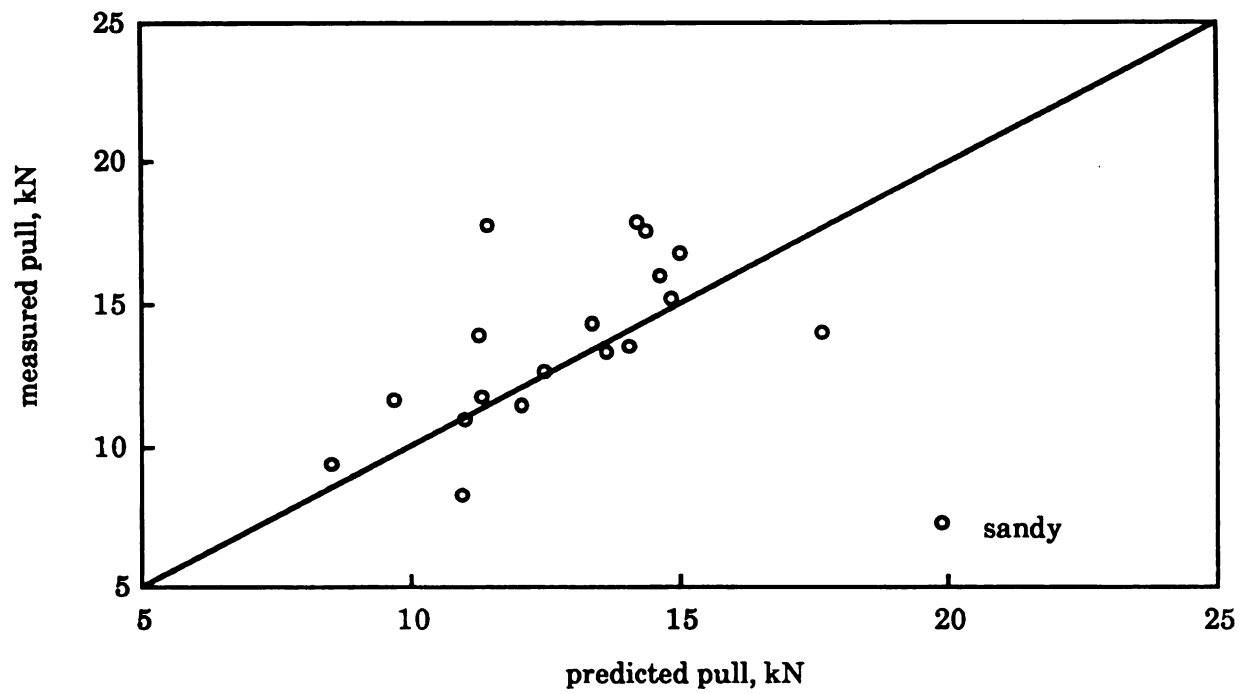
Figure 7.7 - Pull Prediction using variable cone index in sandy soil
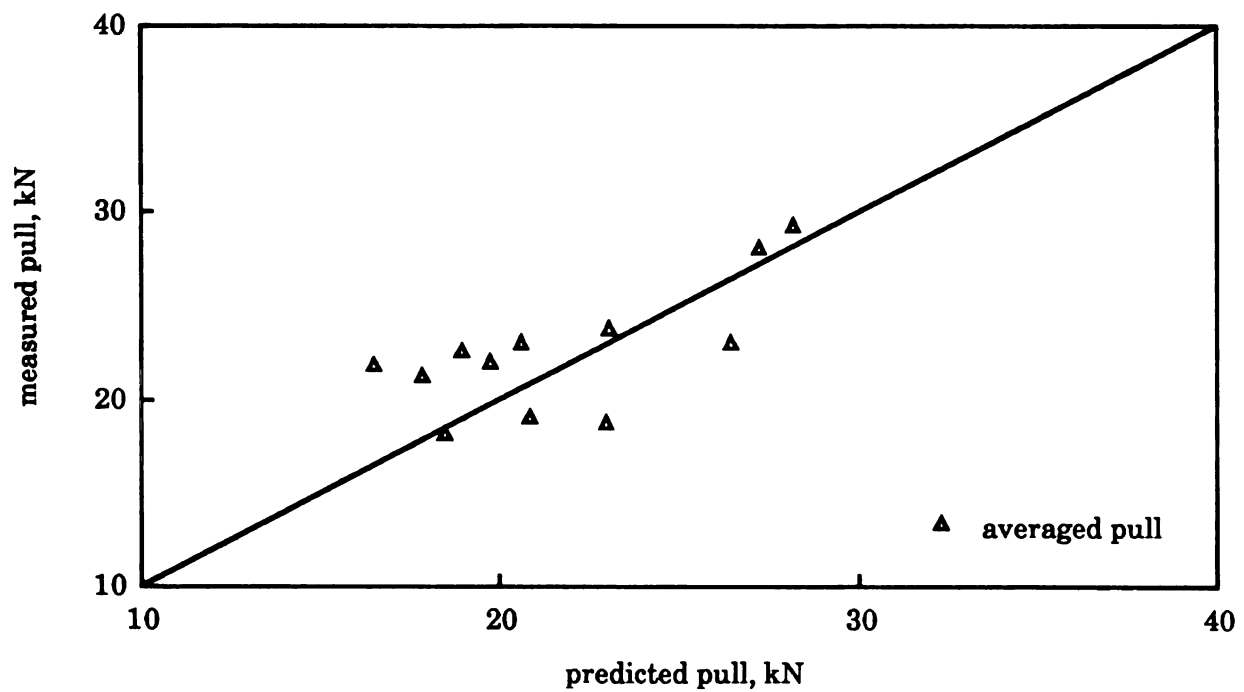
Figure 7.8 - Pull prediction using variable cone index in silty-clay soil
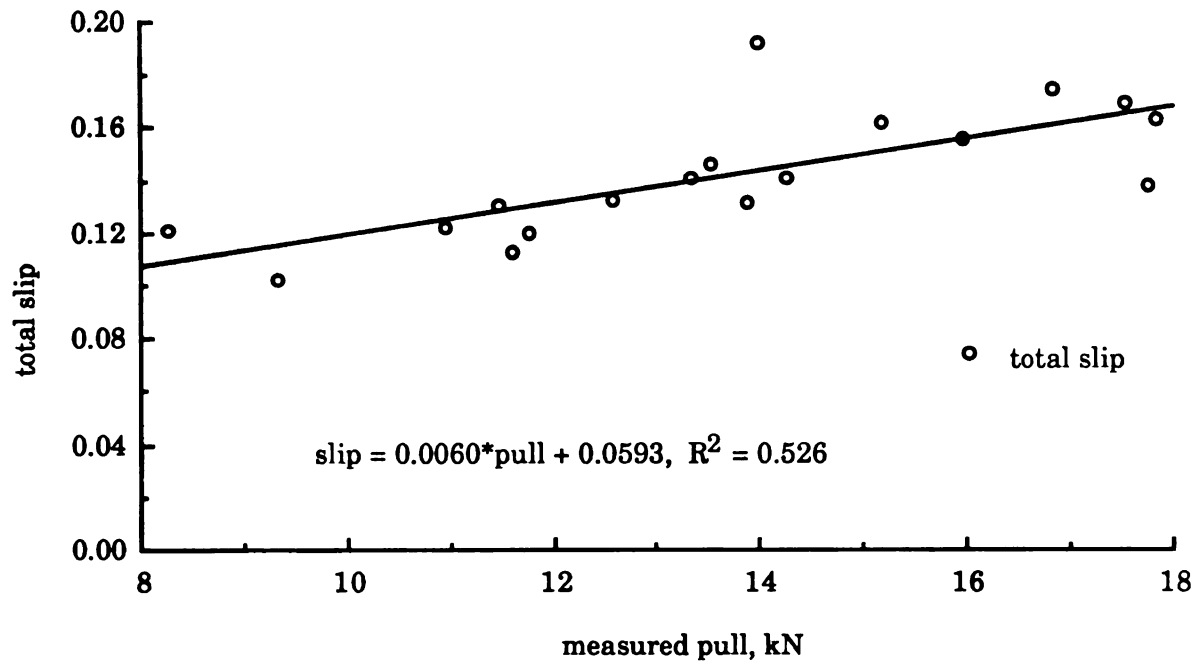
Figure 7.9 - Averaged slip vs measured pull in sandy soil
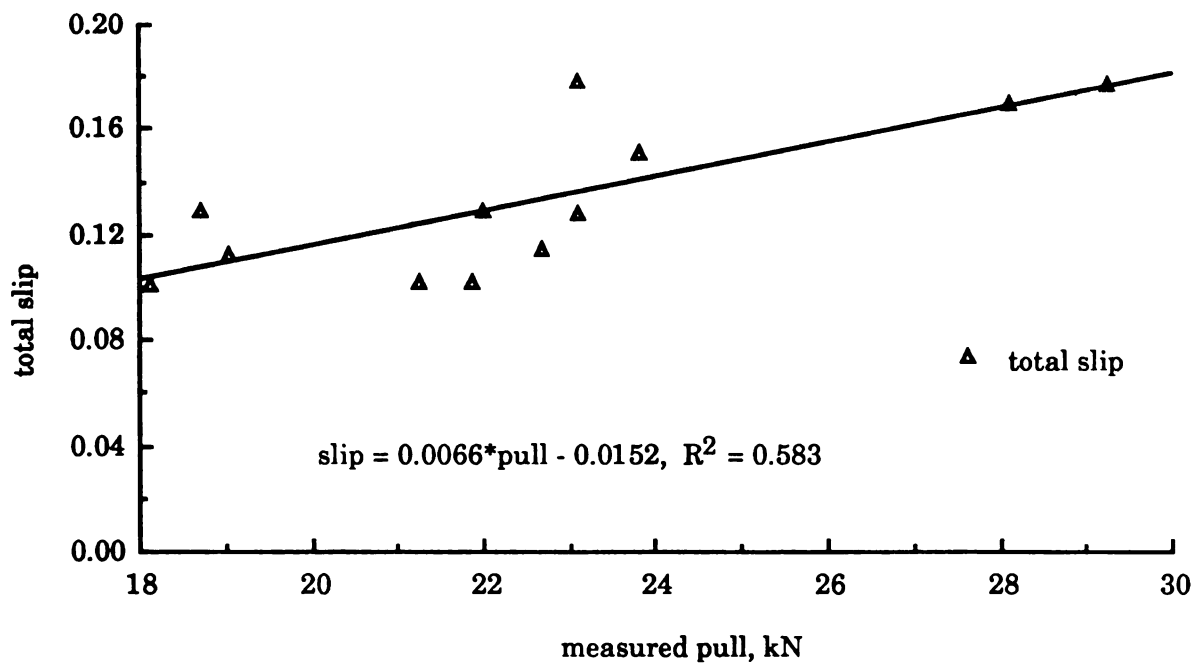
Figure 7.10 - Averaged slip vs measured pull in silty-clay soil

7

p
c
r
s

f
f
f
c
a
s
w
re

ei
ob
ro

tr
ir
s
p

7.2.2 Relationships between dynamic load ratio, slippage, and TE

A major objective of this study was to determine the extent to which performance of an FWA tractor with front and rear implements could be optimized by adjustments affecting dynamic load distribution ratio. The relationships of slippage and TE with dynamic load distribution ratio on sandy and silty-clay soils are illustrated respectively in Figures 7.11 and 7.12.

In the case of the sandy soil there was little change in slip as a function of front load ratio, however, TE increased from about 0.52 to 0.68 as front load ratio increased from 0.2 to 0.4. This magnitude of optimal TE at a front dynamic load ratio of 0.4 in FWA tractors, especially on loose soils, is consistent with essentially all of the published studies. Although no attempt to measure or calculate rolling resistance is being made in this study, it is possible that the 0.4/0.6 f/r load ratio results the best distribution within this experiment's range, and thus a reduction in total rolling resistance and an increase in TE.

In the case of the silty-clay soil there appears to be little change in either slippage or TE. Again, this is consistent with other published observations, and may result because there is less opportunity to minimize rolling resistance on firmer soils.

Finally, the apparent limited opportunity for optimization in this tractor system (i.e. ± 15%) is not surprising since similar values were found in other studies. Furthermore, the front/rear implement system may act to stabilize the tractor (i.e. prevent oscillations) and thus improve performance in the field.
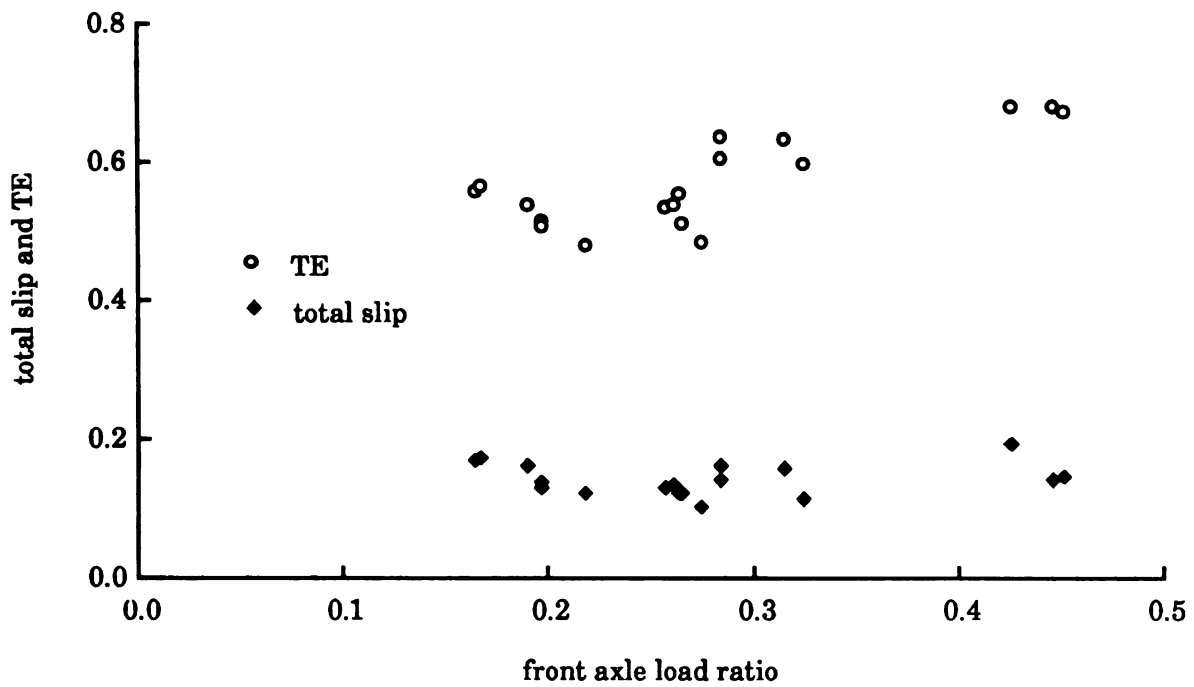
Figure 7.11 - Averaged slip and TE vs front axle load ratio in sandy soil
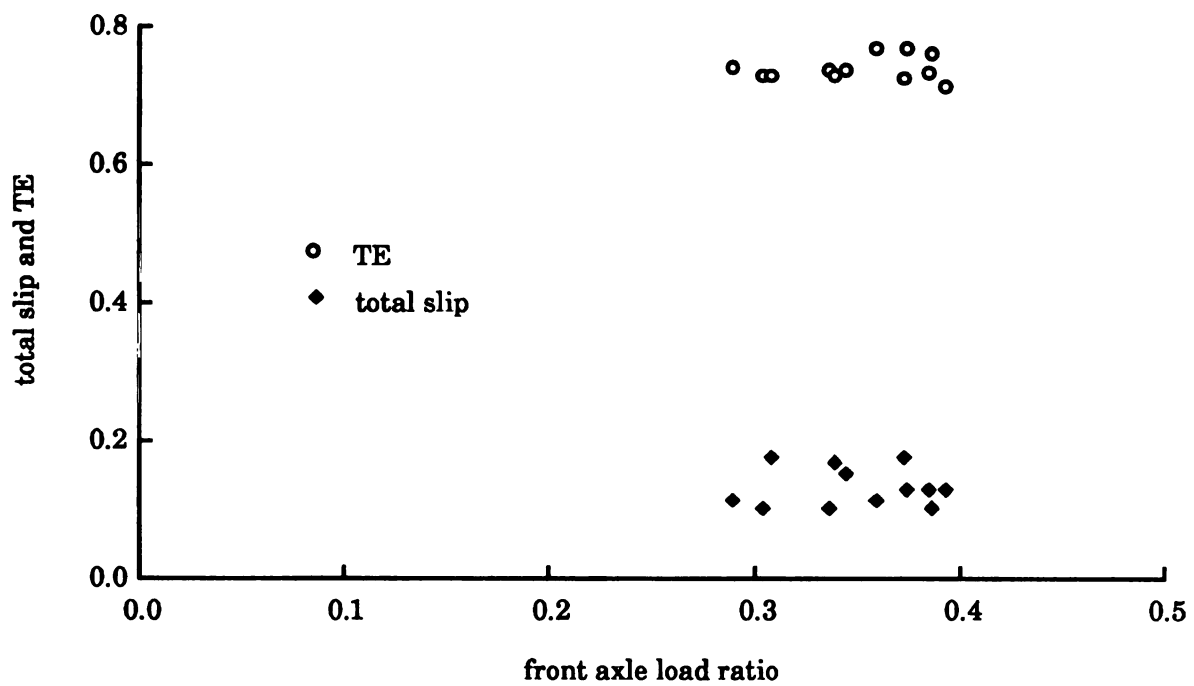
Figure 7.12 - Averaged slip and TE vs front axle load ratio in silty-clay soil

7.3

pr

me

di

va

fo

an

th

tra

we

ot

ru

re

ei

co

co

hi

pa

1.

te

s

y

h

7.3 Simulation results

Throughout all of the published studies, and to some extent in the present study, the f/r load distribution has been emphasized as a possible means of optimizing tractor performance. The exact value of f/r load distribution for optimal tractor performance is not known, and clearly varies from one set of working conditions to another. Therefore the following simulations are aimed only toward determining the sensitivity and trends of f/r load ratios resulting from the varied parameters, rather than attempting to optimize TE or other aspects of tractor performance.

In the following simulations many of the input parameters (i.e tractor and implement dimensions and weights and working conditions) were similar to those used in the field studies. However, since implements other than plows might be used in other field studies, the simulations were run with three different sets of values for the forces acting on the front and rear three-point hitches. These three sets of forces were chosen to generate either tension loading, neutral loading (i.e. almost no loading), or compression loading on the upper links. Then with each set of loading conditions, simulations were conducted by varying the value of a selected hitch dimension, implement dimension, or tractor ballast. Each selected parameter was varied in seven increments; namely, 0.7, 0.8, 0.9, 1.0, 1.1, 1.2, and 1.3 times the original value of that parameter used in the field tests. All other parameters were held constant during the seven simulations at each of the three loading conditions.

The hitch dimensions to be varied in the simulations were the X- and Y-coordinates of the lower and the upper link points of the front and rear hitches, the front and rear lower link length. The implement dimensions

to

ba

7

t.

lo

v

a

e

m

is

va

ha

lin

in

co

ch

hi

to be varied were the front and rear mast heights. The front and rear wheel ballasts of the tractor were also varied.

7.3.1 Effects of hitch dimensions

The first set of simulations was designed to determine the effects of the lower link point X-coordinates of the front and rear hitches on the f/r load ratio (reported as front axle load ratio). In each case, increasing the value of X moves the lower link point away from the tractor. Figures 7.13 and 7.14 illustrate that this parameter in the rear hitch has little or no effect (Fig 7.14), while increased values in the front hitch greatly increase, moderately increase, or slightly decrease f/r load ratio when the upper link is in tension, neutral, or compression loads respectively.

The second set of simulations (Figures 7.15 and 7.16) illustrates that varying the lower link point Y-coordinate of either the front or rear hitches has little or no effect on f/r load ratio.

The third set of simulations indicates that varying the front upper link point X-coordinate moderately decreases, has no effect, or moderately increases f/r ratio when the upper link is in tension, neutral, or compression loads respectively (Figure 7.17). Nevertheless the effect of changing this parameter in the rear hitch is opposite to that of the front hitch (Figure 7.18).

Figure 7.13 - Front axle load ratio vs front lower link point X-coordinate

Figure 7.14 - Front axle load ratio vs rear lower link point X-coordinate
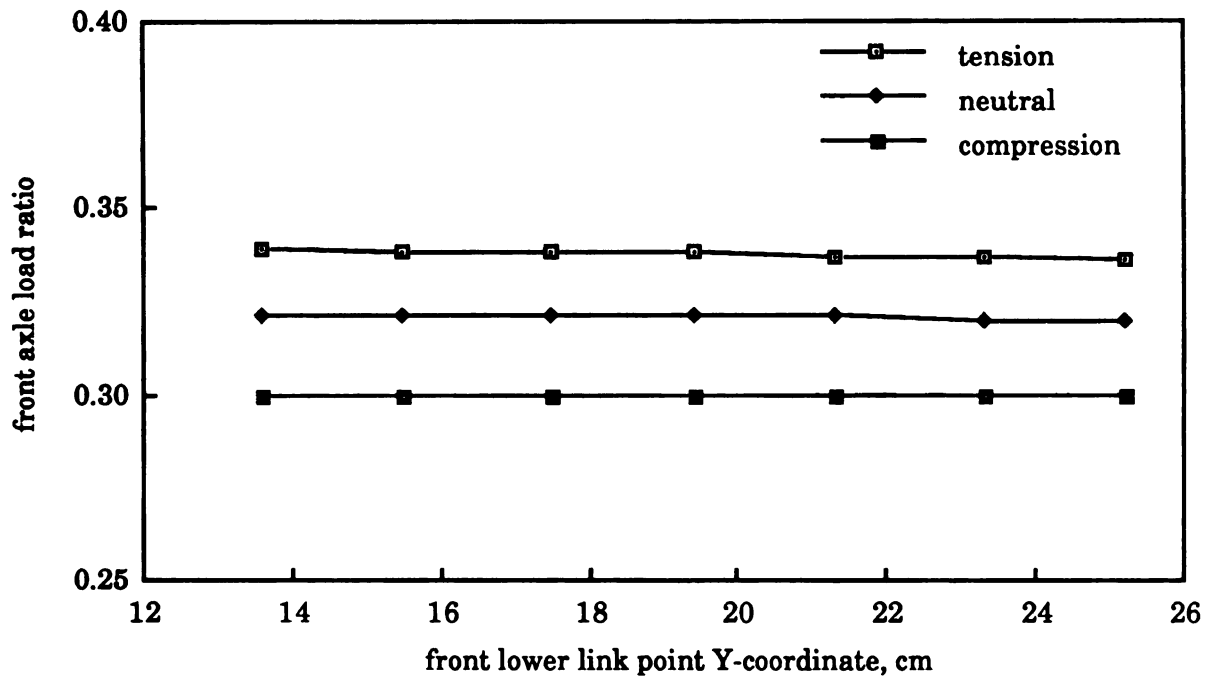
Figure 7.15 - Front axle load ratio vs front lower link point Y-coordinate
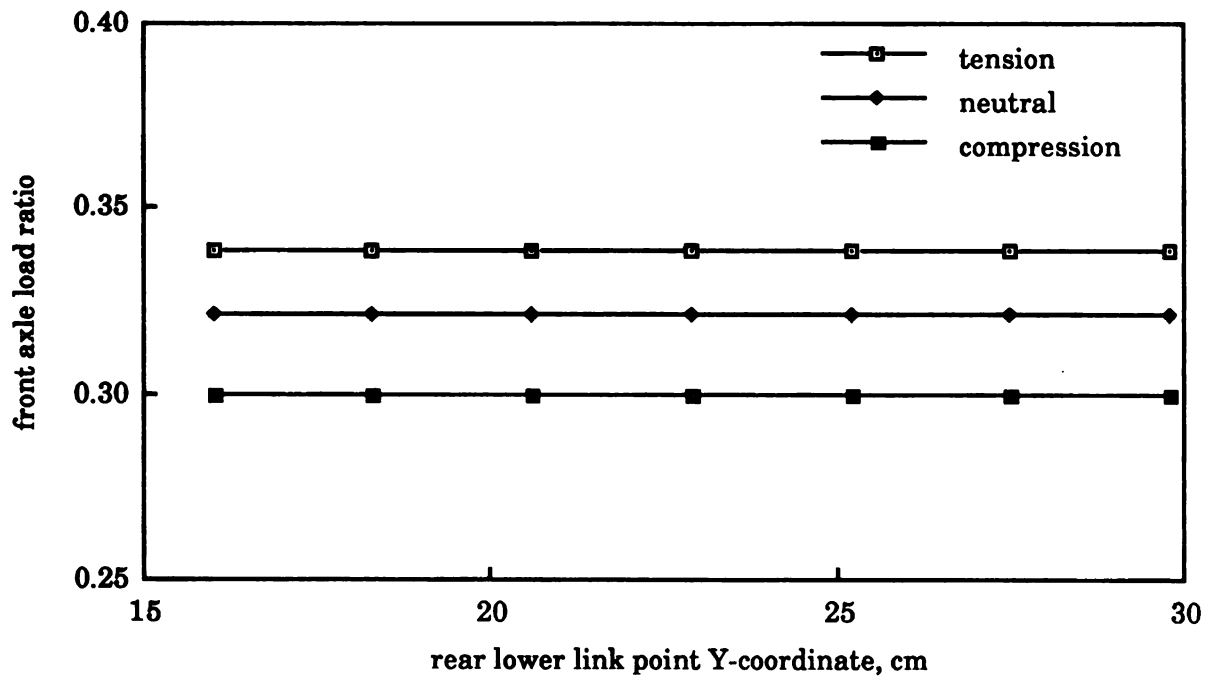
Figure 7.16 - Front axle load ratio vs rear lower link point Y-coordinate
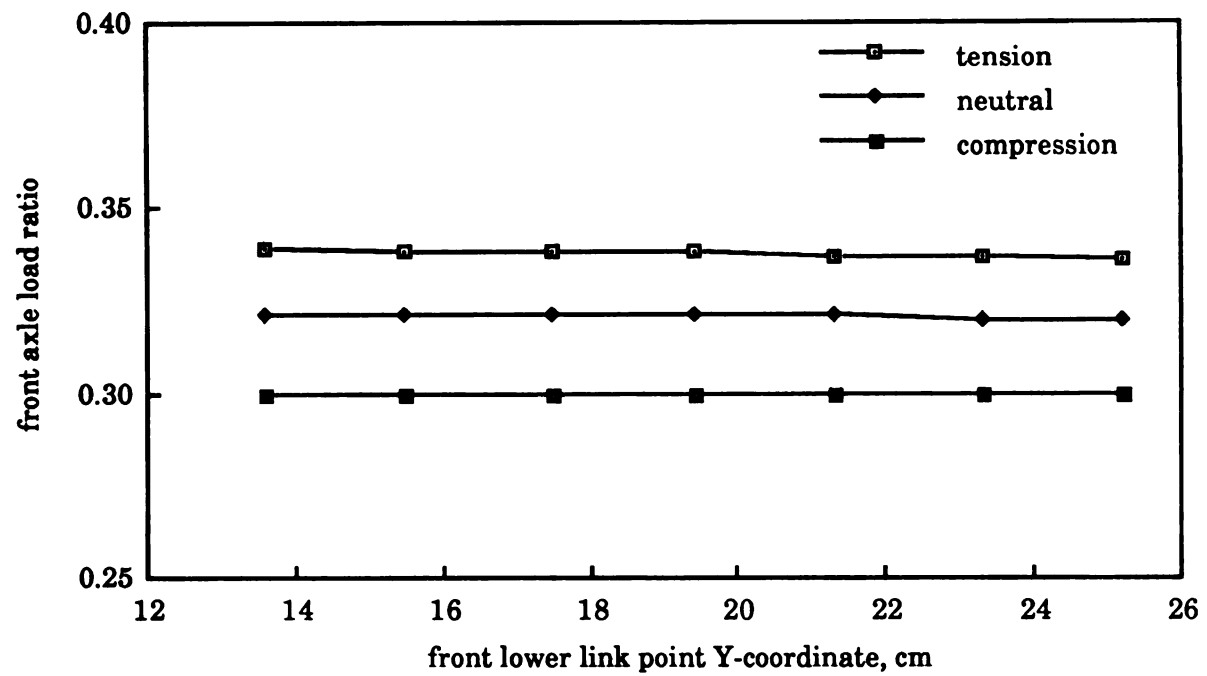
Figure 7.15 - Front axle load ratio vs front lower link point Y-coordinate
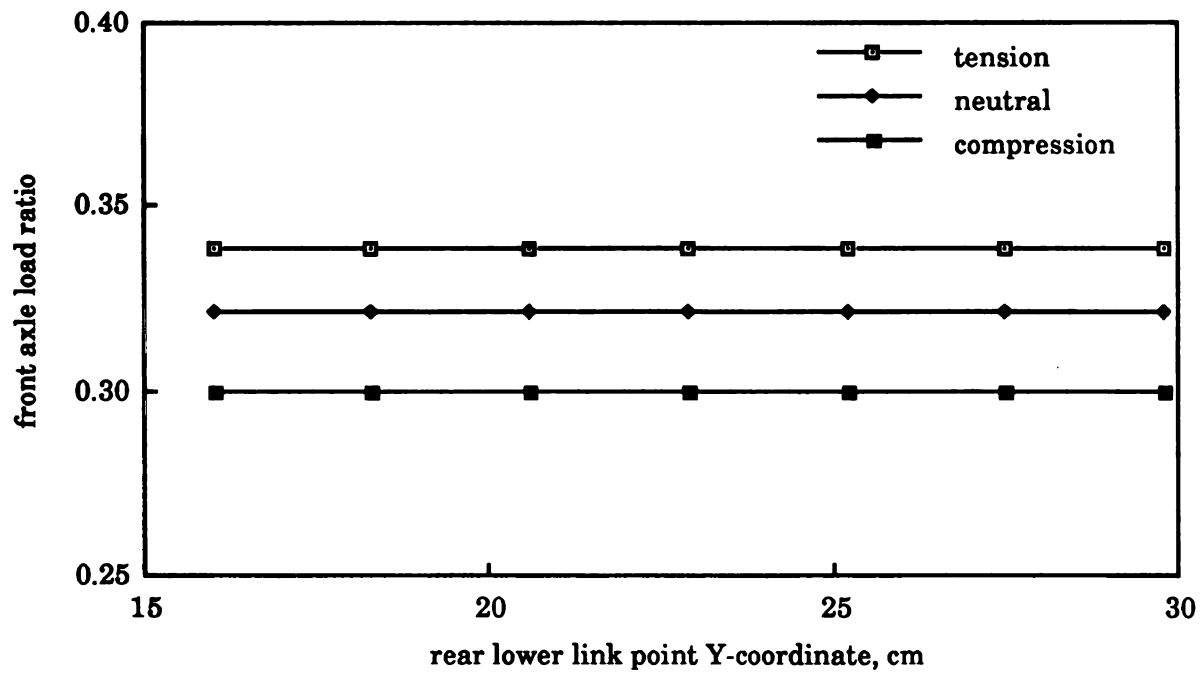
Figure 7.16 - Front axle load ratio vs rear lower link point Y-coordinate
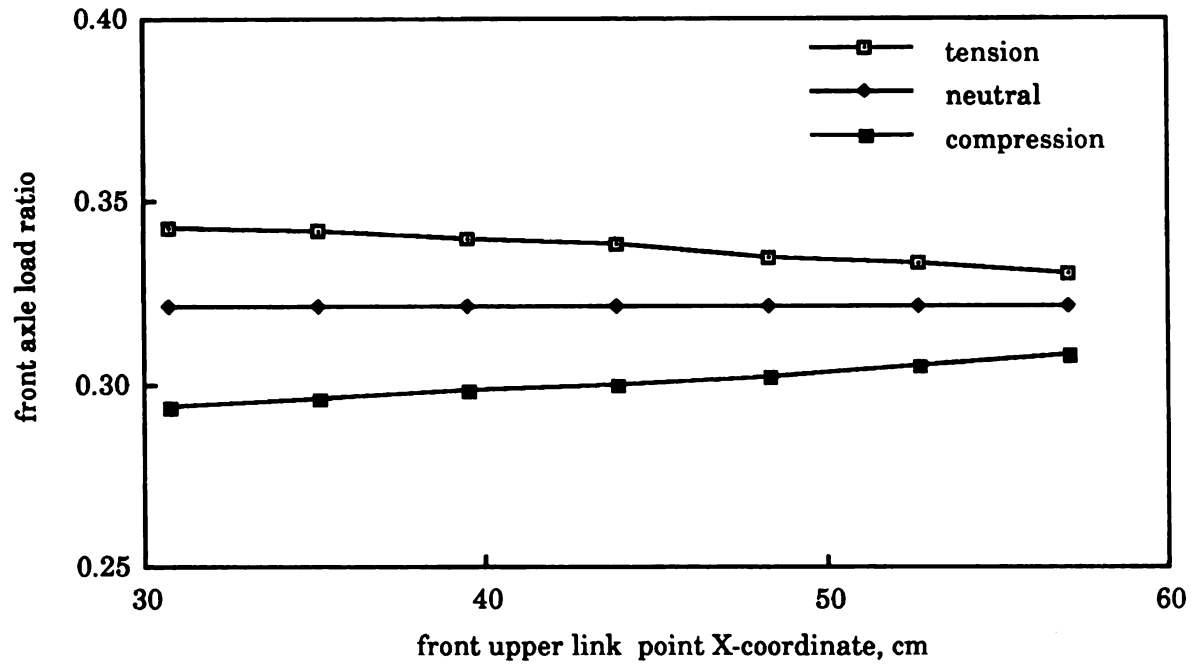
Figure 7.17 - Front axle load ratio vs front upper link point X-coordinate
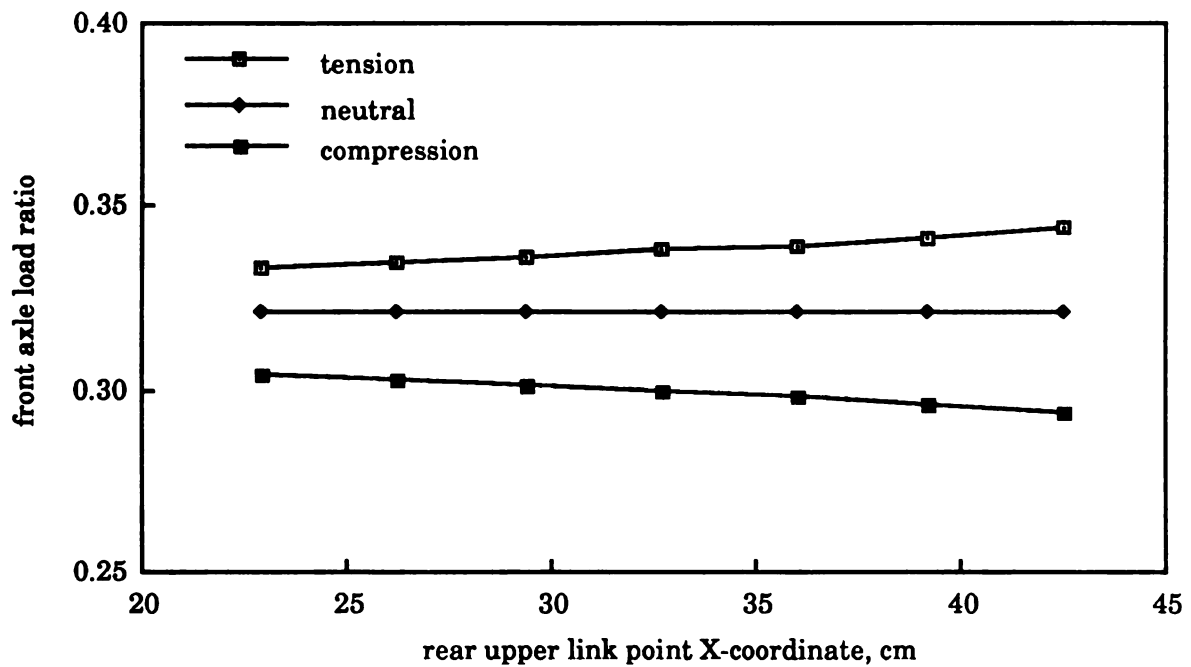
Figure 7.18 - Front axle load ratio vs rear upper link point X-coordinate

The most dramatic effects are observed in the fourth simulation, where increasing the front upper link point Y-coordinate greatly increases, has no effect, or greatly decreases f/r ratio respectively with the upper link in the tension, neutral, and compression modes (Figure 7.19). However, little or no effect occurred when the rear upper link point Y-coordinate was varied (Figure 7.20)

Substantial effects were also obtained in the fifth set of simulations, in this case resulting from changes in both the front and rear hitch dimensions. Increasing the front lower link length greatly increased, moderately increased, or slightly decreased f/r ratio respectively in the tension, neutral, and compression modes of the upper link (Figure 7.21). Increasing the rear lower link length caused a great decrease, moderate decrease, and slight decrease in f/r load ratio with the rear upper link in the tension, neutral, and compression modes respectively (Figure 7.22).
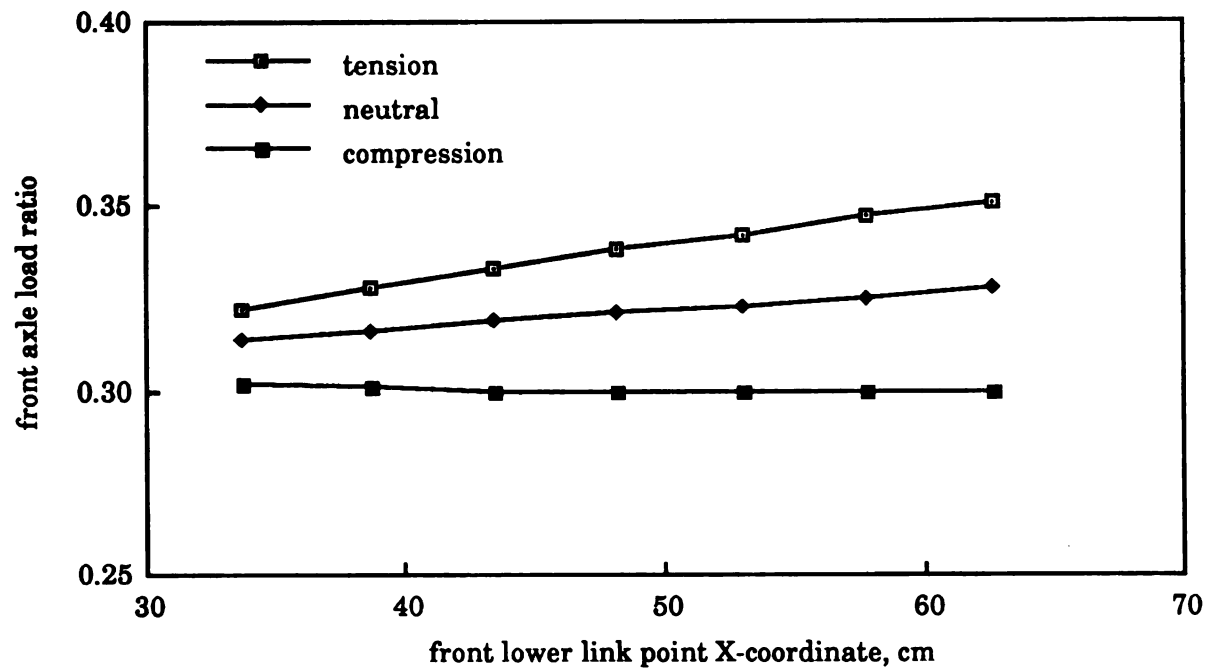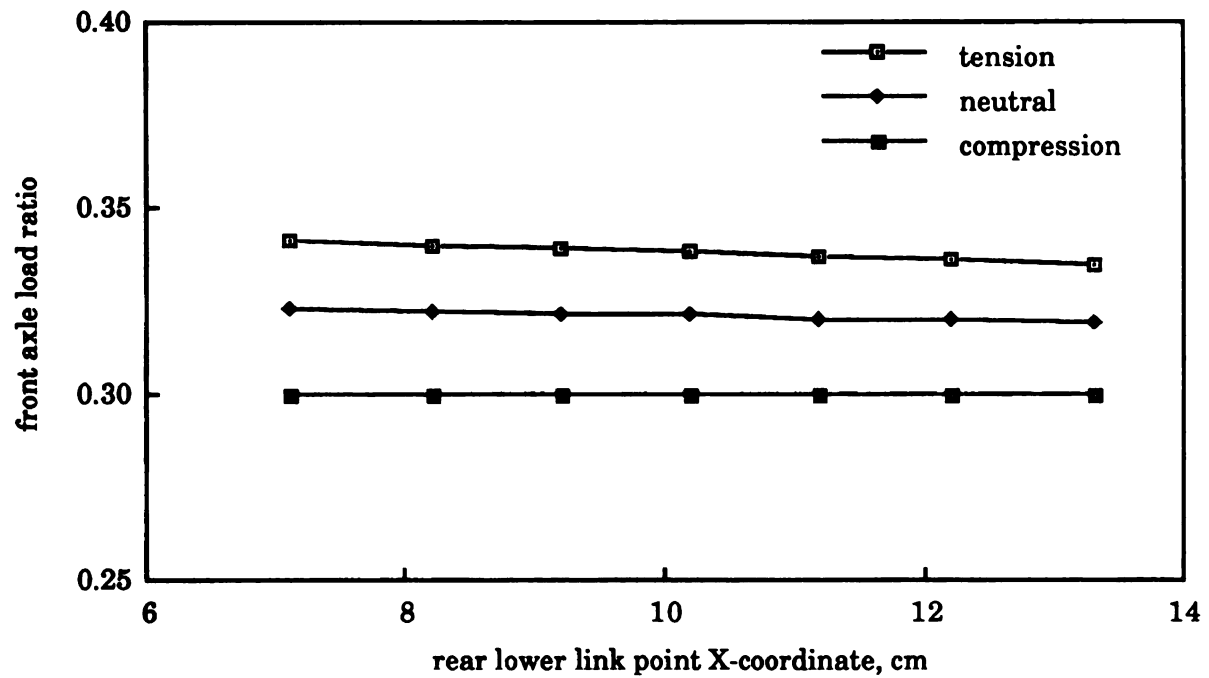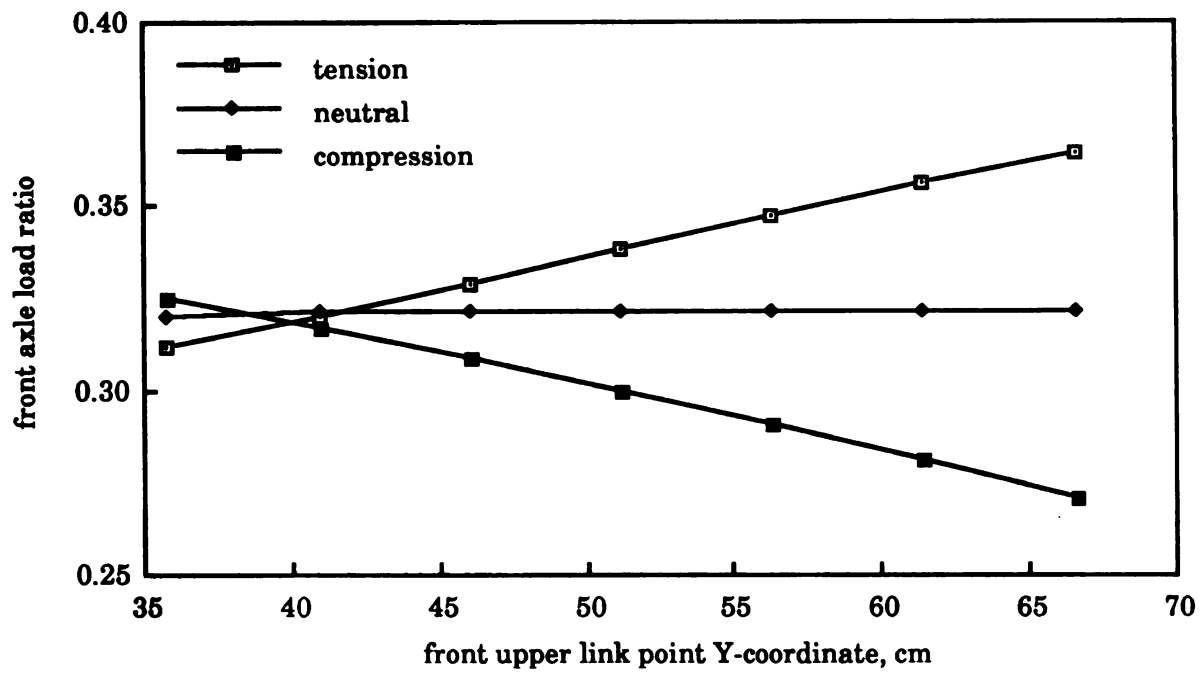
Figure 7.19 - Front axle load ratio vs front upper link point Y-coordinate
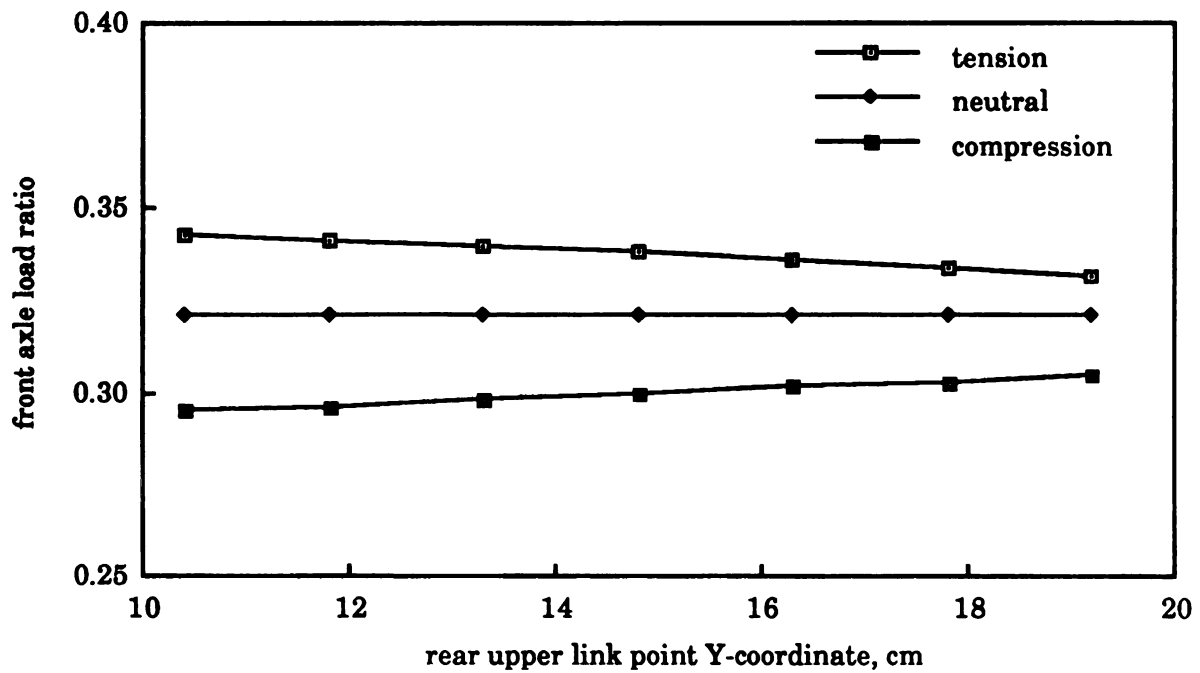
Figure 7.20 - Front axle load ratio vs rear upper link point Y-coordinate
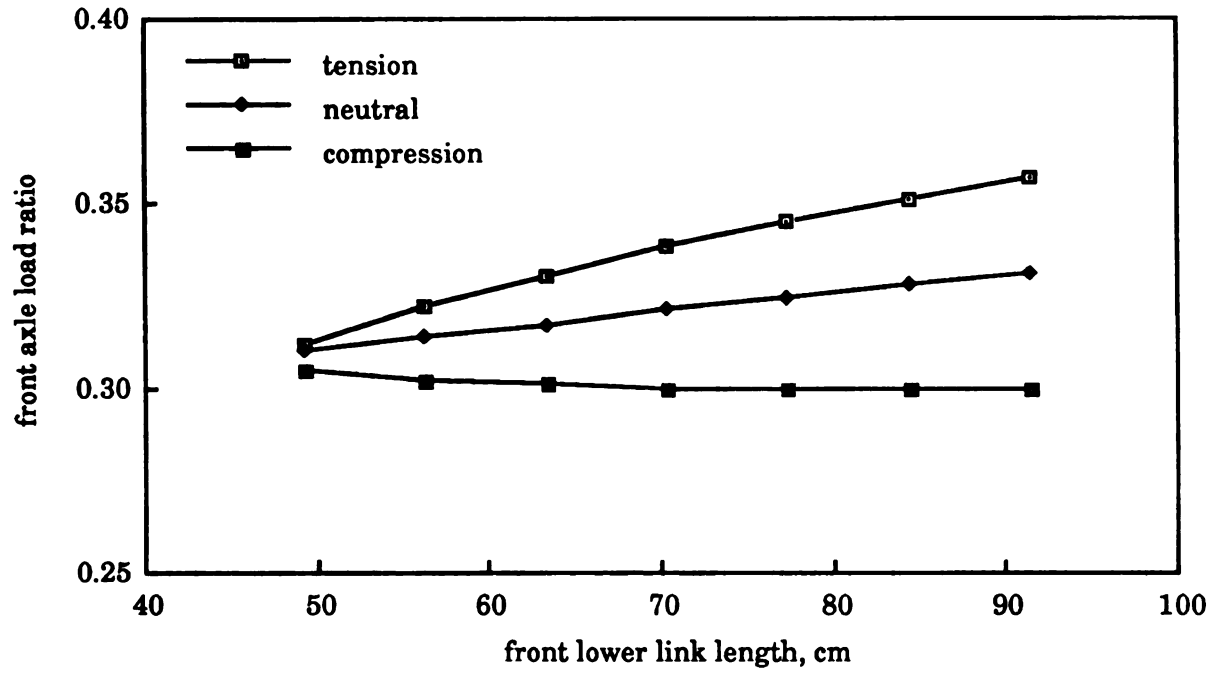
Figure 7.21 - Front axle load ratio vs front lower link length
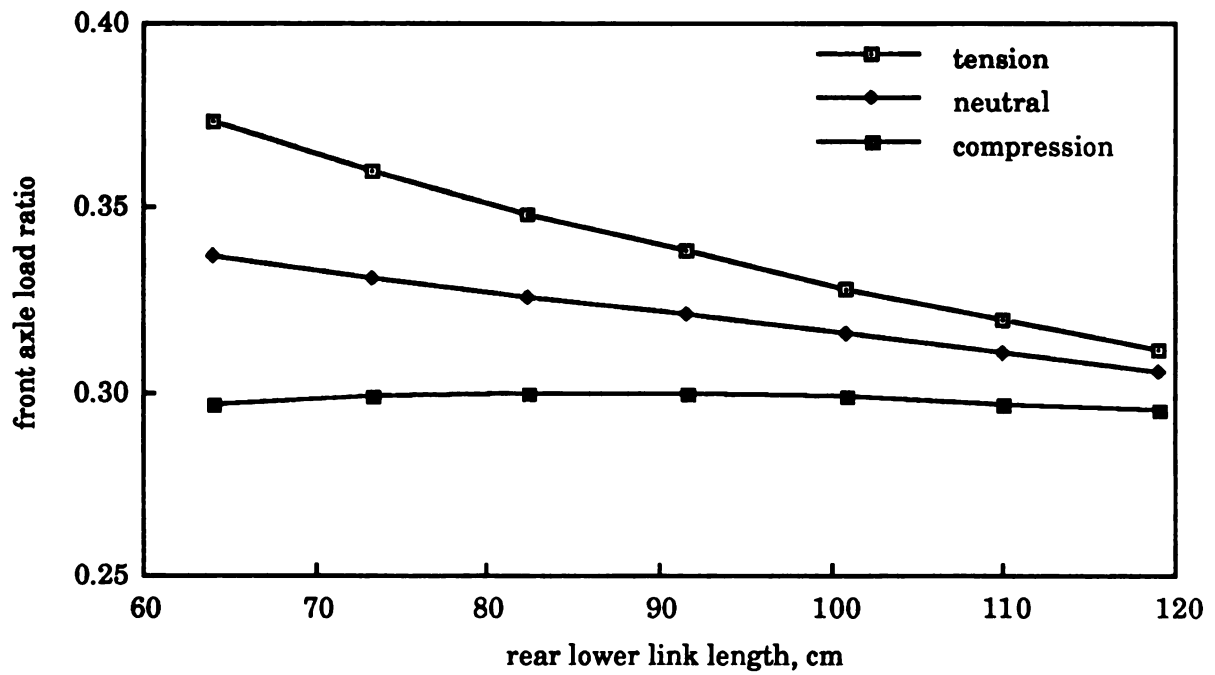
Figure 7.22 - Front axle load ratio vs rear lower link length

7.3.2 Effects of implement dimensions

Only one of the implement dimensions, namely mast height, can be readily changed by an operator, since each implement is designed by the manufacturer to achieve its particular operating conditions. Also, the range of adjustment in this parameter is limited by ASAE Standards. Nevertheless it is interesting to simulate the effects of this parameter and find that increasing the front implement mast height has a pattern of greatly decreasing, not affecting, or greatly increasing f/r ratio respectively with the upper link in the tension, neutral, or compression modes (Figure 7.23). On the other hand, increasing the rear implement mast height has the effects of moderately increasing, not affecting, or moderately decreasing f/r load ratio respectively with the rear upper link in the tension, neutral, or compression modes (Figure 7.24).

7.3.3 Effects of tractor ballast

Finally, tractor ballasting has been frequently used in 4WD and FWA as one way of achieving desired f/r dynamic load ratios. The following simulations confirm the obvious expectation that adding front ballast increases f/r dynamic load ratio (Figure 7.25), and adding rear ballast decreases f/r ratio (Figure 7.26) regardless of upper link loading mode.
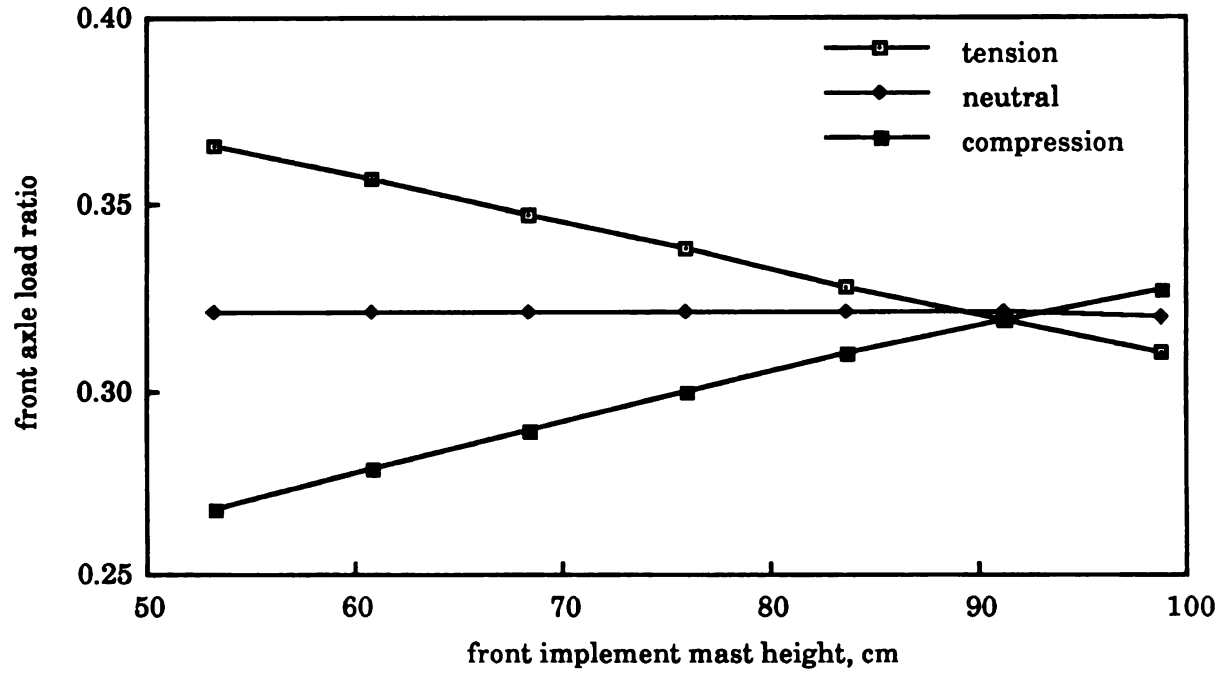
Figure 7.23 - Front axle load ratio vs front implement mast height
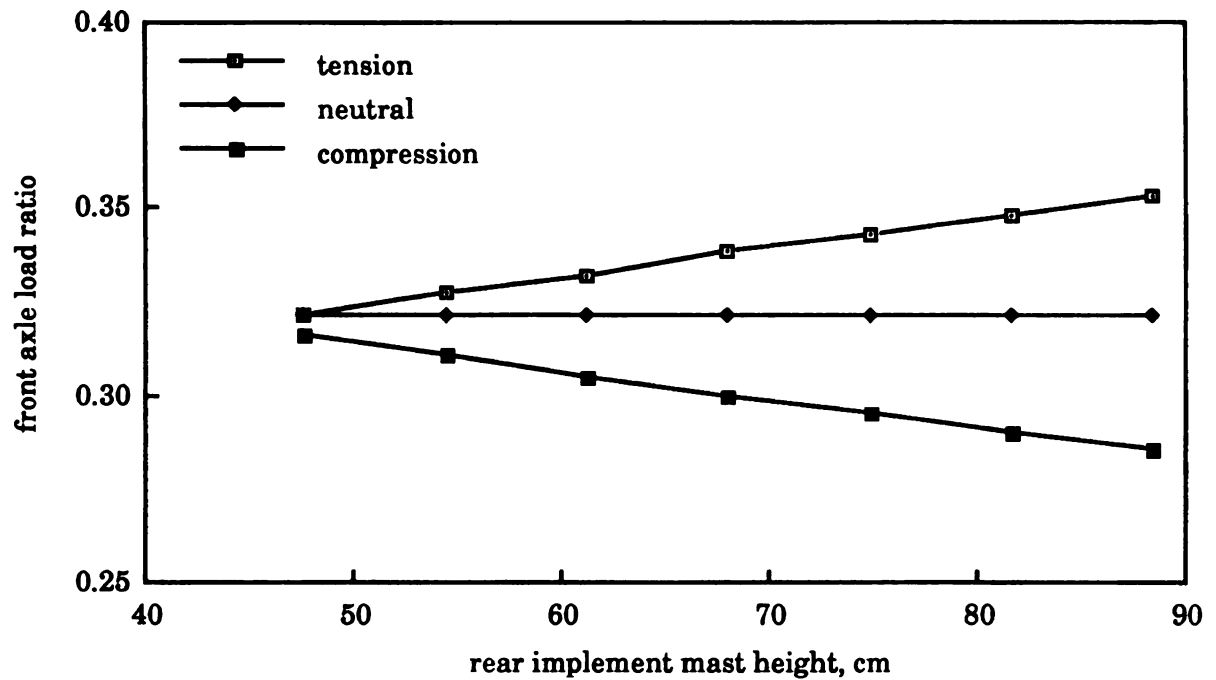
Figure 7.24 - Front axle load ratio vs rear implement mast height
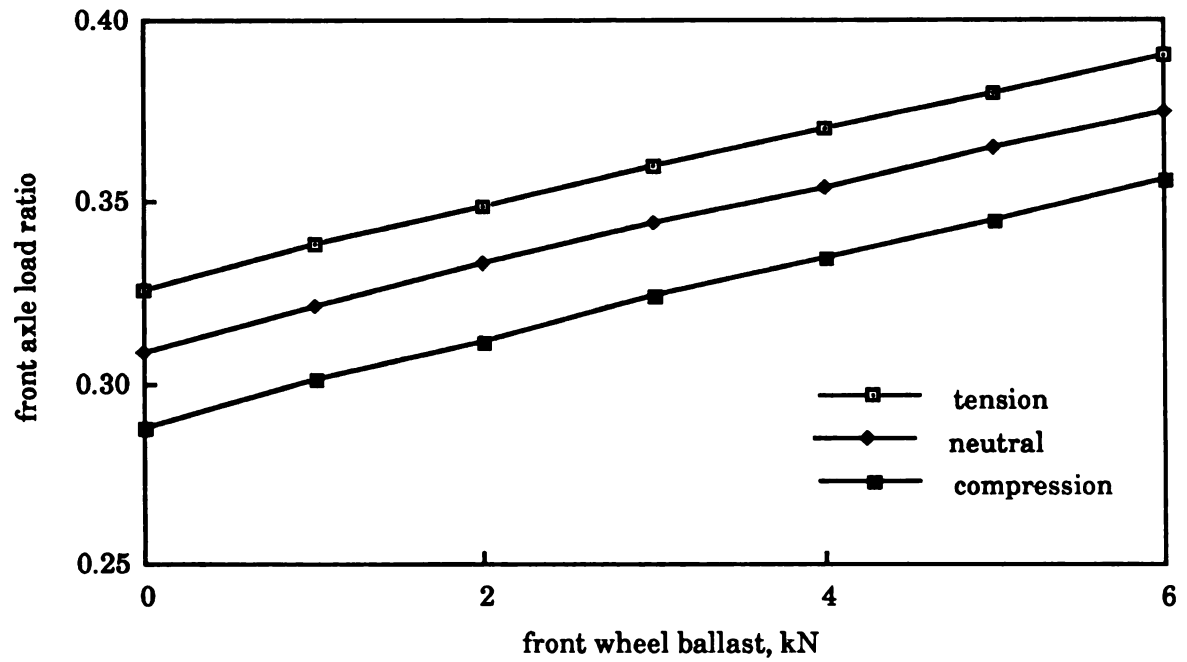
Figure 7.25 - Front axle load ratio vs front wheel ballast
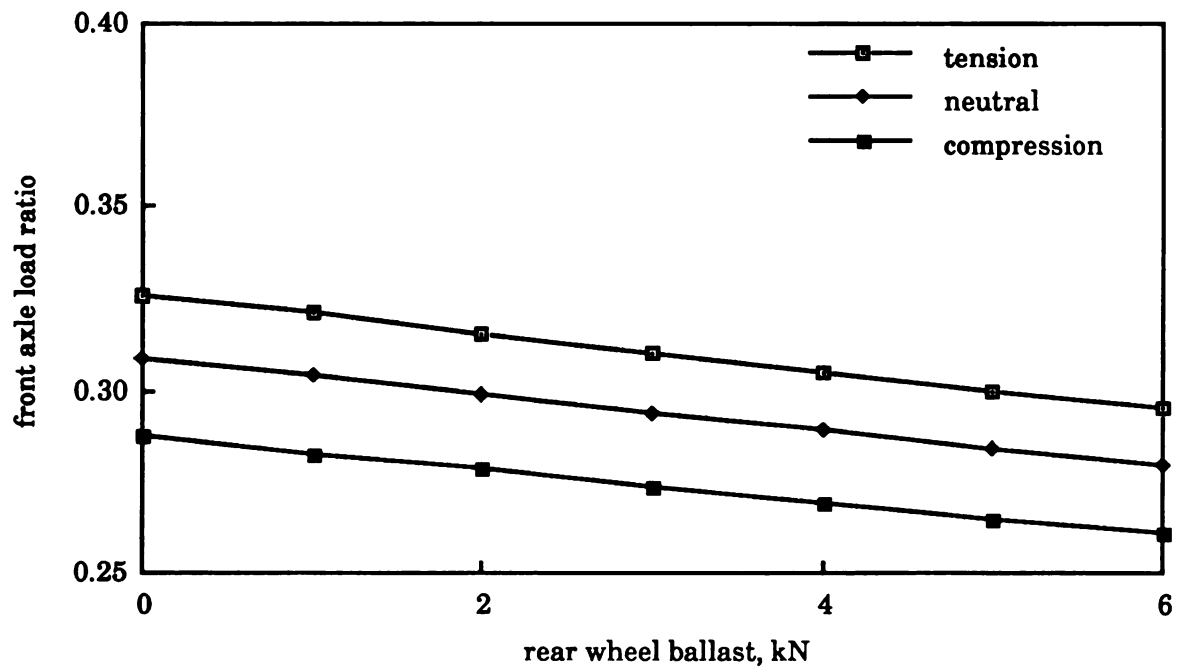
Figure 7.26 - Front axle load ratio vs rear wheel ballast

7.3.4 Practical considerations in the application of simulation data

Attempts to use these simulations to achieve a particular desired f/r load distribution must take into account such practical considerations as the effects that adjustments in hitch configuration would have on the orientation of the implements. In the case of the moldboard plow, altering the hitch geometry could have negative effects on one or more of the three orientation requirements for transport, entry, and normal operation of the plow (see Constraints #3 and #4 in Section 3.3, also discussions in Section 4.1.3 and 4.1.4).

An example of such practical limitations is illustrated in Figure 7.27 (same simulation data as Figure 7.19). In this case the shaded area indicates those values of front upper link point Y-coordinate which would result in the plow having an upward angle while the plow were being lowered into operating position. This would prevent normal entry of the plow into the ground. Similar considerations would have to be applied to the other parameters, and all of these limitations might be different for different implements.
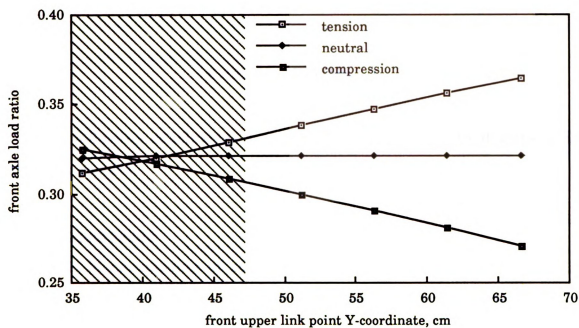
Figure 7.27 - Restriction on adjustment of front upper link point
Y-coordinate with moldboard plow

8. CONCLUSIONS

The following conclusions were drawn based on the field tests and simulation results.

8.1 Field experiments

    8.1.1. Measurements of soil cone index by the standard technique, especially if the values are averaged together for the whole test area, may not be adequate for use in the type of field experiments in this study. Equally important is the fact that the presence of a front implement such as a plow or cultivator presents a special case where the wheels on one side of the tractor may run in a soil condition different from the measured CI.

    8.1.2. Measurements of slippage in only two of the 4 drive wheels (with estimation of slip in the other two) are also less than desirable for a rigorous analysis of tractor performance.

    8.1.3. Despite the considerations in conclusions 8.1.1 and 8.1.2 of present section, the relationships between slippage and pull are reasonable in magnitude and curve shape as compared with results of other published studies.

    8.1.4. The relationships between TE and f/r dynamic load ratio on loose and firm soils are also consistent with other studies. Specifically, on loose soil there are some opportunities for

optimization (i.e. apparent optimum f/r ratio near 0.4/0.6), but a nearly flat response on firm soil may limit the opportunity for optimization in these conditions.

8.2 Simulations

8.2.1. Adjustments of all front hitch dimensions, except the lower link point Y-coordinate, had moderate to substantial effects on f/r dynamic load ratio when the upper link was in either tension or compression load, but little or no effects when there was no load on the upper link.

8.2.2. Adjustments of rear hitch dimensions have little or no effect on f/r dynamic load ratio, except rear lower link length.

8.2.3. Adjustment of front implement mast height has dramatic effects on f/r dynamic load ratio. Adjustment of rear implement mast height has moderate effects on F/R load ratio.

8.2.4. The known effects of adjusting front and/or rear ballast are confirmed by these simulations. The f/r dynamic load ratio changes proportionally to the change of ballast.

8.2.5. Some practical limitations in the range of adjustment in some dimensions must be observed since these adjustments also may change the orientation of the implements, and thus interfere with various aspects of their operation. This must be done on an implement by implement basis.

8.2.6. Overall, the simulations pinpoint several parameters such as front lower link point X-coordinate, front upper link point X- and Y- coordinates, front and rear lower link lengths, front

implement mast height, and front and rear wheel ballast whose adjustment alone or in combination could be used to achieve a desired f/r dynamic load ratio, thus the model has good potential for practical application.

9. RECOMMENDATIONS

9.1 Improved measurements of soil properties

9.1.1 Possible measurements of CI in each test area

Variability in the value of CI in different areas of a given field could first be established by the random sampling method. In those cases where the standard deviation exceeds 10% in soils where penetration is relatively uniform with depth, or 15% in soils with crusts or other distinct layers, then, according to the sensitivity analysis of this parameter, one should sample the specific area of each test, and use those local values of CI in the analyses of data.

9.1.2 Develop some means of measuring CI in those cases where the soil is disturbed by a front implement before passage of the front wheels

This task will not be easy because the only means of making such measurements is after the tractor has stopped at the end of each run, leaving a short length of furrow or tillage between the rearmost part of the front implement and the front wheel. In the case of the plow used in these studies such measurements would have been nearly impossible because components of the plow extended back over this area obstructing the use of the penetrometer. Assuming that some means were developed to achieve this measurement, it would have the weakness of sampling only a small portion of soil at the end of the run. Another alternative is to measure CI in

the furrow from the rear implement after each test and on the surface before each test. This measurement would be an improvement over the method used in these studies.

9.1.3 Develop some means of measuring CI in the tracks after passage of the front wheels

This problem is similar to that of 9.1.2, since only a short length of front tire track remains between the front and rear wheels at the end of the run.

9.1.4 Possible development of techniques to measure soil parameters such as cone index while the tractor is in motion during a field test run

The ideal solution to both of the above problems would be a continual measurement of soil properties in front of all of the wheels while the tractor is in motion during the tests. At present there are no ASAE methods for this purpose, and apparently no formal proposals to develop such instrumentation. Perhaps this is because the value of such measurements has only become more noticeable in the types of tests conducted in these studies and other recent studies of 4WD and FWA tractors. Indeed, an examination of many recent publications reveals variabilities in calculated values of slip, pull, and/or TE which could be entirely accounted for by variations in actual CI in the test fields.

Mechanical devices (e.g. some type of knife blade being pushed through the soil in front of each wheel) are likely to be extremely troublesome. Thus one might consider some form of acoustic or radar reflectivity.

9.2 Improved measurements of wheel slippage and rear axle torque

The addition of wheel motion measurements on all driving wheels is primarily a matter of installing additional sprockets, sensing devices, signal processing channels, and data acquisition capability of the types already in use. It is quite possible that wheel motion sensors on all wheels would greatly minimize the need for more elaborate soil property measurements, since slippage would not have to be estimated in unmeasured wheels. This addition would be relatively easy, however in the case of the present instrumentation system it would require at least one more channel of signal processing electronics since none of the other measurements could be deleted.

Addition of torquemeters (i.e. Wheatstone bridge type of strain gage) to the rear axles would be highly desirable, but extremely difficult because they are enclosed in housings and immersed in oil. The same consideration applies to the rear driveshaft.

9.3 Determine ideal dynamic load distribution for FWA tractors

The above improvements in measurement of soil properties and instrumentation would make it possible to obtain rigorous analyses of field performance, and thus determine the ideal load distributions for the conditions and implements tested. The same data could also be used for further validation and development of the model. If a better relationship between soil properties, dynamic load, and slippage could be established by these or other studies, then the model could be used to predict and optimize tractor performance over a wide range of conditions.

APPENDICES

APPENDIX A

ASAE Standard Definitions

1) Ballast : Mass that can be added or removed for the purpose of changing total load or load distribution. (ASAE Standard: ASAE S296.3)

2) Dynamic load : Total force normal to the reference plane of the predisturbed supporting surface exerted by the traction or transport device under operating conditions. This force may result from ballast and/or applied mechanical forces. (ASAE Standard: ASAE S296.3)

3) Hitch point : The articulated connection between a link and the implement. For geometrical analysis, the hitch point is established as the center of the articulated connection between a link and the implement. (ASAE Standard: ASAE S217.10)

4) Implement frame length : The distance between lower hitch point and the farthest supporting point of the implement away from the hitch point.

5) Implement height : The distance between lower hitch point and the lowest point of implement while it is at working position.

6) Link point : The articulated connection between a link and the tractor. For geometrical analysis, the link point is established as the center of the articulated connection between a link and the tractor. (ASAE Standard: ASAE S217.10)

7) Load transfer : The change in normal forces on the traction and transport devices of the vehicle under operating conditions, as compared to those for the static vehicle. (ASAE Standard: ASAE S296.3)

8) Mast height : The perpendicular distance between the upper hitch point and common axis of the lower hitch points. (ASAE Standard: ASAE S217.10)

9) Motion resistance : Force required in the direction of travel to overcome the resistance from the supporting surface and the internal resistance of the device. (ASAE Standard: ASAE S296.3)

10) Static load : Total force normal to the surface plane of the predisturbed supporting surface exerted by the traction or transport device while stationary with zero net traction and zero input torque. (ASAE Standard: ASAE S296.3)

11) Vehicle traction ratio : Ratio of the drawbar pull of the vehicle to the gross vehicle load. (ASAE Standard: ASAE S296.3)

12) Tractive efficiency : Ratio of output power to input power. The output power is the product of net traction and forward velocity of a traction device. The input power is the product of input torque and angular velocity of the driving axle of a traction device. (ASAE Standard: ASAE S296.3)

13) Travel reduction : One minus travel ratio. Travel ratio is defined as the ratio of distance traveled per revolution of the traction device when producing output power to the rolling circumference under the specified zero conditions. (ASAE Standard: ASAE S296.3)

14) Working depth : The distance between soil surface and the lowest point of implement while it is at working position. The irregularity of soil surface is ignored.

APPENDIX B

Simulation Program and Input Templates

This appendix lists the Pascal-like pseudo program of simulation model developed in this dissertation along with three tables of input parameters used by the simulation model. The pseudo program can be easily translated into any high level programming language. The input parameters are listed as three templates which can be used directly as model input.

The in-line comments (e.g. (* Eq. 4.1 *), (* Fig. 4.1 *)) refer to the implementation of that piece of code by the use of that particular equations or figures in the dissertation.

B1. <u>Pseudo program of simulation model</u>

```
program Simulation;

    include variable declaration file;

(* ============================ *)

  procedure Initialization;

    begin

        GetTracData       := false;
        GetImplData       := false;
        GetWorkData       := false;

        TracDataChanged := false;
        ImplDataChanged := false;
        WorkDataChanged := false;

        finished          := false;

        input data file path name prefix;
        input parameters title;

    end;

(* ============================ *)

  procedure MainMenu (var option);

    begin

        option := 0;
        set up main menu;

        while ( option not in [1..5, 9] ) do
          beep;
          input option;
        end of while;

    end;

(* ============================ *)

  procedure SaveTractorData;

    begin

        input file name;
        save parameters to file;
        TracDataChanged := false;

    end;

(* ============================ *)
```

```
procedure TractorDataHandling;

(* ------------------------------- *)

   procedure TractorDataMenu (var option);

      begin

         option := 0;
         set up option menu;

         while ( option not in [1..4, 9] ) do
            beep;
            input option;
         end of while;

      end;

(* ------------------------------- *)

   procedure InputFromFile;

      begin

         input file name;
         input data from file;
         GetTracData := true;

      end;

(* ------------------------------- *)

   procedure InputFromKeyboard;

      begin

         for loop := 1 to # of parameters do
            write parameter title[loop];
            input parameter[loop];
         end of for;

         GetTracData      := true;
         TracDAtaChanged := true;

      end;

(* ------------------------------- *)

   procedure EditData;

      begin

         while (not quit) do

            for loop := 1 to # of parameters do
               write parameter title[loop];
            end of for;
```

```
        input parameter#;

        write parameter title[parameter#];
        write parameter[parameter#];
        input parameter[parameter#];      (* get new value *)

        if (new parameter <> old parameter) then
          TracDataChanged := true;
        end of if

      end of while;

    end;

(* ------------------------------ *)

  begin      (* of procedure TractorDataHandling *)

    quit := flase;

    while (not quit) do

      TractorDataMenu (option);

      case option of

          1 : InputFromFile;
          2 : InputFromKeyBoard;
          3 : EditData;
          4 : SaveTractorData;
          9 : quit := true;

      end of case;

    end of while;

    end;        (* of procedure TractorDataHandling *)

(* ============================== *)

  procedure SaveImplementData;

    begin

        input file name;
        save parameters to file;
        ImplDataChanged := false;

    end;

(* ============================== *)

  procedure ImplementDataHandling;

    (* ------------------------------ *)
```

```
procedure ImplementDataMenu (var option);

    begin

        option := 0;
        set up option menu;

        while ( option not in [1..4, 9] ) do
            beep;
            input option;
        end of while;

    end;
```

(* ---------------------------- *)

```
procedure InputFromFile;

    begin

        input file name;
        input data from file;
        GetImplData := true;

    end;
```

(* ------------------------------ *)

```
procedure InputFromKeyboard;

    begin

        for loop := 1 to # of parameters do
            write parameter title[loop];
            input parameter[loop];
        end of for;

        GetImplData     := true;
        ImplDataChanged := true;

    end;
```

(* ------------------------------ *)

```
procedure EditData;

    begin

        while (not quit) do

            for loop := 1 to # of parameters do
                write parameter title[loop];
            end of for;

            input parameter#;

            write parameter title[parameter#];
            write parameter[parameter#];
```

```
            input parameter[parameter#];     (* get new value *)

            if (new parameter <> old parameter) then
              ImplDataChanged := true;
            end of if;

        end of while;

    end;

  (* ------------------------------ *)

    begin     (* of procedure ImplementDataHandling *)

      quit := flase;

      while (not quit) do

        ImplementDataMenu (option);

        case option of

            1 : InputFromFile;
            2 : InputFromKeyBoard;
            3 : EditData;
            4 : SaveImplementData;
            9 : quit := true;

        end of case;

      end of while;

    end;        (* of procedure ImplementDataHandling *)

(* =========================== *)

  procedure SaveWorkingData;

    begin

      input file name;
      save parameters to file;
      WorkDataChanged := false;

    end;

(* =========================== *)

  procedure WorkingDataHandling;

    (* ------------------------------ *)

    procedure WorkingDataMenu (var option);

      begin

        option := 0;
        set up option menu;
```

```
    while ( option not in [1..4, 9] ) do
      beep;
      input option;
    end of while;

  end;

(* ---------------------------- *)

  procedure InputFromFile;

    begin

      input file name;
      input data from file;
      GetWorkData := true;

    end;

(* ---------------------------- *)

  procedure InputFromKeyboard;

    begin

      for loop := 1 to # of parameters do
        write parameter title[loop];
        input parameter[loop];
      end of for;

      GetWorkData     := true;
      WorkDataChanged := true;

    end;

(* ---------------------------- *)

  procedure EditData;

    begin

      while (not quit) do

        for loop := 1 to # of parameters do
          write parameter title[loop];
        end of for;

        input parameter#;

        write parameter title[parameter#];
        write parameter[parameter#];
        input parameter[parameter#];      (* get new value *)

        if (new parameter <> old parameter) then
          WorkDataChanged := true;
        end of if;
```

```
      end of while;

   end;

(* ------------------------------ *)

   begin     (* of procedure WorkingDataHandling *)

      quit := flase;

      while (not quit) do

         WorkingDataMenu (option);

         case option of

            1 : InputFromFile;
            2 : InputFromKeyBoard;
            3 : EditData;
            4 : SaveWorkingData;
            9 : quit := true;

         end of case;

      end of while;

   end;        (* of procedure WorkingDataHandling *)

(* =========================== *)

   procedure RearUpperLinkLength (var NewLength; WorkDepth);

      begin

         calculate effective rear lower link length;   (* Fig. 4.4 *)
         calculate rear alpha angle using WorkDepth;    (* Eq.  4.1 *)
         calculate rear beta angle;                     (* Eq.  4.2 *)
         calculate distance of AB;                      (* Fig. 4.1 *)
         calculate diagonal distance BD;                (* Eq.  4.3 *)
         calculate rear delta angle;                    (* Eq.  4.4 *)
         calculate rear gamma angle;                    (* Eq.  4.6 *)

         calculate NewLength;                           (* Eq.  4.5 *)

         calculate rear theta angle;                    (* Eq.  4.8 *)

      end;       (* of procedure RearUpperLinkLength *)

(* =========================== *)

   procedure FrontUpperLinkLength (var NewLength; WorkDepth);

      begin

         calculate effective front lower link length;  (* Fig. 4.4  *)
         calculate front alpha angle using WorkDepth;   (* Eq.  4.9  *)
         calculate front beta angle;                    (* Eq.  4.10 *)
         calculate distance of EF;                      (* Fig. 4.5  *)
```
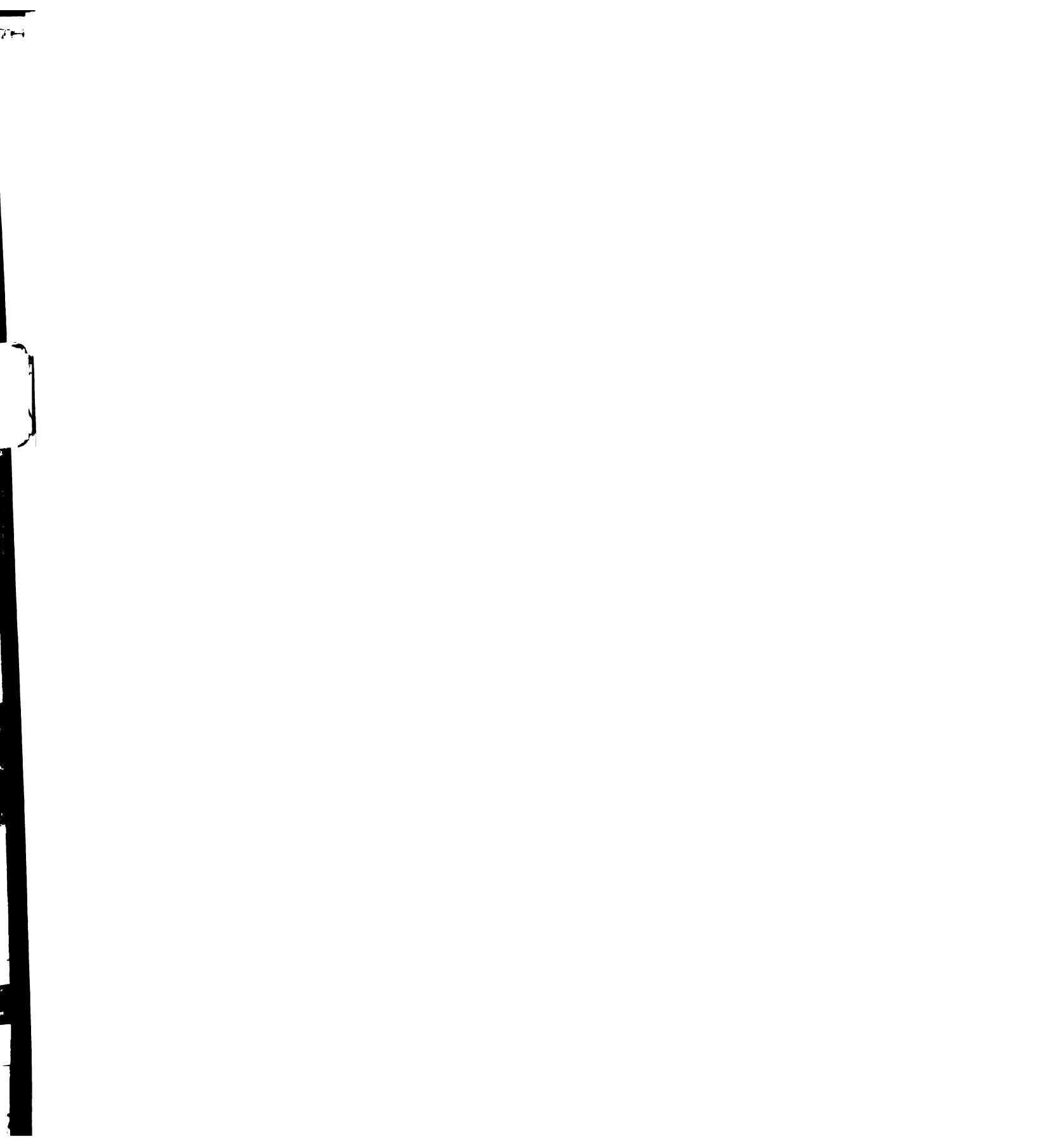
```
        calculate diagonal distance FH;            (* Eq.  4.11 *)
        calculate front delta angle;               (* Eq.  4.12 *)
        calculate front gamma angle;               (* Eq.  4.14 *)

        calculate NewLength;                       (* Eq.  4.13 *)

        calculate front theta angle;               (* Eq.  4.15 *)

    end;      (* of procedure FrontUpperLinkLength *)

(* ============================= *)

   procedure CalculateDynamicLoad (forces on hitches;
                                   var wheels dynamic load);

      begin

        calculate front axle dynamic load;         (* Eq. 4.18 *)
        calculate  rear axle dynamic load;         (* Eq. 4.17 *)
        calculate effective tread width;           (* Eq. 4.21 *)
        calculate in-furrow  rear wheel dynamic load; (* Eq. 4.19 *)
        calculate on-surface rear wheel dynamic load; (* Eq. 4.20 *)
        calculate front wheels dynamic load;

      end;      (* of procedure CalculateDynamicLoad *)

(* ============================= *)

   procedure OptimizeGeometry;

     (* ------------------------------ *)

      procedure SimulationMenu (var option);

        begin

          option := 0;
          set up option menu;

          while ( option not in [1..4, 9] ) do
            beep;
            input option;
          end of while;

        end;

     (* ----------------------------- *)

      function FrontPenetrateAngle (UpperLinkLength) : real;

        begin

          calculate effective front lower link length;  (* Fig. 4.4  *)
          calculate front alpha angle with WorkDepth=0;  (* Eq.  4.9  *)
          calculate front beta angle;                    (* Eq.  4.10 *)
          calculate distance of EF;                      (* Fig. 4.5  *)
          calculate diagonal distance FH;                (* Eq.  4.11 *)
          calculate front delta angle;                   (* Eq.  4.12 *)
```

```
    calculate front gamma angle;                    (* Eq.  4.13 *)
    calculate FrontCutAngle;                         (* Eq.  4.14 *)


  end;    (* of function FrontPenetrateAngle *)

(* ---------------------------- *)

  begin    (* of procedure OptimizeGeometry *)

    while (not quit) do         (* main while loop *)

      while (not GetTracData) do
        TractorDataHandling;
      end of while;

      while (not GetImplData) do
        ImplementDataHandling;
      end of while;

      while (not GetWorkData) do
        WorkingConditionHandling;
      end of while;

      RearUpperLinkLength (RearUpperLength, WorkDepth);
      FrontUpperLinkLength (FrontUpperLength, WorkDepth);

      FrontCutAngle := FrontPenetrateAngle (FrontUpperLength);

      if (FrontCutAngle >= 0) then
        ErrorMessage ('Can not penetrate');
      else
        CalculateDynamicLoad (forces on hitches, wheels dynamic load);

        if (wheel dynamic load > permissible load) then
          ErrorMessage ('Overloading the tires');
        else
          output FrontUpperLength, RearUpperLength, FrontCutAngle,
                 wheel dynamic loads, dynamic load ratio;
        end of if;
      end of if;

      while (option not in [4, 9]) do
        SimulationMenu (option);

        case option of

          1 : TractorDataHandling;
          2 : ImplementDataHandling;
          3 : WorkingConditionHandling;
          4 : ;
          9 : quit := true;

        end of case;
      end of while;

    end of while;           (* main while loop *)

  end;    (* of procedure OptimizeGeometry *)
```

```
(* ============================== *)

 procedure VerifyFieldData;

  (* ---------------------------- *)

   procedure CalculateGeometry;

     begin

        done := false;
        UpperLimit := 100;
        LowerLimit := 1;

        RearUpperLinkLength (CurrentLength, (LowerLimit+UpperLimit)/2);

        while (not done) do

           if (abs(CurrentLength - RearUpperLength) > tolerance) then

              if (CurrentLength > RearUpperLength) then
                LowerLimit = (LowerLimit+UpperLimit)/2;
              else
                UpperLimit = (LowerLimit+UpperLimit)/2;
              end of if

              RearUpperLinkLength (CurrentLength,
                              (LowerLimit+UpperLimit)/2);
           else
              rearWorkDepth := (LowerLimit+UpperLimit) / 2;
              done := true;
           end of if

        done := false;
        UpperLimit := 100;
        LowerLimit := 1;

        FrontUpperLinkLength (CurrentLength, (LowerLimit+UpperLimit)/2);

        while (not done) do

           if (abs(CurrentLength - FrontUpperLength) > tolerance) then

              if (CurrentLength > FrontUpperLength) then
                LowerLimit = (LowerLimit+UpperLimit)/2;
              else
                UpperLimit = (LowerLimit+UpperLimit)/2;
              end of if

              FrontUpperLinkLength (CurrentLength,
                              (LowerLimit+UpperLimit)/2);
           else
              FrontWorkDepth := (LowerLimit+UpperLimit) / 2;
              done := true;
           end of if

     end;     (* of procedure CalculateGeometry *)
```

```
(* ------------------------------ *)

    procedure EvaluatePerformance (wheels dynamic load, field data;
                                   var wheels pull, TE);

      begin

        calculate non-instrumented wheels slip;
        calculate wheel numerics;                    (* Eq.  2.2  *)
        calculate wheels pull;                       (* Eq.  4.24 *)
        calculate TE;                                (* Eq.  4.25 *)

      end;    (* of procedure EvaluatePerformance *)

(* ----------------------------- *)

    begin   (* of procedure VerifyFieldData *)

      while (not GetTracData) do
        TractorDataHandling;
      end of while;

      while (not GetImplData) do
        ImplementDataHandling;
      end of while;

      while (not GetWorkData) do
        WorkingConditionHandling;
      end of while;

      while (not done) do

        input field data file name;
        initialize accumulators to zeros;
        CalculateGeometry;

        for loop := 1 to # of data set do

          input field data;
          CalculateDynamicLoad (field data, wheels dynamic load);
          EvaluatePerformance (wheels dynamic load, field data,
                               wheels pull, TE);
          accumulators := accumulators + new results;

        end of for;

        averages := accumulators / # of data set;

        output averages;
        input option whether done;

      end of while;

    end;    (* of procedure VerifyFieldData *)

(* ============================== *)
```

```
procedure Finalization (finished);

   begin

      if (TracDataChanged) then
        input option whether save data;
        if (WantToSave) then
          SaveTractorData;
        end of if;
      end of if;

      if (ImplDataChanged) then
        input option whether save data;
        if (WantToSave) then
          SaveImplementData;
        end of if;
      end of if;

      if (WorkDataChanged) then
        input option whether save data;
        if (WantToSave) then
          SaveWorkingData;
        end of if;
      end of if;

      input whether quit program;
      if (quit) then
        finished := true;
      else
        finished := false;
      end of if;

   end;    (* of procedure Finalization *)

(* ============================== *)

begin  (* of main program *)

   Initialization;

   while (not finished) do

     MainMenu (option);

     case option of

        1 : TractorDataHandling;
        2 : ImplementDataHandling;
        3 : WorkingConditionHandling;
        4 : OptimizeGeometry;
        5 : VerifyFieldData;
        9 : Finalization (finished);

     end of case;

   end of while;

end.    (* of main program *)
```

B2. Model input templates

Table B.1 - Tractor parameters template

```
FORD 7610 2x3
X-coordinate of rear lower link point   =        10.200
Y-coordinate of rear lower link point   =        22.900
rear lower link length (cm)             =        91.600
rear lower link width (cm)              =        52.100
X-coordinate of rear top link point     =        32.700
Y-coordinate of rear top link point     =        14.800
X-coordinate of front lower link point  =        48.200
Y-coordinate of front lower link point  =        19.400
front lower link length (cm)            =        70.300
front lower link width (cm)             =        67.000
X-coordinate of front top link point    =        43.900
Y-coordinate of front top link point    =        51.200
the tractor wheel base (cm)             =       225.600
the tractor rear wheels tread (cm)      =       163.200
unloaded rear wheel radius (cm)         =        82.700
unloaded front wheel radius (cm)        =        60.500
rear axle load (Newton)   =               26867.000
front axle load (Newton) =                17348.000
tractor total weight (Newton)         =   44215.000
center of gravity from rear axle (cm) =       91.900
rear wheel ballast (Newton)                 =        .000
front wheel ballast (Newton)                =        .000
ballast in front of tractor (Newton)        =        .000
distance from front ballast to front axle = 1.000
front ballast height from front axle (cm) = 1.000
Y-coordinate of center of gravity (cm)      =      23.300
Z-coordinate of center of gravity (cm)      =       0.000
number gear = 16
LO1     11.780
HI1      9.160
LO2      8.102
HI2      6.300
LO3      5.543
HI3      4.310
LO4      3.807
HI4      2.960
LO5      3.331
HI5      2.590
LO6      2.289
HI6      1.780
LO7      1.569
HI7      1.220
LO8      1.080
HI8      0.840
rear differential ratio    =              23.790
front differential ratio   =              15.820
rear final drive ratio     =               1.000
front final drive ratio    =               1.000
front drop box ratio       =               1.096
```

Table B.2 - Implement parameters template

no of front bottom	=	3
rear mast height	=	68.0
rear hitch width	=	89.5
rear frame angle phi	=	0.0
rear implement height	=	73.0
rear clear point	=	49.0
rear cut point	=	49.0
rear frame angle	=	0.0
front mast height	=	76.0
front hitch width	=	89.0
front frame angle phi	=	0.0
front implement height	=	73.0
front clear point	=	63.0
front cut point	=	210.0
front frame angle	=	0.0

Table B.3 - Working condition parameters template

left plowing		
ground slope	=	0.01
cone index	=	45.0
rear roll radius(furrow)	=	76.5
rear roll radius(land)	=	79.5
rear wheel width	=	46.7
rear work depth	=	20.0
rear tire perm. load	=	22100.0
front roll radius(furrow)	=	56.6
front roll radius(land)	=	57.2
front wheel width	=	34.5
front work depth	=	20.0
front tire perm. load	=	13200.0

APPENDIX C

Front axle pivot force and power distribution to axles

Figures C.1 and C.2 show the forces acting on the tractor's front axle pivot point. Each point in the figures represents the average value of each test run. There were 500 data set recorded during each test run.

Figures C.3 and C.4 illustrate the power distribution to the tractor's front and rear axles. The power delivered to each wheel was calculated by equations 4.25 and 4.26. The front axle power ratio was obtained by dividing the sum of the power delivered to the front wheels by total power delivered to four wheels.
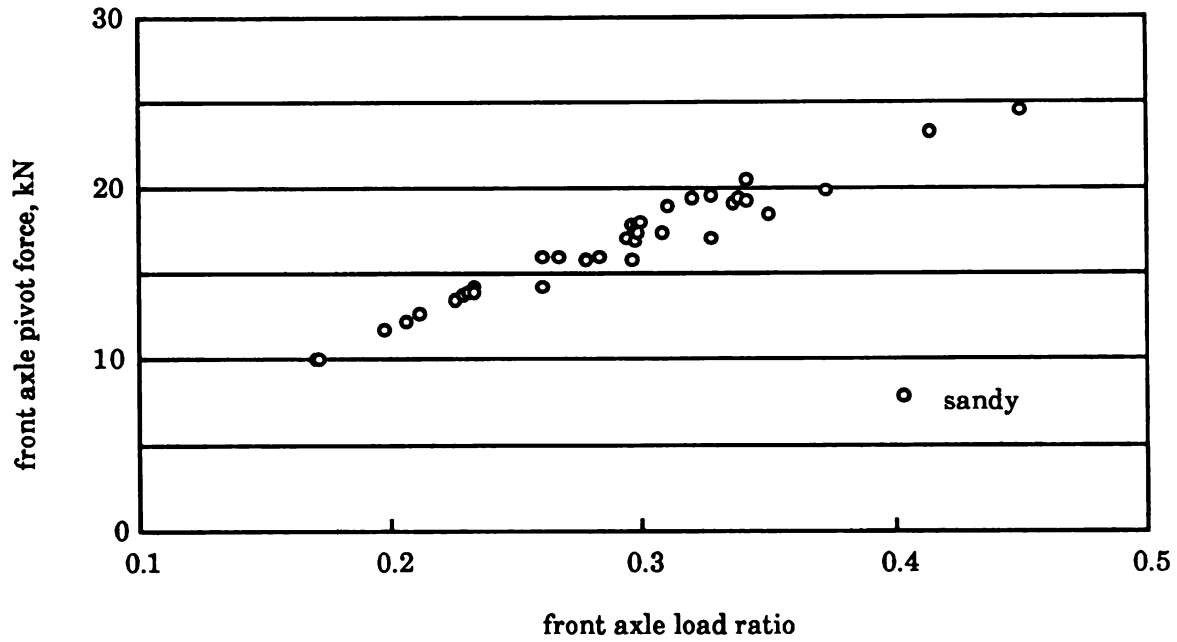
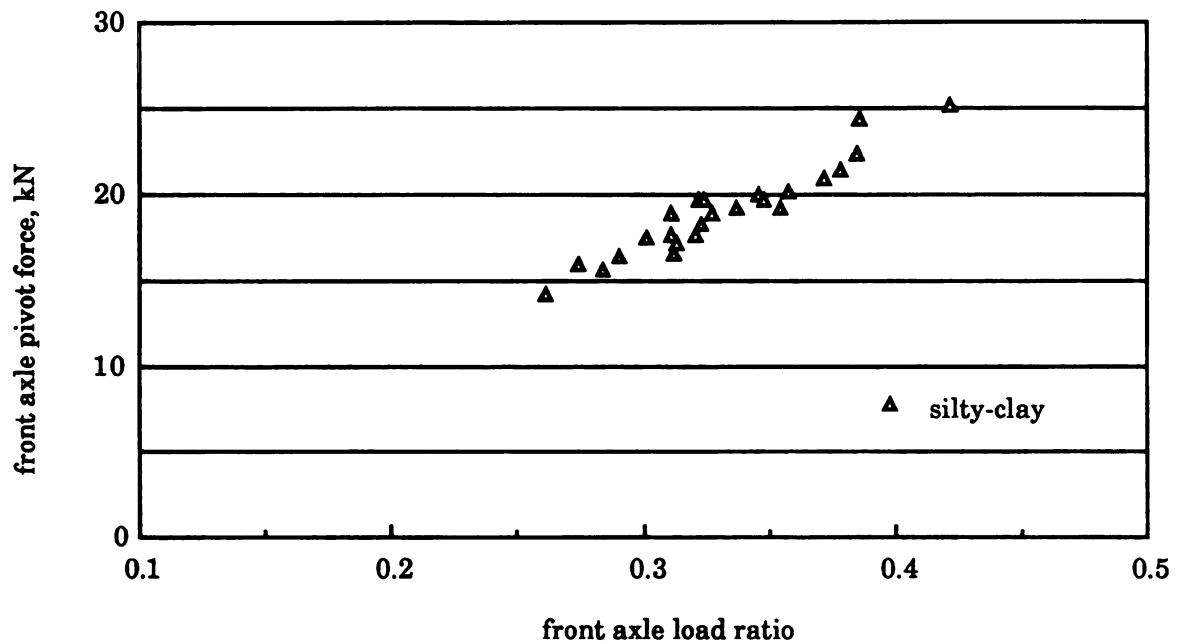Figure C.1 - Front axle pivot force vs front axle load ratio in sandy soil

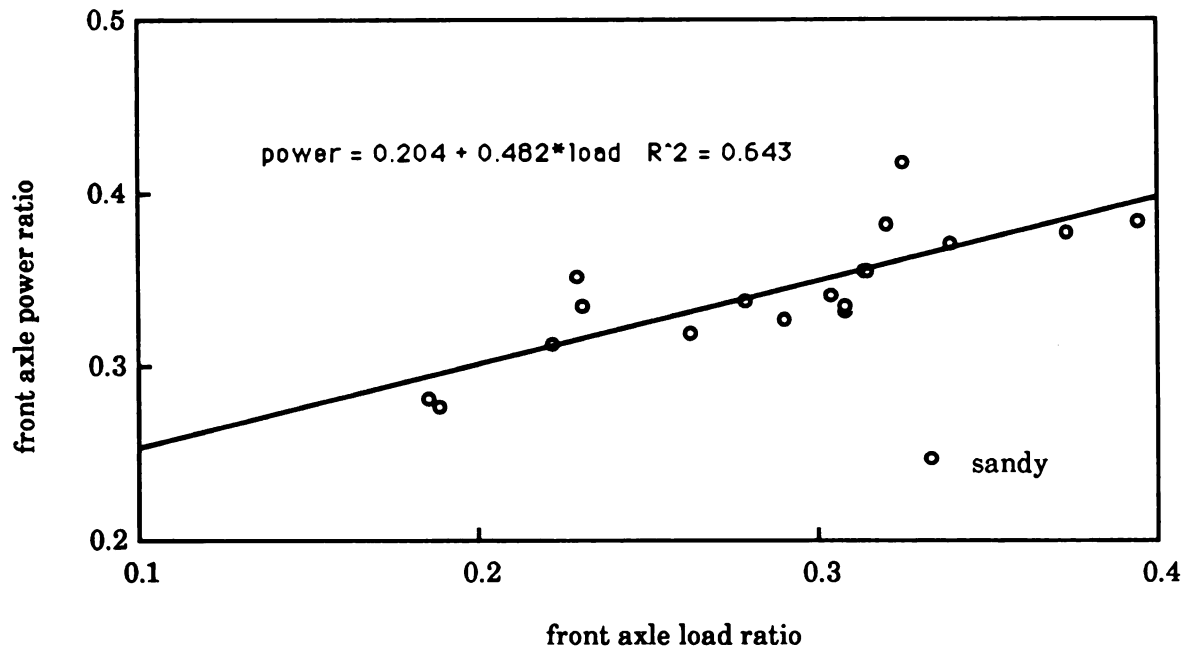Figure C.2 - Front axle pivot force vs front axle load ratio in silty-clay soil

Figure C.3 - Front axle power ratio vs front axle load ratio in sandy soil
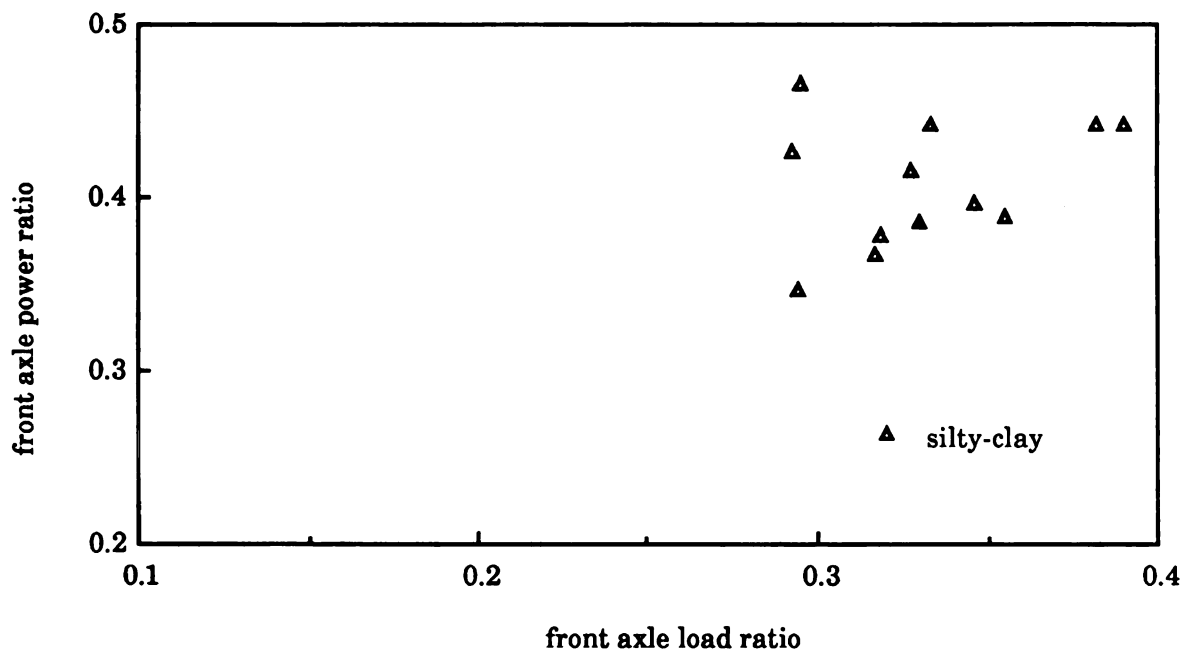

Figure C.4 - Front axle power ratio vs front axle load ratio in silty-clay soil

BIBLIOGRAPHY

BIBLIOGRAPHY

Anonymous. 1986. Tire and Rim Association Yearbook. Published by the Tire and Rim Association, Inc., Akron, OH 44313.

ASAE D230.4. 1988. Agricultural machinery management data. ASAE Data. St. Joseph, MI 49085.

ASAE S209.5. 1988. Agricultural tractor test code. ASAE Standards. St. Joseph, MI 49085.

ASAE S313.2. 1988. Soil cone penetrometer. ASAE Standards. St. Joseph, MI 49085.

Babacz, W.A., G. Felsenstein, C. Kotazabassis, S.W. Searcy and B.A. Stout. 1986. Mechanical front wheel drive tractor performance. ASAE Paper nº 86-1548. ASAE, St. Joseph, MI 49085.

Bailey, A.C., E.C. Burt, J.H. Taylor. 1976. Thrust-dynamic weight relationships of rigid wheels: II. The effects of soil and wheel surface. Transactions of the ASAE 19(1):37-40.

Bailey, A.C. and E.C. Burt. 1976. Theoretical considerations of a rigid wheel mechanics. Transactions of the ASAE 19(5):1005-1007.

Bailey, A.C. and E.C. Burt. 1981. Performance of tandem, dual, and single tires. Transactions of the ASAE 24(4):1103-1107.

Bandy, S.M., W.A. Babacz, J. Grogan, S.W. Searcy, and B.A. Stout. 1985. Monitoring tractor performance with a three-point hitch dynamometer and an on-board microcomputer. ASAE Paper nº 85-1078. ASAE, St. Joseph, MI 49085.

Barger, E. L., Liljedahl, J. B., Carleton, W. M. and McKibben, E. G. 1963. Tractors and their power units. 2nd ed., John Wiley & Sons, Inc., New York, NY.

Bashford, L.L. 1984. Power losses due to slip and motion resistance. ASAE Paper nº 84-1564. ASAE, St. Joseph, MI 49085.

Beggs, J. S. 1955. Mechanism. McGraw-Hill Book Co., Inc., New York, NY.

Bekker, M.G. 1960. Off-the-road locomotion. The University of Michigan Press, Ann Arbor, MI.

Bekker, M.G. 1983. Prediction of design and performance parameters in agro-forestry vehicles. National Research Council of Canada, 22880 Ottawa, Ontario, K1A 0R6.

Brixius, W.W. 1987. Traction prediction equations for bias ply tires. ASAE Paper n° 87-1622. ASAE, St. Joseph, MI 49085.

Burt, E.C. and A.C. Bailey. 1975. Thrust-dynamic weight relationship of rigid wheels. Transactions of the ASAE 18(4):811-813.

Burt, E.C., A.C. Bailey, J.H. Taylor. 1980. Effect of dynamic load distribution on the tractive performance of tires operated in tandem. Transactions of the ASAE 23(5):1395-1400.

Burt, E.C. and A.C. Bailey. 1982. Load and inflation pressure effects on tire. Transactions of the ASAE 25(4):881-884.

Burt, E.C., P.W.L. Lyne, P. Meiring and J.F. Keen. 1983. Ballast and inflation effects on tire efficiency. Transactions of the ASAE 26(5):1352-1354.

Chironis, N. P. 1965. Mechanics, linkages, and mechanical controls. McGraw-Hill Book Co., Inc., New York, NY.

Clark, R.L. 1984. Tractor performance in two- and four-wheel drive. Transactions of the ASAE 27(1):8-11.

Cowell, P.A. and P.F. Herbert. 1988. The design of a variable geometry linkage to improve depth control of tractor mounted implements. Journal of Agricultural Engineering Research 39(2):85 - 97.

Devine, R.J. and C.E. Johnson. 1972 A three-point hitch force dynamometer accessory. ASAE Paper n° NC-72-403. ASAE, St. Joseph, MI 49085.

Dodd, R.B., D. Wolf, T.H. Garner, S.A. Hale, U.R. Pieper. 1986. Preliminary design and testing of a variable geometry three point hitch. ASAE Paper n° 86-1085. ASAE, St. Joseph, MI 49085.

Dwyer, M.J. and D.P. Heigho. 1984. The tractive performance of some large tractor drive wheel tyres compared with dual wheels. Journal of Agricultural Engineering Research 29(1):43 - 50.

Ellis, R.W. 1977. Agricultural tire design requirements and selection considerations. ASAE Distinguished Lecture Series, Tractor Design n° 3, St. Joseph, MI 49085.

Erickson, L.R. and W.E. Larsen. 1983. Four wheel drive tractor field performance. Transactions of the ASAE 26(5):1346-1351.

Felsenstein, G., C. Kotzabassis, B.A. Stout and S.W Searcy. 1987. Performance characteristics of a JD 4450 tractor with a mechanical front wheel drive. ASAE Paper n°87-1053. ASAE, St. Joseph, MI 49085.

Gee-Clough, D., G. Pearson, and M. MaAllister. 1982. Ballasting wheeled tractors to achieve maximum power output in frictional-cohesive soils. Journal of Agricultural Engineering Research 27(1):1 - 19.

Gibson, H. G. and Biller, C. J. 1974 Side-slope stability of logging tractors. Transactions of the ASAE, 17:245-250.

Hartenberg, R. S. and Denavit, J. 1964. Kinematic synthesis of linkages. McGraw-Hill Book Co., Inc., New York, NY.

Hoag, D.L. and R.R. Yoerger. 1974. Designing load rings for measruement. Transactions of the ASAE, 17:251-253, 261.

Johnson, C.E. and W.B. Voorhees. 1979. A force dynamometer for three-point-hitches. Transactions of the ASAE, 22:226-228, 232.

Kendall, C.K., C.L. Nachtigal, and J.H. Dooley. 1984. Three-point hitch dynamometer data acquisition system. ASAE Paper n° 84-1596. ASAE, St. Joseph, MI 49085.

Kepner, R. A., Bainer, Roy and Barger, E. L. 1980 Principles of farm machinery. 3rd ed., Avi Publishing Co., Inc., Westport, CT.

Kucera, H.L., K.L. Larson, V.L. Hofman. 1985. Field performance tests of front wheel assist tractors. ASAE Paper n° 85-1047. ASAE, St. Joseph, MI 49085.

Langewisch, S.A and J.C. Frisby. 1976. Portable, interchangeable instrumentation to mearsue draft and fuel consumption. ASAE Paper n° MC-76-806. ASAE, St. Joseph, MI 49085.

Long, G., T.H. Burkhardt and M.M. Mah. 1987. Performance evaluation of front and rear mounted plows. ASAE Paper n° 87-1617. ASAE, St. Joseph, MI 49085.

Luth, H.J., V.G. Floyd, and R.P. Heise. 1978. Evaluating energy requirements of machines in the field. ASAE Paper n° 78-1588. ASAE, St. Joseph, MI 49085.

Lyne, P.W.L. and E.C. Burt. 1987. Real time optimization of tractive efficiency. ASAE Paper n° 87-1624. ASAE, St. Joseph, MI 49085.

Martin, G. H. 1969. Kinematics and dynamics of machines. McGraw-Hill Book Co., Inc., New York, NY.

Mueller, G.R. and J.J. Freer. 1986. Evaluation of mechanical front drive tractor performance. ASAE Paper nº 86-1591. ASAE, St. Joseph, MI 49085.

Murillo-Soto, F. and J.L. Smith. 1977. Weight transfer in 4WD tractors: a model study. Transaction of the ASAE 20(2):253-257.

Murillo-Soto, F. and J.L. Smith. 1978. Traction efficiency of 4WD tractors: a model study. Transaction of the ASAE 21(5):1051-1053.

Rackham, D.H. and D.P. Blight. 1985. Four-wheel drive tractors -- a review. Journal of Agricultural Engineering Research 31(3):185 - 201.

Reynolds, W.R., G.E. Miles, T.H. Garner. 1982. Microcomputer system for data acquisition and processing in the field. ASAE Paper nº 82-5510. ASAE, St. Joseph, MI 49085.

Shell, L.R., R. Fox and K. Moss. 1986. Comparative evaluation of FWDA to two-wheel drive tractors. ASAE Paper nº 86-1067. ASAE, St. Joseph, MI 49085.

Smith, J.L. and M. Khalid. 1982. Hitch position control for 4WD tractors. Transactions of the ASAE 25(3):530-533, 537.

Tao, D. C. 1964. Applied linkage synthesis. Addison-Wesley Publishing Co., Inc., Reading, MA.

Tembo, S. 1986. Performance evaluation of the power disk - a PTO driven disk tiller. M.S. Thesis, Michigan State University, East Lansing, MI.

Taylor, J.H. 1976. Comparative traction performance of R-1, R-3, and R-4 tractor tires. Transaction of the ASAE 19(1):14-16.

Upadhyaya, S.K., D. Wulfsohn, G. Jubbal. 1987. Traction prediction equations for radial ply tires. ASAE Paper nº 87-1625. ASAE, St. Joseph, MI 49085.

Wilkinson, R. 1988. Personal communication. Agricultural Engineering Department, Michigan State Unviersity, East Lansing, MI 48824.

Wilson, C. E. Jr. and Michels, W. J. 1969. Mechanism - design-oriented kinematics. American Technical Society, Chicago, IL.

Wismer, R.D. and H.J. Luth. 1974. Off-road traction prediction for wheeled vehicles. Transactions of the ASAE, 17:8-10, 14.

140

Woerman, G.R. and L.L. Bashford. 1983. Performance of a front wheel assist tractor. ASAE Paper nº 83-1560. ASAE, St. Joseph, MI 49085.